Assessment and comparative study of design method for onshore wind power plant foundations

Master's thesis in Structural Engineering

MARCUS AHLSTRÖM
CARL HOLMQUIST

Department of Civil and Environmental Engineering
Division of Structural Engineering
Concrete Structures
CHALMERS UNIVERSITY OF TECHNOLOGY
Gothenburg, Sweden 2017
Master's thesis BOMX02-17-82

MASTER'S THESIS BOMX02-17-82

Assessment and comparative study of design method for onshore wind power plant foundations

Master's thesis in Structural Engineering

MARCUS AHLSTRÖM
CARL HOLMQUIST

Department of Civil and Environmental Engineering
Division of Structural Engineering
Concrete Structures
CHALMERS UNIVERSITY OF TECHNOLOGY

Gothenburg, Sweden 2017

Assessment and comparative study of design method for onshore wind power plant foundations
MARCUS AHLSTRÖM
CARL HOLMQUIST

Master's thesis BOMX02-17-82
ISSN 1652-8557
Department of Civil and Environmental Engineering
Division of Structural Engineering
Concrete Structures
Chalmers University of Technology
SE-412 96 Gothenburg
Sweden
Telephone: +46 (0)31-772 1000

Colophon:
The thesis was created using LaTeX 2_ϵ and `biblatex` and edited on `www.sharelatex.com`. The typesetting software was the TeX Live distribution. The text is set in Times New Roman. Graphs were creating using PGFPLOTS and MS Excel. Figures were created using AUTOCAD.

Cover:
Onshore Wind Power plant

Chalmers Reproservice
Gothenburg, Sweden 2017

Assessment and comparative study of design method for onshore wind power plant foundations
Master's thesis in Structural Engineering
MARCUS AHLSTRÖM
CARL HOLMQUIST
Department of Civil and Environmental Engineering
Division of Structural Engineering
Concrete Structures
Chalmers University of Technology

ABSTRACT

In recent years the demand for renewable energy has increased significantly, resulting in a large number of wind power plants being built. There has also been an increase in size of these towers and due to that an increase in the foundation size. The design of these foundations is a complicated process due to the complex loading on these towers. Especially the cyclic loads results in potential fatigue damage which gives cumbersome calculations with a lot of uncertainties.

The company WSP has designed several foundations over the years using a method developed by a professor at the Royal Institute of Technology in Stockholm. There was however a wish within the company to investigate the process and increase the knowledge. Another aim was to make the design process more efficient and for this a document capable of designing a foundation in little time was developed.

The aim of this study was to present a method that fulfills the standards set by the norms. In addition, some of the more problematic concepts will be discussed in more detail. The two major concepts analyzed in detail were wind loads and fatigue verification. The wind loads are often provided by the manufacturer of tower and are maybe not known in an early stage. Fatigue is one of the areas where designers have limited knowledge and it is an area where a lot of assumptions needs to be made in the design. Therefore, a more thorough investigation was done into this for both Eurocode and Model Code 2010. A comparison between the methods presented was also conducted to investigate potential improvements in the design process.

With the developed method three different case studies were made using three different wind towers. The studies concerned the influence of tower height, the life span of the foundation and the difference between using different partial safety factors, taken from Eurocode and IEC. The first study showed a clear relationship between the height and the design forces on the tower, and a moderate correlation between the height and the dimensions of the foundation. This study also showed that the influence of fatigue on the reinforcement increases with height and has a larger influence on the reinforcement in the top of the foundation. The second study showed that there is no major gain in designing a foundation for a 20-year life span instead of 50 years which is the value determined from Eurocode. Finally, the third study showed that there is little difference when designing according to IEC instead of designing according to Eurocode.

Keywords: Wind power plant foundations, Fatigue, Design methodology, Wind loads, Eurocode

Utvärdering och jämförande studie av konstruktion för vindkraftverksfundament
Examensarbete inom Konstruktionsteknik
MARCUS AHLSTRÖM
CARL HOLMQUIST
Institutionen för Bygg- och Miljöteknik
Konstruktionsteknik
Betongbyggnad
Chalmers tekniska högskola

SAMMANFATTNING

Under de senaste åren har det skett en ökad efterfrågan efter förnybar energi vilket lett till att ett stort antal vindkraftverk har byggts. Storleken på vindkraftverken har också ökat för att ge högre effekt, vilket i sin tur lett till ökad storlek på fundamenten. Konstruktionen av dessa fundament är en komplicerad process, främst på grund av de komplexa lasterna. Framförallt är det de cykliska laster som fundamentet utsätts för som ger potentiella utmattningsproblem och som leder till omfattande beräkningar.

Företaget WSP har konstruerat ett flertal fundament de senaste åren med en metod utvecklad av en professor vid Kungliga Tekniska Högskolan i Stockholm. Det fanns dock en önskan inom företaget att öka förståelsen för processen som använts. Ett annat mål är tidseffektivisera processen och i det syftet har ett dokument tagits fram för att utföra dimensioneringen.

Målet med denna studie var att presentera en konstruktionsmetod som uppfyller gällande normer. Utöver det kommer några av de mer problematiska delarna att presenteras i mer detalj. Detta gäller huvudsakligen vindlaster och dimensionering med hänsyn till utmattning. Vindlaster tillhandahålls oftast av tornleverantören och är inte alltid kända tidigt i processen. Utmattning är ett av de områden där konstruktörers kunskap kan vara begränsad och där det ofta krävs antaganden i processen. Av den anledningen gjordes en genomgång av Eurocode och Model Code 2010 samt en jämförelse mellan de olika metoderna i förhoppning om att hitta förbättringar i konstruktiongången.

Med den framtagna metoden genomfördes tre fallstudier utifrån tre olika vindkraftverk. I studierna utreddes tornhöjdens påverkan, skillnader för olika livslängder på konstruktionen samt effekten av att dimensionera med partialkoefficienter från IEC istället för Eurocode. Den första studien visade på ett tydligt samband mellan tornhöjden och de dimensionerande lasterna på fundamentet, samt viss korrelation mellan höjden och dimensionerna på fundamentet. Den visade också att utmattning får större effekt vid ökad tornhöjd samt har större påverkan på armering i överkanten av fundamentet. Den andra studien visade att det inte finns några större vinster med att konstruera med avsikt på 20 års livslängd istället för 50 som är riktlinjen i Eurocode. Slutligen så visade den tredje studien att det var liten skillnad mellan att dimensionera för IEC jämfört med Eurocode.

Nyckelord: Vindkraftsfundament, Utmattning, Designmetodik, Vindlaster, Eurocode

CONTENTS

PREFACE

This study was conducted on the initiative of the company WSP and done in order to clarify uncertainties regarding the design of wind power plant foundations. The study was conducted between January and May 2017 and made in collaboration between WSP and the Department of Structural Engineering, research group Concrete Structures, at Chalmers University of Technology.

We would like to thank WSP for the opportunity to conduct this study in their regime and for the constant support. A special thanks to our supervisor Erik Gustavsson for his insight into previous project and his help with difficulties regarding calculations. We would also like to thank Hans Helling and Joel Gustafsson for providing the initial idea to this thesis.

Next, we would like to thank our supervisor at Chalmers Alexandre Mathern for answering questions surrounding the process and for taking the time despite being abroad during the major part of the writing. We would also like to show our gratitude to our examiner Rasmus Rempling for his invaluable knowledge and experience in the field, and for helping with some of the most difficult design models.

Lastly, we want to thank our opponents David Gustafsson and Martin Ingvarsson for comments and suggestions during the process and for company during coffee breaks and lunches.

Göteborg, May 2017

Carl Holmquist & Marcus Ahlström

Nomenclature

Subscripts

c	Concrete
d	Design value
e	Extreme
equ	Equivalent
g	Permanent
k	Characteristic value
m	Material
tm	Mean tensile
u	Ultimate

Greek letters

ϵ	Strain
γ	Partial factor
Λ	Turbulence scale parameter
ω	Reinforcement ratio
ϕ	Bar diameter (m)
ρ	density (kg/m^3)
σ	standard deviation (m/s)

Roman lower case letters

c	Confinement factor
f	Strength (MPa)
k	Stiffness ratio
m	Relative moment
n	Applied number of cycles
z	Height (m)

Superscripts

α	Power law exponent
k	Exponent for S-N curve

Roman capital letters

R	Resistance
A	area (m^2)
E	Young's modulus (MPa)
G	Permanent load
I	Turbulence intensity
N	Resisting number of cycles
Q	Variable load
R	Stress ratio
S	Stress level
V	Wind speed

1 Introduction

"Structural engineering is the art of using materials that have properties which can only be estimated, to build real structures that can only be approximately analyzed, to withstand forces that are not accurately known, so that our responsibility with respect to public safety is satisfied."

Taken from: Shaopei Lin and Zhen Huang. "Comparative Design of Structures". iBooks.

1.1 Background

With the increasing effect of climate change the need for alternative energy sources has risen in order to decrease the dependency on fossil fuels. According to the Swedish organization Svensk Energi, wind power is the fastest growing renewable energy source in Sweden. In 2015 the total production in Sweden was 16.6 TW h, which can be compared to the 0.9 TW h produced in 2005 (Svensk Energi, 2016). This is an increase to more than 18 times in just 10 years. A graph representing the number of plants, effect and total energy production can be seen in Figure 1.1.

As can be expected, a large number of wind power plants have been built during this period. There has also been an increase in the size of the wind towers themselves in order to increase the effect, which has also lead to an increase in the size of the foundations in order to resist the resulting forces from these high structures. These foundations are subjected to a complex loading situation, mainly from the ever-changing wind, with sizable cyclic forces.

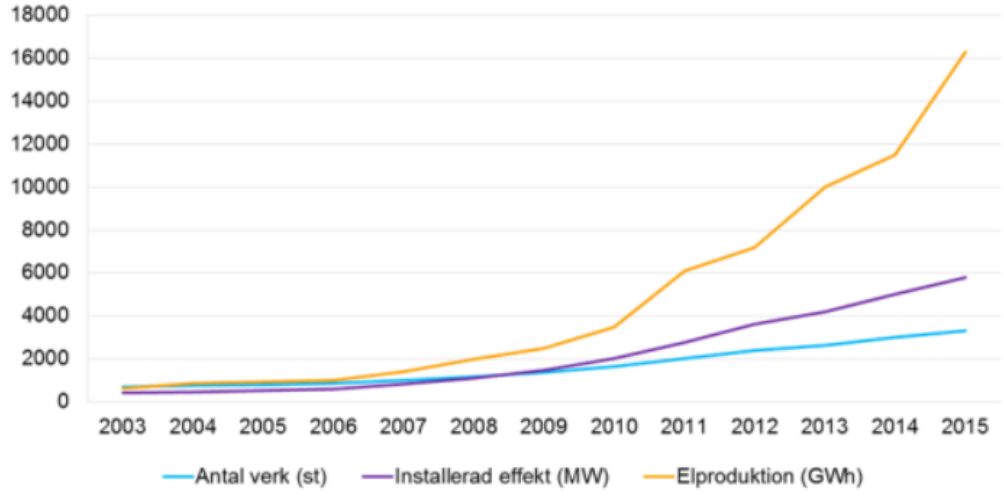

Figure 1.1: The development of wind power in Sweden. Source: Johansson, 2015.

At the company WSP a number of different foundations has been designed over the years with the help of experts in the field. There is, however, a feeling within the company that the internal level of knowledge surrounding this problem has to be increased through a deeper study of the method that has been used

previously. There is also a wish to potentially improve the design process and the way the results are obtained.

One of the main challenges is the estimation of fatigue capacity in the foundation due to difficulties with determining stress concentrations and structural behaviour under cyclic loading. There are a lot of uncertainty among the active designers on how the loads shall be treated and which standards shall be used. Especially on a wind power project with actors from several different companies, potentially based in different countries, there is an uncertainty on which standard is governing. There are International, European and, in some cases, National standards that all have different methods on how fatigue strength shall be calculated or what factors should be used. A clarification and study of the governing parameters for each standard has the potential to improve the understanding of the design process in a significant way.

1.2 Problem description

"Understand and develop an analytical design methodology for wind power plant foundations"

1.3 Purpose

The purpose of the project was to gain a deeper understanding of how to design wind power plant foundations and how different norms affect the design outcome. This included comprehension of methodologies and modeling choices used in designs today. Furthermore, the intention was that this knowledge should enable designers to make use of the materials in the structure more efficiently, and thus create more accurate designs. Finally, the intention was to make the design process more efficient in both preliminary and detailed phases.

1.3.1 Objectives

The main objective of this study was to investigate a design methodology for wind power plant foundations and from that propose recommendations for future work. In order to reach the aim of the project some specific objectives were mapped out:

- describe the design method used by WSP today with underlying theory and increase the knowledge
- study the norms governing the wind loads in order to increase understanding
- study fatigue behaviour with an emphasis on how it is treated in different norms
- develop tools to use the described design method in an efficient way
- investigate how the height of the tower affect the final design of the foundation.

- study what influence the life-span has on the final design
- study the influence of using different partial safety factors

1.4 Limitations

In order to keep this study focused the following limitations have been made. Another motivation behind the limitations may be to keep in order with the wishes made by the examiner and WSP:

- The scope of the study was limited to onshore gravitational foundations only. Other types of foundations are introduced briefly but not studied in depth.
- Only quadratic foundations with a centrally placed tower are considered in design.
- Only the method used and developed by WSP was studied. Other potential design methods are not investigated.
- Reference cases used were taken from WSPs earlier projects. The same external conditions were used for all towers.
- The thesis treats only the design of the foundation, meaning that there was no consideration to the design of the tower.
- The study was focused to the following norms
  - Eurocode
  - fib Model Code 2010 for fatigue
  - IEC 61400 for wind loads.
- All norms were only used for the discussion and comparisons. For WSP's method only Eurocode was used.

1.5 Method

The first part of the project mainly focused on a literature study of methods to design wind power plants. This was done in order to attain an understanding of how the design is performed in general and how it is done in particular at WSP. This included understanding the underlying theory behind the assumptions that are made in the calculations, and also fully comprehend the calculations, in order to clearly convey the knowledge to others who are not as familiar with design of wind power plant foundations.

When this was achieved, the next step was to establish a calculation document in order to easily produce foundation designs. One of the goals with the document was to make it easy for the designer to discover how different design choices affect the outcome and also make the calculations easy to overview.

Therefore it was deemed appropriate to use Excel for the calculations. This proved very efficient in later parts of the study.

In order to easily convey the knowledge about the design of foundations to others a document explaining each step in the calculation process was established. This included the formulas used, explanatory text and figures when needed.

Two aspects of the design was studied in more depth in order to improve the knowledge. These were the calculations of wind loads and the fatigue. A deeper literature study was made on both subjects in order to improve the knowledge. That involved reading books on the subject as well as articles attained from the Internet, other master theses and material that WSP have used as a base for their assumptions in previous projects. The study resulted in recommendations on how to proceed in future work and was used as basis for discussions.

The major aim of the study was to conduct three case studies to find out more about the governing parameters. The first of these concerned the tower height and was done in order to find relations to the design forces, foundation dimensions and the governing parameters with regard to height. The second study concerned the life span of the foundation and the potential gain of shortening it from 50 to 20 years. Lastly, the influence of designing with partial safety factors from IEC instead of Eurocode was studied.

The results from the case studies was discussed along with some other issues that had arisen during the process and conclusions were drawn that resulted in recommendations regarding future design work.

2 Introduction to wind power plants

2.1 Wind towers today

The amount of energy produced from wind power plants (WPP) in Sweden has been increasing during the last few years. According to the Swedish organization Svensk Energi (2016) the energy from WPPs in 2015 compiled 12 % of the total energy production in Sweden. It is expected to rise even further as the knowledge within the area has been increased and thus making it easier and cheaper to produce new WPPs. Another contributing factor for this development is that the conditions are very good in Sweden. A long coast line and windy environment renders a lot of good locations for placing WPPs (Svensk Energi, 2016).

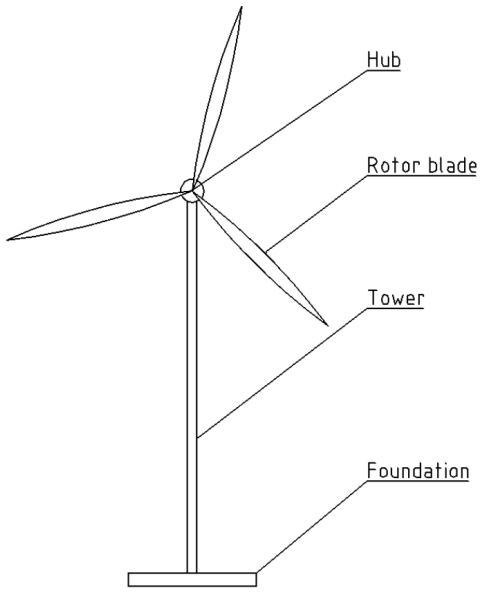

Figure 2.1: Schematic figure showing some of the basic components in a WPP

The rotor which converts the wind energy into electrical energy can be placed in front of or behind the tower according to Gasch and Twele (2012). The most beneficial is to place it in front due to the extra load that is created when wind passes the tower and then hits the rotor. The moment driving the generator comes from the blades, which are usually three. The material used for the blades is either glass fibre or carbon fibre where the former is less expensive but the latter has better material properties. The glass or carbon fibres come in sheets that are placed in moulds and glued together by a polyester or epoxy resin. Using epoxy based resin is more beneficial since it is lighter which implies lower loads and thus less strain on the structure.

The tower of the WPP is very important for the whole structure because of economic aspects. The wind conditions influence the height of the hub and how much energy that can be generated. Usually the towers

are made of steel but concrete is also an option. However, using concrete requires a post-tensioning system due to the limited tensile strength of concrete. There are also so called hybrid towers consisting of both concrete and steel where the intention is to make use of the strength of each material. The lower part of the tower is thus made of concrete whereas the upper part is made of steel (Gasch and Twele, 2012).

The foundation is the connection to the ground and its purpose is to provide stability for the WPP. That includes handling tilting moments, horizontal and vertical forces and also torsional moments that arise due to wind effects. The design of the foundation may vary depending on which type of tower that is used, e.g. tubular, lattice or guyed which are described more in depth in Section 2.2. However, one common trait among all types of onshore foundations is the use of reinforced concrete for the foundation.

2.2 Wind power plants

There exist a variety of different designs of WPPs depending on which context it is situated in. There are, for example, offshore WPPs which are placed in marine environments and onshore WPPs which can be further categorized depending on the ground conditions. If the soil is not able to carry the weight of the WPP, a pile foundation is to prefer. The piles can either be driven to bedrock or to a layer of soil that has higher strength. If the top layer of the soil has the capability to withstand the resulting forces, a gravity based foundation can be used which is stabilized by the ground pressure. Generally offshore WPPs are more expensive to produce and maintain due to more difficult conditions, however, the wind conditions for offshore WPPs are very good. Furthermore, the development within the industry has lead to higher and more powerful WPPs capable of producing more energy. The latest onshore models being designed have an effect of 7.5 MW and a height of 137 m, which is the same height as one of the reference projects but more than twice the capacity (Campbell, 2016). The difference is that this tower is designed for higher wind speeds which is advantageous since the power of the turbine is approximately proportionate to the cube of the wind speed (Gasch and Twele, 2012). However, this puts higher demands on the foundation since bigger loads have to be resisted.

There are several types of towers used when constructing WPPs. The most common is according to Hanser Verlag (2014) the tubular tower. This type of tower has a circular section which grants benefits like good torsional resistance and fast erection. The tower is delivered in separate sections that are bolted together. This type of tower also benefits from the possibility of prefabricating the sections and thus limiting the on-site construction.

Another type of tower is the lattice mast which is a lighter construction than the tubular tower. As for the tubular tower, the degree of prefabrication is high and the components can be brought easily to the construction site. The downside of this design is an extensive erection and maintenance required due to the vast amount of components.

A third type is the guyed mast which uses cables or guy lines for stabilizing the structure. The tower has to be able to withstand the compression force from its self-weight and the guy lines. This design enables material savings but, due to comprehensive ground investigations that are necessary, this design is rarely used (Hanser Verlag, 2014).

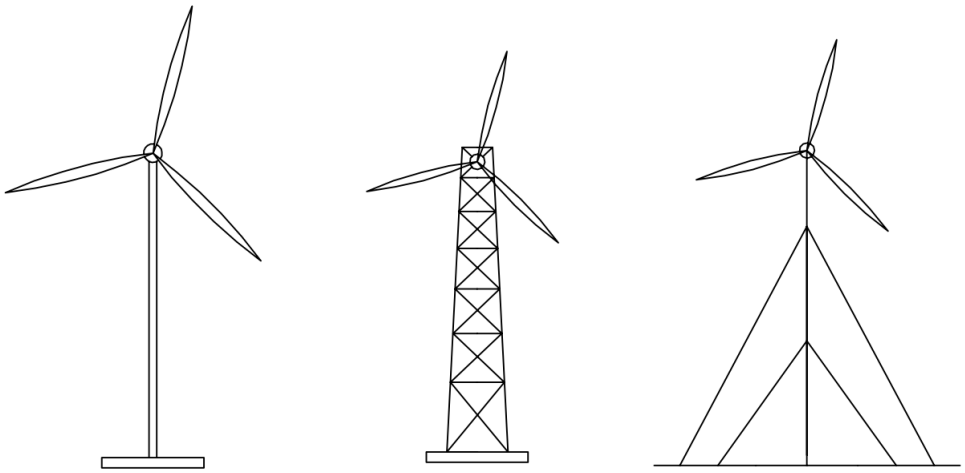

(a) (b) (c)

Figure 2.2: Different types of towers (a) tubular (b) lattice (c) guyed.

.

2.3 Wind Power Plant foundations

With the increased size of the wind towers there has been an increased demand on the foundations to fulfill the different requirements needed. The design requirements will be explained in more detail in the following sections. The purpose of this section is to explain the different types of foundations and describe when the different types are suitable to use.

The three foundations mentioned by Hanser Verlag (2014) as the most common are

- gravity force foundations
- cabled foundations
- piled foundations.

They are appropriate in different situations depending on the bearing capacity of the soil and the construction of the tower itself (Hanser Verlag, 2014).

2.3.1 Gravity force foundations

These types of foundations are the most commonly used foundations for WPPs. Two different types exist, the raft and the monopile foundation, where the difference is the ratio between depth and width. The monopile foundation consists of a single pile driven deep into the soil according to Burton (2011). It is also stated that monopiles may be used for sites with good soil conditions but is seldom used due to an excessive use of materials (Burton, 2011). Two different examples of monopiles can be seen in Figure 2.6, type (b) and (c).

The second type of gravity foundation is the raft foundation where in contrast to the pile the width is larger than the depth, and is therefore designed as a shallow foundation according to Eurocode. In Figure 2.3 four different types of raft foundations can be seen. Notice that type (d) is a rock-anchored foundation which can be used when the distance to solid rock is small. Type (a)-(c) show different ways of designing raft foundations.

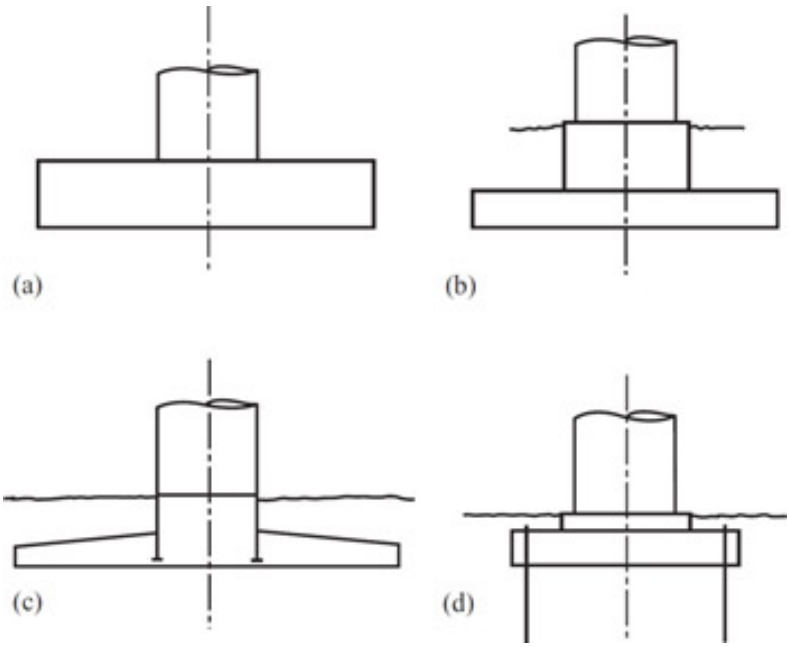

Figure 2.3: (a)-(c) show different designs types of raft foundations whereas (d) is rock anchored. Source: Burton, 2011.

The raft foundation's function is to resist the forces coming from the tower and the foundation itself. With the exception of the rock-anchored foundation the forces are resisted only by the weight of the foundation and the tower. The bending moment results in an eccentric support reaction to the ground and large internal forces.

Construction details of raft foundations

Since this report will focus on the design of a raft foundation with a square crossection this will be presented a bit more thorough. In Figure 2.4 a raft foundation can be seen before the casting of concrete. These are heavily reinforced structures with most of the reinforcement placed in the main directions, with additional reinforcement in radial direction nearest to the tower.

An anchorage ring that consists of two steel plates connected with post-tensioned bolts is used to attach the tower to the foundation. This will ensure that the concrete is always in compression and avoid large cracks due to tension. However, this will lead to very high pressures under the upper steel ring when the moment creates a positive reaction on that side. Therefore, it is required to use a high-strength concrete grout under the plate, often with a characteristic compressive strength in the range of 80 MPa. An example of a construction can be seen in Section 2.5.

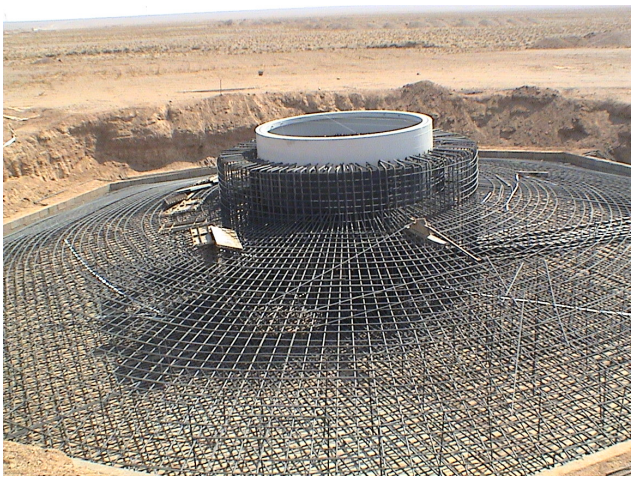

Figure 2.4: A typical reinforcement arrangement for a gravity foundation

2.3.2 Cabled foundations

This foundation is used for guyed masts where the loads are transferred using prestressed cables which are anchored into the ground, see Figure 2.5. This gives a very complicated force flow within the soil and is dependent on satisfactory bearing capacity.

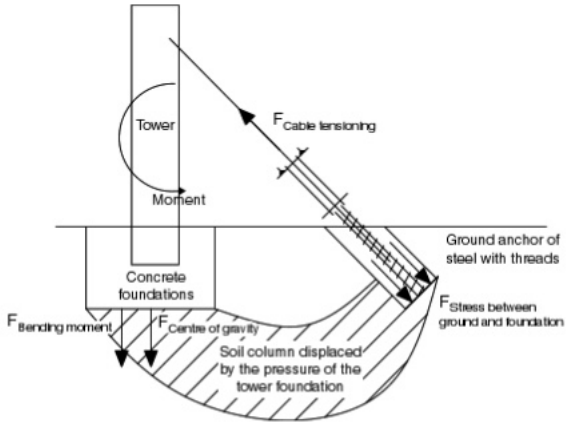

Figure 2.5: Sketch of a typical cabled foundation where forces are indicated. Source: Hanser Verlag, 2014.

2.3.3 Piled foundations

These kinds of foundations are used both on- and offshore when the soil conditions are unfavorable, or there is a need to avoid excessive settlements (Knappett and Craig, 2012). Long piles made of concrete, timber or steel are driven into the ground to give a satisfactory bearing capacity on weak soil. Depending on whether the soil is cohesive or non-cohesive the design process differs.

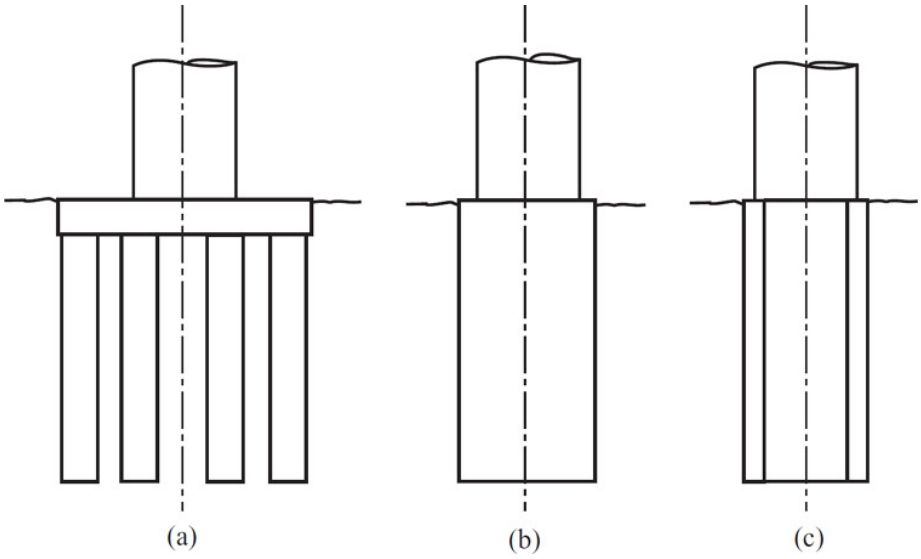

Figure 2.6: Different types of pile foundations. (a) multi-pile (b) solid monopile (c) hollow monopile Source: Burton, 2011.

2.4 Actions on WPPs

A WPP is subjected to different types of loads during its life where some are more prominent and have to be considered when designing. The most apparent might be the self weight. The wind is the most significant load causing the highest stress on the structure. These loads have to be resisted and for gravity foundations this is achieved by the soil pressure acting on the foundation of the WPP.

The aim of this section is to give the reader a brief view of the forces acting on a WPP. A more thorough study of the wind loads can be found in Section 3.4. The reason for looking more into detail on this matter was that there have been interests in understanding how the wind loads are calculated, since today the tower manufacturer, e.g. Vestas, simply delivers the loads acting on the foundation without any detailed background information.

2.4.1 Permanent

The permanent loads acting on the WPP is the self-weight of the foundation, the tower, the nacelle and the rotor. Moreover electrical machinery that is used in the WPP along with other equipment like, for example, stairs should also be considered.

2.4.2 Wind loads

The wind is the main variable load that has to be considered when designing WPPs and the intensity of the wind is site specific, meaning that the average speed and other parameters can vary from one location to another, and this has resulted in the development of wind classes. Gasch and Twele (2012) state that

there are four different classes in the IEC-standard. Each class provides the designer with appropriate values for wind speeds, see Table 2.1, in order to attain representative loads for the location of the WPP to enable accurate and profitable designs.

The selection of wind class has to be verified by site specific investigations. This is important since small variations in wind speed can cause big differences in how much energy that can be generated. A 10% difference in wind speed leads to 33% difference in power output. The survey includes measuring wind conditions at the intended location and thorough investigations of the surrounding environment. The latter involves, for example, locating other WPPs and determining surface roughness of the ground (Gasch and Twele, 2012). How wind loads are determined and modelled will be introduced further in Chapter 3.

Table 2.1: Wind speeds for different different wind classes (Gasch and Twele, 2012).

Wind Class	I	II	III	IV		
Extreme load					Unit	Comment
$V_{ref} = V_{50}$	50.0	42.5	37.5	30.0	m/s	Expected extreme 50-years wind, 10m-min average
V_{e0}	70.0	59.5	52.5	42.0	m/s	Extreme 50-year wind, 3-sec average
V_{ml}	37.5	31.9	28.1	22.5	m/s	Expected annual extreme wind, 10min-average
V_{el}	52.5	44.6	39.4	31.5	m/s	Annual average wind, 3-sec average
Fatigue strength						
T_{IA}	18	18	18	18	%	Characteristic turbulence intensity at V = 15 m/s Class A
T_{IB}	16	16	16	16	%	Characteristic turbulence intensity at V = 15 m/s Class B

2.5 Introduction to case studies

The aim of this study was to investigate the influence of three different parameters of the WPP. In order to do this three case studies were conducted. The following parameters were examined:

- the influence of tower height
- the life-span of the WPP
- the effect of different partial factors.

In order to make the comparisons as accurate as possible the same soil conditions were used for all towers, taken from a reference case. The three towers are all designed by the same manufacturer, Vestas, and have been used for foundation design by WSP. The data for these can be seen in Table 2.2.

Table 2.2: Data for the three Wind towers used in case studies.

Name	Hub height	Rotor diameter	Effect	Wind class
V126-3.3 MW ™	137 m	126 m	3.3 MW	III A
V112-3.0 MW ™	124 m	112 m	3.0 MW	II A
V100-1.8 MW ™	95 m	100 m	1.8 MW	III A

The reference case used for introduction and choice of parameters derives from one of WSP's earlier projects that was designed and built in Sweden during the year 2014. The WPP is of type V126-3.3 MW ™ and is designed specifically for locations with lower wind speeds. The data for this tower can be seen in Table 2.2. The loads used when designing for ULS and SLS were provided by Vestas and are displayed in Table 2.3. In Table 2.3 loads for fatigue are presented in the form of equivalent moments which are calculated in accordance with the method presented in Section 4.8.

Table 2.3: Loads acquired from Vestas acting on the foundation for V126.

Serviceability limit state				Unit	Comment
Characteristic value		*Design value*			
$M_{ex.k}$	104.9	$M_{ex.d}$	104.9	MN m	Tilting moment
$H_{ex.k}$	850.4	$H_{ex.d}$	850.4	kN	Horizontal force
Ultimate limit state					
Characteristic value		*Design value*			
$M_{ex.k}$	104.9	$M_{ex.d}$	157.4	MN m	Tilting moment
$M_{ex.k.torsion}$	6429.0	$M_{ex.d.torsion}$	9643.5	kN m	Torsional moment
$H_{ex.k}$	850.4	$M_{ex.d}$	1275.6	kN	Horizontal force
Fatigue limit state					
$M_{fatigue.tower}$	53800			kN m	Macalloy bolts
$M_{fatigue.bottom.reinforcement}$	15450			kN m	Bottom reinforcement
$M_{fatigue.top.reinforcement}$	13900			kN m	Top reinforcement
$M_{fatigue.steel}$	46000			kN m	Distribution ring

For the different towers there are extreme external forces divided into two different categories, normal and abnormal. Normal loads correspond to situations that are expected to occur frequently during the towers life span. Abnormal situations are expected to occur less frequently and therefore have a lower safety factor than the normal load cases. Which case that results in the largest design load may vary between different towers.

A bolt cage, shown in Figure 2.7 and Figure 2.8, is used to anchor the tower to the foundation. All the loads from the tower have to be transferred through this element. Pressure acts on the upper flange and is transferred through the plate to the concrete. Tension, on the other hand, is carried through the bolts to the lower flange where it is compressing the concrete. The bolts are post-tensioned to roughly 65 % of their tensile strength.

In the center of the foundation under the tower a so called soft layer is used. This consists of expanded polysterene (EPS) which has low capacity for compression. The purpose of using the EPS is to ensure beam behaviour in the foundation and moving the extreme stress to the edges. Another benefit is that it prevents the soil at the edges from becoming too soft after a high number of load cycles, which would otherwise cause severe tilting of the foundation. This would, in turn, reduce the electricity that can be produced from the tower.

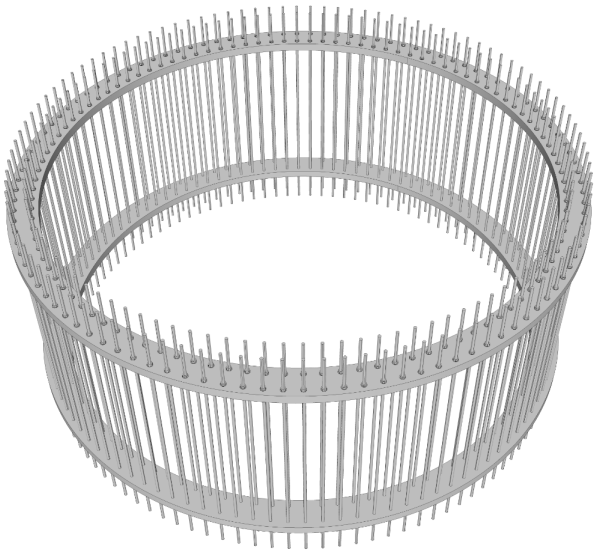

Figure 2.7: Bolt cage used in the reference case.

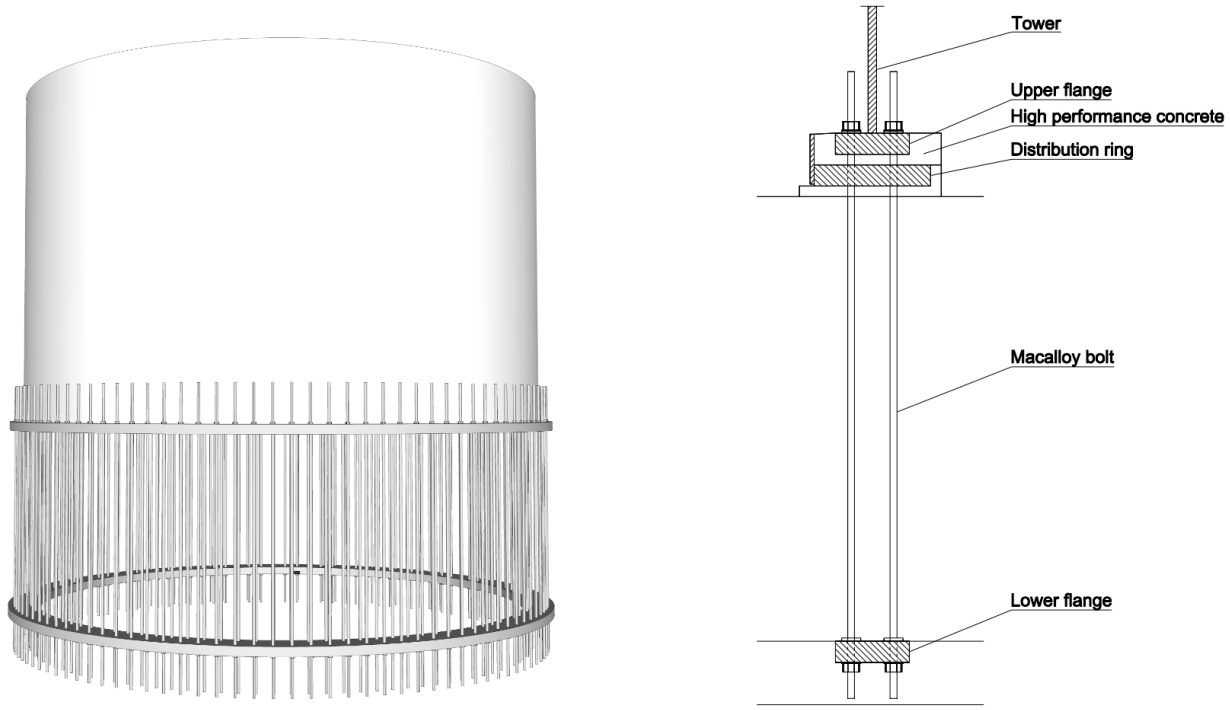

(a) (b)

Figure 2.8: The connection between the tower and the bolt cage.

The design method presented in Chapter 4 will be used for all three case studies. The aim of each case study is introduced in the following Sections.

2.5.1 Case study 1 - Influence of tower height

In order to get more effect from the tower the height can be increased since the wind speed increases with height. With a higher tower there is also the option to use larger rotor blades and get more power. However, this will also lead to larger forces on the tower and a larger foundation. Therefore a comparison for different heights to examine the relation between foundation size and height was of interest. The relation for design forces was also studied.

Another aspect of interest was to study the governing parameter in design. This was done to find out if the damage from fatigue is more severe for a high tower compared to a low tower and also to potentially find a threshhold were the governing parameter changes.

2.5.2 Case study 2 - Influence of life span

All of the towers in the case study are designed for a life span of 20 years during which it is in production. This has an effect on the size of the fatigue loads. However, the governing norm in Europe states that the life span of most structures should be 50 years. This raises the question of what influence this increased

life span has. The effect is also dependent on if the foundation is intended to be used a second time after the initial tower has been worn out.

2.5.3 Case study 3 - Conflicts between norms

The design of WPPs should according to IEC (2005), which is the International standard governing the design of wind towers, be done with partial safety factors. This is also a concept presented by the other norms. The purpose is to account for stochastic variations for loads and the strength of materials. For load calculations this moderates how big the chances are for a certain load occurring. These may vary when considering different types of loads like ultimate and fatigue loads. When it comes to materials, the purpose is to account for the uncertainty in the production methods and thus the reliability of the materials strength class.

The same load type or material can have different partial safety factors depending on which norm is used, and therefore the combination of different norms can provide difficulties. By applying the different partial factors from Eurocode and IEC (2005), introduced further in Section 3.1, the effect of different parameters can be seen. In order to see the effect of only the partial factors the same method, presented in Chapter 4, was used for all partial factors.

3 Theory

Recalling the quote from the beginning, the design of a structure is a complex process where a lot of data has to be combined using the knowledge and experience of the designer. Using a quote from Lin and Huang (2016) *"Design is the bridge between subjective function and objective reality"*. At the beginning of a design process a couple of functions are defined that the final structure are supposed to fulfill. In these processes there are no single correct solution because in the early phase decisions are made that will have a large impact on later phases in the design process.

Focus in this study will lie on the detailed design of structures when the bearing system and loading conditions are known. The challenge comes in translating the structure and loads into something that can be verified by either analytical or numerical methods. Some of the things that have to be accounted for in this process can be seen in Figure 3.1.

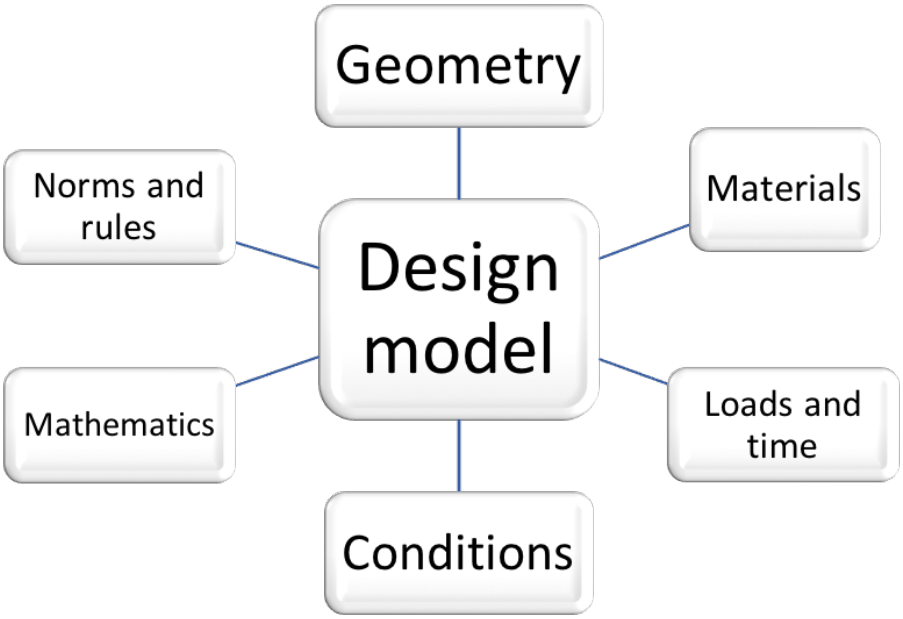

Figure 3.1: Parameters influencing a Design Model

By establishing these in a satisfactory way a structure can be transformed from something complex into something that is known, e.g. an Euler-Bernoulli beam, from which design values for sections can be calculated. Another alternative which has been introduced over the last years with the increased capacity of computers are numerical methods, e.g. the Finite Element Method (FEM), where the structure is divided into smaller elements in order to calculate section forces. The main challenge is to know the limitations of assumptions and the potential risks by doing them, referring back to the quote from Chapter 1.

Three different concepts will be introduced as part of the literature study. Firstly, the governing standards that influence the design. Secondly, how the wind loads are calculated in order to increase the knowledge surrounding this and finally, the theory and governing norms surrounding fatigue is presented. This was done in order to provide basis for further discussions surrounding the different issues. It was also

done in order to attain an increased knowledge which supported the presentation of the design method in Chapter 4. However, the theory presented in this section has limited influence on the case studies conducted and should be seen as a separate part of the study.

3.1 Standards

In order to ensure that a structure is functioning during the course of its use there are standards that regulate what a structure must fulfill in order to safely predict its function during the intended life span. An important aspect in design is the concept of limit states which are the state beyond which the performance of the structure no longer satisfies the design criteria (Gulvanessian, Calgaro, and Holický, 2012). In Eurocode the two standard states are Ultimate and Servicability limit state, with several checks needed to be made for different states. For structures subjected to varying loads the Fatigue limit state is also necessary to check. Examples of checks are listed below.

- Ultimate limit state (ULS)
  - Moment capacity
  - Shear force capacity
  - Structural stability
- Servicability limit state (SLS)
  - Vibrations
  - Deflections
- Fatigue (FLS)

The standards normally give guidelines for how to combine different loads into the design stress (S_d) on the structure and how to calculate the relevant design resistances (R_d) of the materials and sections used. The safety of the structure is ensured by controlling that the stress on the structure is less than the resistance of the structure, i.e.

$$S_d \leqslant R_d \tag{3.1}$$

The process may vary a bit between different norms but the general process will be described using Eurocode as an example, as this is the governing norm in Sweden. The procedure is done by taking a characteristic load which represents a condition that has a certain return-time, normally 50 years. In the same manner a characteristic value is considered for each material parameter which represents a certain probability, e.g. the lower 5-percentile. These two different characteristic values are then modified with *partial safety factors* in order to provide a satisfactory margin of safety. The partial safety factors are determined based on a number of parameters, e.g. which limit state and what type of load. Normally

these are treated as load combinations which are stated in EN-1990 (2005). In a generic way the safety check can be expressed as follows

$$\gamma_{Sd}\mathbf{S}\left\{\gamma_g G_k; \sum_{i=1}\gamma_{q,i}Q_{k,i}\right\} \leqslant \frac{1}{\gamma_{Rd}}\mathbf{R}\left\{\frac{\mathbf{R}_k}{\gamma_m}\right\} \tag{3.2}$$

where

G_k is the characteristic permanent load,
Q_k is the characteristic variable load,
R_k is the characteristic resistance of the structure,
γ_{Sd} is a partial factor for the uncertainty of the load model,
γ_g is a partial factor for permanent load,
$\gamma_{q,i}$ is a partial factor for live loads,
γ_{Rd} is a partial factor for the uncertainty of the material model,
γ_m is a partial factor for material properties.

This is shown visually in Figure 3.2 reprinted from Gasch and Twele (2012).

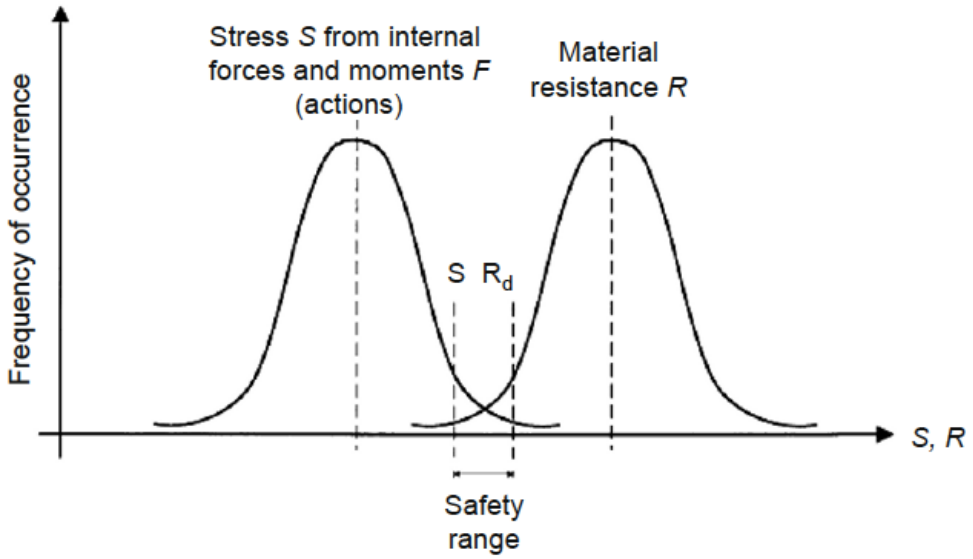

Figure 3.2: Visual represenation of structural verification. Source: Gasch and Twele, 2012.

Since a large focus of this study will be on comparing approaches from different standards a short introduction to these will follow. Interesting points are differences and eventual conflicts between norms that can be governing.

3.1.1 Eurocodes

Since 2010 it is mandatory for countries within the European Union to design structures to meet the requirements set by the European Norms (EN). There are a total of 10 different norms and the relation

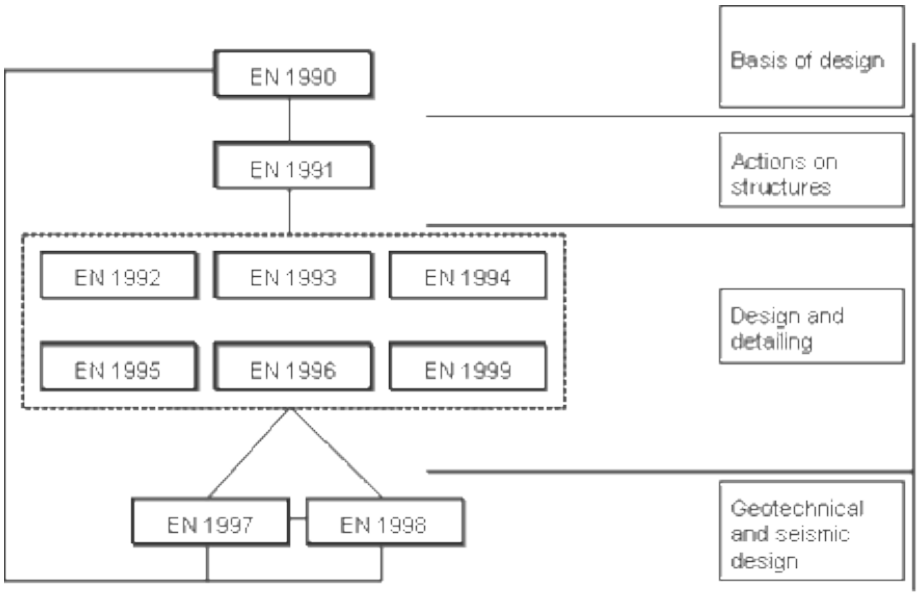

Figure 3.3: The links between different parts in the Eurocode. Source:`http://www.standardsforhighways.co.uk`

between them can be seen in Figure 3.3. The aim of these norms was to cover as many design situations as possible and not all of the norms are applicable to the design of WPP. The ones that are of interest for this study are listed in Table 3.1.

There are some important aspects to know about the Eurocodes. They are reviewed every five years with a new update coming out in 2018. Another aspect is that countries have a way of influencing the norm via the national parameters in Eurocode. These are parameters that are left open within the norm for each country to decide about, with a recommended value stated in the norm which may be used. For each country there is a National Annex (NA) which states the choices made. In Sweden the governing NA is the EKS where the latest version is EKS10.

Table 3.1: Eurocode documents of interest for this thesis (EN-1990, 2005).

Number	Description
EN 1990	Basis on Structural Design
EN 1991	Actions on structures
EN 1992	Design of concrete structures
EN 1993	Design of steel structures
EN 1997	Geotechnical design

3.1.2 fib Model Code 90 and 2010

One of the major organizations concerned with concrete structures is the International Federation for Structural Concrete, commonly refered to as fib from their french name. The organization has over the years released several different codes, the first code-like documents were released in 1964. This was done as a joint endeavour by the organizations predecessors Comité Euro-International du Béton (CEB) and Fédération Internationale de la Précontrainte (FIP) in order to provide documents that national code commisions could use when writing their documents. In this fashion the Model Code 90 was used as a basis when writing EN 1992 (fib, 2013). Therefore the Model Code is not a norm in itself, instead providing a basis for the writing of new norms.

One important aspect in the fib Model Code that differs from Eurocode is the term *level of approximation*. This indicates how simplistic the model is where I represents the most approximate method and is reserved for structures where the need for accuracy is low (fib, 2013) . The level which provides the highest accuracy is IV, however this often requires more cumbersome calculations. This is shown visually in Figure 3.4 reprinted from Model Code 2010. For each load effect Model Code provides methods for different levels depending on the wanted accuracy.

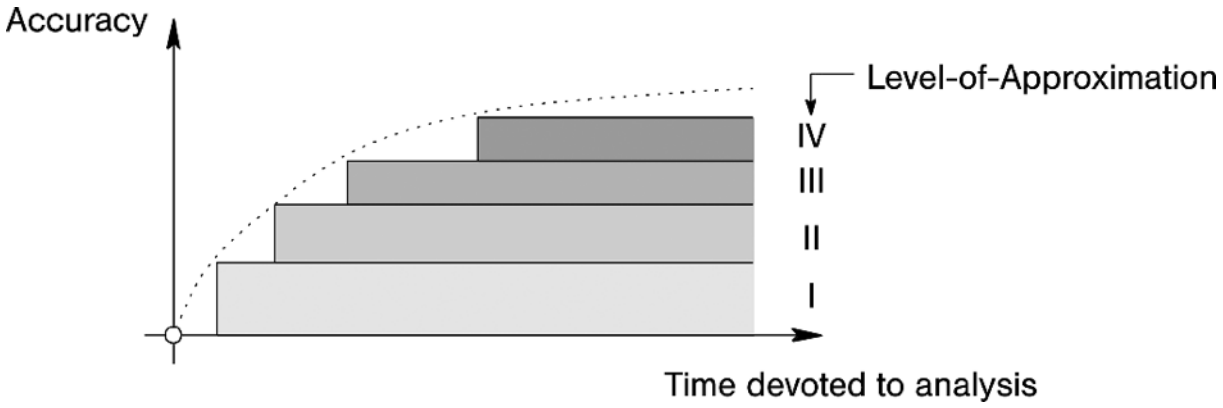

Figure 3.4: Visual representation of level of approximation in Model Code 2010. Source: fib, 2013

3.1.3 IEC-61400

IEC is an international organization that was founded 1906 and provides International standards for all fields of electrotechnology (IEC, 2017). Their standard series IEC-61400 concerns the design of wind turbines and their supporting structures. This standard is only valid for onshore structures. IEC-61400-1 is the governing document and is used to calculate the wind loads, e.g. the data in Table 2.1 is taken from this standard. There are also several load cases that are used as a basis for calculating the loads used in FLS.

3.1.4 Basis of design

The WPP has to be designed with regard to ULS, SLS and FLS. Examples of loads for each respective case are displayed in Table 2.3. The loads for ULS and SLS are taken directly from the data provided by

Vestas where one of the major uncertainties surround the partial load factors accompanying the loads. For the fatigue load the standard load provided is a mean load and a range which come in two different sets depending on the fatigue behaviour of the studied material. These load levels are valid for 10^7 cycles. Two alternatives are given, namely a Rainflow matrix and a Markov matrix. The latter is used for the design.

The Markov matrix is a load matrix and the load capacity is represented by the S-N curve for the material in question. The Markov matrix is described in more detail in Section 3.5.2. The damage equivalent bending moment in the tower is derived by trial-and-error calculations by varying the moment until the sum of all partial damages according to Palmgren-Miner hypothesis becomes 1.0. The calculated loads can be seen Table 2.3 for the different parts subjected to fatigue loading.

The loads acting on the bottom of the tower except for the horizontal force can be seen in Figure 3.5. How these loads are transferred to and resisted by the foundation will be the main objective of Chapter 4 as well as verification according to the governing norm, Eurocode.

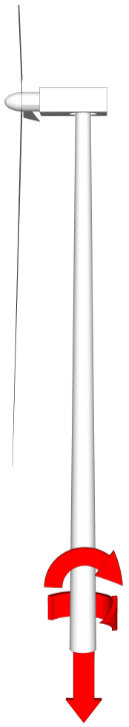

Figure 3.5: Tilting and torsional moments and normal force acting on the foundation. In this study the loads are provided by Vestas.

One of the major problems when designing a foundation is the origin of the loads, especially the wind loads. Live loads and self-weights are tabulated in the norms but for wind loads there are some major problems. One is that the international norm IEC-61400 demands that the calculations of loads should be made in a certain way without giving detailed guidelines for how these should be performed. Secondly, the structure is often designed according to different norms which give other safety parameters and can in the worst case lead to an unsatisfying margin of safety for the structure.

In previous projects WSP have received the dimensioning loads from the manufacturer of the tower and the degree of detail have varied from case to case. For one of the cases the characteristic loads are presented in Table 2.3.

3.2 Partial factors in Eurocode and IEC

This section aims to give the reader a brief introduction to partial factors and their origin. Therefore, it has been deemed sufficient, in some cases, to only state the partial factor of interest and omitting the theory behind.

As explained in Section 2.5.3, stochastic variations of loads and strength of materials is handled by the use of partial safety factors. However, different norms might state various partial factors even though they are used with the same parameter. This is the case between Eurocode and IEC, where Eurocode tend to supply the designer with greater partial factors for the loads. In Figure 3.6 a scheme of how the different partial factors are combined is shown.

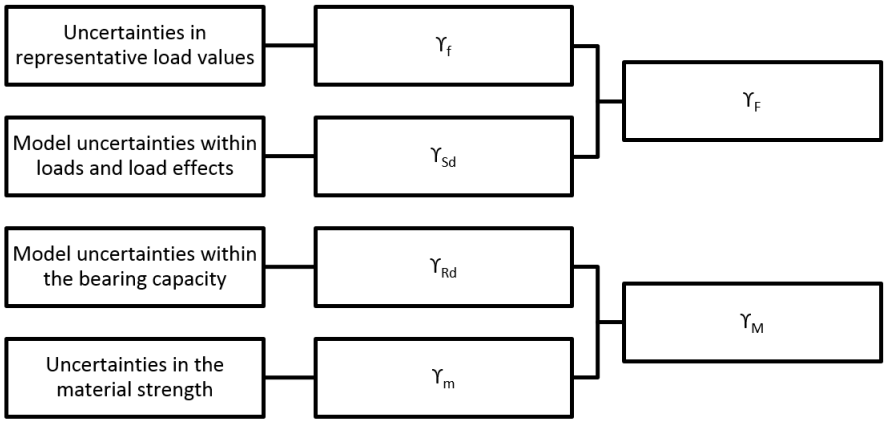

Figure 3.6: Link between different partial factors. Source: EN-1990, 2005.

Safety factors can be developed in different ways, ranging from empirical methods to pure mathematical models as well as combinations of these. The empirical method is based on observing the results from earlier designs and thereafter adjusting the factors accordingly. The pure mathematical model is supposed to represent the exact reality whereas the semi-probabilistic methods take basis in well defined approximations. In Eurocode, the safety factors are mainly derived by empirical methods and experience, and in some cases further development has been done using mathematical models.

The methods presented in Annex C of EN-1990 (2005) are only informative, meaning that the designer is not bound to use any of them but recommended to do so. This, in turn, means that the designer is free to choose any of the three methods. However, the most common choice is to use recommended partial factors given by Eurocode. One of the major reasons for this is most likely convenience. The probabilistic methods are complicated and cumbersome to perform and the norms already provide well substantiated values. Another reason is that statistical data is missing and therefore making it impossible to perform any probabilistic evaluations.

fib (2013) provides an approach to calculate the partial safety factors probabilistically. The method requires that statistical data is available so that the average value, μ and coefficient of variation, δ can be calculated. Using, e.g. the case with material partial safety factors the equations are stated as

$$\gamma_m = \frac{R_k}{R_d} = \frac{\mu_R(1 - k\delta_R)}{1 - \alpha_R \beta \delta_R} \tag{3.3}$$

if a normal distribution is used and

$$\gamma_m = \frac{R_k}{R_d} = \frac{exp(\mu_{lnR} - k\delta_{lnR})}{exp(\mu_{lnR} - \alpha_R \beta \delta_{lnR})} = exp(-k\delta_{lnR} + \alpha_R \beta \delta_{lnR}) \tag{3.4}$$

if a log-normal distribution is used, where

α_R is a sensitivity factor,
β is a factor dependant on the consequences of an eventual failure,
δ_R is a coefficient of variation or relative standard deviation.

The β-values can be found EN-1990 (2005) and represent a safety index that is dependant on the life span and safety class of the building. The processof deriving the partial factors for loads is more complicated since the statistical data is often lacking. In Table 3.2 the partial factors used in the case studies are displayed. These are limited to permanent and main variable actions and thus excluding prestress forces and other variable actions.

Table 3.2: Partial load factors used in Eurocode and IEC.

	Eurocode		IEC	
Action	Unfavourable	Favourable	Unfavourable	Favourable
Permanent, γ_G	1.35	1.0	1.05-1.1	0.9-0.95
Leading variable action, γ_Q	1.5	Neglected	1.5	Usually neglected

3.3 Theory behind wind-loads

In order to understand how the loads for the design of wind towers are calculated, an introduction to the different characteristics of wind loads is needed. In order to do this two different books are used as reference, firstly a book by Hau (2013) and secondly another book by Gasch and Twele (2012).

The wind loads can be divided into steady and unsteady loads and the latter can be divided into cyclic and non-cyclic loads. Or in short form:

- steady loads
- unsteady cyclic loads, e.g. wind shear on the tower

- unsteady non-cyclic loads, e.g. action from turbulence.

The resulting stress from each of these loads as well as the sources for them will be presented briefly in the following sections.

3.3.1 Steady loads

The steady loads originate from gravity, centrifugal and steady wind where gravity acts as one of the major limiting forces for the size of the WPP according to Hau (2013). For the design of the foundations, the gravity has a positive effect in resisting the overturning moment, limiting the eccentricity of the resulting force, see Section 4.1. The weight of the tower in the reference case is also significantly smaller than the weight of the foundation itself. Centrifugal forces have little impact on the rotors of a WPP due to the low rotational speed (Hau, 2013).

Of more interest is the effect of a steady, uniform wind acting on the structure. According to Hau (2013) this is not a realistic load model but is still relevant to check the mean loads acting on the tower over a longer duration of time (Hau, 2013). An example of how the wind varies can be seen in Figure 3.7. Gasch and Twele (2012) states that the mean wind speed is also important as the energy generated is proportional to the cube of the wind. This information is used when designing the layout of the WPP parks. The final important thing to note regarding the mean wind speed is that a strong correlation exists between the mean wind speed over a certain time and the maximum wind speed during that interval (Gasch and Twele, 2012). As will be explained later this is used to calculate the maximum wind speed during the life-time of the tower.

3.3.2 Unsteady cyclic loads on the tower

Cyclic loads are loads that occur with a certain frequency that will result in alternating forces. The simplest way to explain this with regard to WPP is the effect of gravity acting on the rotors. As they rotate 180° the forces will change so the side that was in tension will be in compression and vice versa. The frequency of this is proportionate to the rotational speed of the rotors, normally denoted Ω [rad s^{-1}].

The wind also contributes to cyclic loads which are dependent on both the nature of the wind and the operation of the WPP. The first of these effects originates from wind shear which is caused by the uneven wind load on the tower. Due to the influence from the ground the wind will increase with the height until it reaches stable condition, called geostrophic wind. The region below which is influenced by the ground is called the atmospheric boundary layer and varies in height between 100 and 2000 m (Gasch and Twele, 2012). Due to the uneven loading the load on the tower will vary as the rotor blades rotate and create a cyclic load. How large this effect is varies and Hau (2013) cites four phenomena that influence the shape of the wind profile, and therefore the wind shear. These are:

Terrain inclination a surrounding slope can disrupt the flow at the tower severely.

Obstacles if the tower is placed close to an obstacle the wind velocity in the bottom will decrease.

Distance between wind turbines a tower causes turbulence in the wind flow which can have negative effect on the following towers. In worst case a horizontal gradient is caused as well.

Atmospheric stability a changing temperature can cause extra wind flow in certain direction.

The three first can be influenced by the design of the park. This effect is deemed to be more severe for the design of rotor blades than it is for the foundation.

Another source of cyclic loads is oblique wind flow which can be both vertical and horizontal, normally called cross winds. This happens when the direction of the wind flow is at an angle to the rotor and creates a bending or torsional moment in the tower. For the horizontal cross wind an important parameter is the *yaw angle* which describes the angle between the wind and the normal to the hub. This angle is not constant and can vary significantly over time due to turbulence. The rotor adjusts itself after the wind to prevent too large effects from this.

The final source of cyclic loads that will be introduced is produced from the effect that the tower itself has on the wind. When the wind passes the tower, the flow is separated from the tower resulting in a wake on the rear side which will create turbulence and cause stresses on the tower. The effect is dependent on two major factors, the first being if the rotor is upwind or downwind. The second is the Reynolds number (Re) for the flow around the tower which will result in different phenomena (Hau, 2013). For more information about this see Section 6.3.5 in Hau (2013).

3.3.3 Unsteady non-cyclic loads

The final type of loads that influence the tower and foundation, and the most difficult to handle, is the turbulence. These loads are non-cyclic and cannot be predicted accurately over time. One illustration of turbulence can be seen in Figure 3.7. The changing loads will cause a lot of stress on the tower and be one of the major factors for design, especially for the rotors, since they are the main contributors to the fatigue loads.

Due to the large uncertainties regarding turbulence effect it is handled with a statistical approach which is outside the scope of this study. One of the main parameters of interest for calculating loads however is the turbulence intensity I_v which is defined in Gasch and Twele (2012) as the ratio between the standard deviation σ_v and the mean velocity $\bar{v}$, or in mathematical terms:

$$I_v = \frac{\sigma_v}{\bar{v}}. \tag{3.5}$$

The value for the turbulence intensity varies along the line of 12 to 18%. It can also be used to estimate the speed of gusts during a certain period due to the previously mentioned correlation between mean and maximum speed. The intensity is influenced by parameters such as obstacles, terrain inclination and surface roughness (Gasch and Twele, 2012).

For a visual summary of the loads presented in this section reference is made to (Hau, 2013, Figure 6.1) or (Gasch and Twele, 2012, Table 8.1).

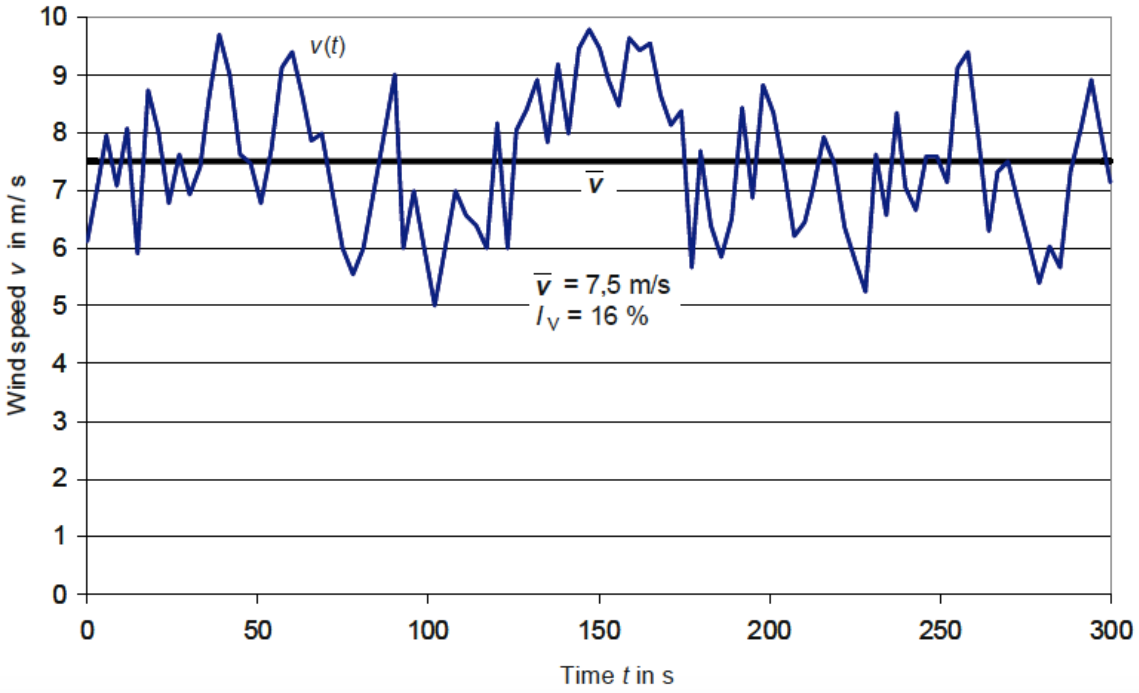

Figure 3.7: The variation of wind speed over time due to turbulence. Source: Hau (2013)

3.4 Modelling of windloads according to IEC 61400

In IEC (2005) a total number of 22 design load cases (DLC) are defined with varying wind intensity. All of these will not be discussed in this study, focusing on some relevant cases. The load cases are divided between Ultimate (U) and Fatigue (F) depending on which analysis they are used for. The main parameters used for calculating loads are presented in Table 2.1 and the usage of them will be introduced in the following sections. On some occasions reference will be made to relevant theory. Before going into the design loads the normal wind conditions will be presented since they are used for calculating both U and F loads and provide a base for further models.

Normal wind conditions

The wind profile over the tower is based on the Hermann Power Law (Gasch and Twele (2012)) and states that

$$V(z) = V_{hub}\left(\frac{z}{z_{hub}}\right)^{\alpha} \tag{3.6}$$

where

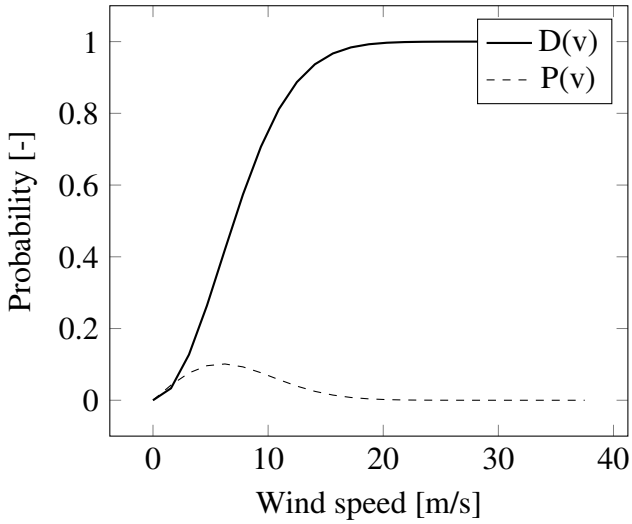

Figure 3.8: The distribution function for normal wind condition using $V_{ref} = 37.5\,\mathrm{m/s}$.

α is the power law exponent,
V_{hub} is the wind speed at the tower hub,
z is the height at which the speed is calculated,
z_{hub} is the height of the hub.

The power law exponent α is given a value of 0.2 in IEC (2005). In Gasch and Twele (2012) the given value is 0.14. However, it is noted that the exponent varies with height and surrounding conditions. Therefore a measured exponent is only valid for the individual site (Gasch and Twele, 2012). The wind speed at hub height is predicted over time using a statistical distribution called Rayleigh distribution. This is used to predict the mean wind speed over a 10-min interval and both the distribution and the probability functions can be seen in Figure 3.8. In IEC (2005) the distribution function is stated as

$$D_R(V_{hub}) = 1 - e^{-\pi\left(V_{hub}/2V_{ave}\right)^2} \tag{3.7}$$

where $V_{ave} = 0.2V_{ref}$, with V_{ref} taken from Table 2.1. As can be seen in the figure the wind speed with the highest probability is close to the average wind speed, in this case $7.5\,\mathrm{m/s}$.

The final part in modelling the normal wind conditions is the modelling of turbulence for normal conditions, the normal turbulence model (NTM). This is used by calculating a representative value for the standard deviation σ_1 which depends on the wind speed at the hub according to the following formula

$$\sigma_1 = I_{ref}\left(0.75V_{hub} + b\right); b = 5.6\,\mathrm{m/s} \tag{3.8}$$

where

I_{ref} is reference value for turbulence intensity from Table 2.1

3.4.1 Loads concerning failure of the structure

For design in ULS, loads from both normal and extreme wind conditions are used. In this section some of the extreme conditions will be described in order to understand their implications.

Extreme wind speed model (EWM)

This model consists of two different models, one steady model and one turbulent model. Firstly, the steady wind model is similar to Equation (3.6) where the extreme wind speed with a recurrence period of 50 years, V_{e50}, is modelled as

$$V_{e50} = 1,4V_{ref}\left(\frac{z}{z_{hub}}\right)^{0,11}. \tag{3.9}$$

It is related to the annual extreme wind speed according to $V_{e1}(z) = 0.8V_{e50}(z)$. The similarities with Equation (3.6) are noticeable with only the exponent and maximum value changing between them. The difference can be seen in Figure 3.10. These models are combined with the possibility of a yaw misalignment of $\pm 15°$ which causes extra stress in the structure.

The turbulent model is similar and is modelled using the same formula as in Equation (3.9) without the 1,4 factor. For this model the standard deviation is determined using

$$\sigma_1 = 0,11V_{hub}. \tag{3.10}$$

Extreme turbulence model (ETM)

This model uses the normal wind profile from Equation (3.6) with the standard deviation calculated using

$$\sigma_1 = cI_{ref}\left(0,072\left(\frac{V_{ave}}{c}+3\right)\left(\frac{V_{hub}}{c}-4\right)+10\right); c = 2\,\mathrm{m/s}. \tag{3.11}$$

The standard deviation for both the ETM and the NTM presented in Equation (3.8) for different V_{hub} can be seen in Figure 3.9, using $V_{ref} = 37.5\,\mathrm{m/s}$ and $I_{ref} = 18\%$. It can be seen that the difference between the two is highest at low wind speeds and is equal for V_{ref}.

Extreme operation gust (EOG)

The extreme gust is the highest wind speed that will occur during operation. The magnitude of the gust at hub height is calculated using

$$V_{gust} = Min\left(1,35(V_{e1}-V_{hub}); 3,3\left(\frac{\sigma_1}{1+0,1\frac{D}{\Lambda_1}}\right)\right). \tag{3.12}$$

where

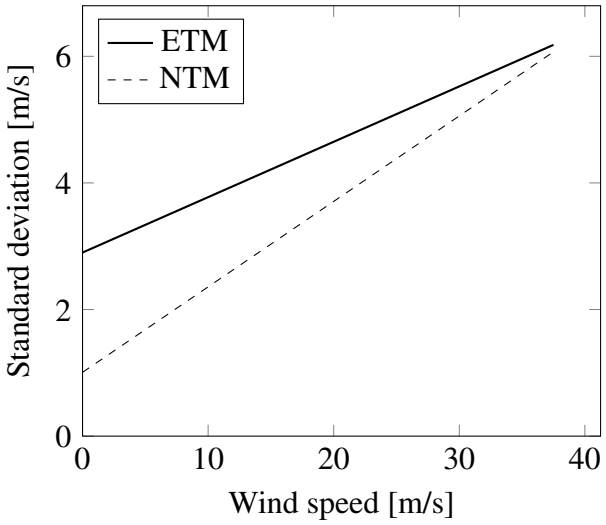

Figure 3.9: The standard deviation between 0 m/s and 37.5 m/s for ETM and NTM.

V_{e1} is calculated according to Section 3.4.1,
σ_1 is calculated using Equation (3.8),
D is the rotor diameter,
Λ_1 is a turbulence scale parameter calculated from Equation (3.13).

$$\Lambda_1 = \begin{cases} 0,7z & z \leqslant 60\,\text{m} \\ 42\,\text{m} & z \geqslant 60\,\text{m} \end{cases} \tag{3.13}$$

With the value for V_{gust} the wind model can be calculated using $V(z)$ from Equation (3.6) and combining it with a time-dependent function for the effect of the gust according to

$$V(z,t) = \left\{ V(z) - 0,37V_{gust}sin(3\pi t/T)(1 - cos(2\pi t/T)) \quad \text{for } 0 \leqslant t \leqslant T \right. \tag{3.14}$$

where T is a defined time period of 10.5 s. For other times the wind is modelled using Equation (3.6). It should be noted that the value for the gust is constant over the whole tower, i.e. independent of the z-coordinate. It can be seen as moving the entire wind profile at the same time which can be seen in Figure 3.10.

Extreme wind shear (EWS)

The wind shear is modelled for both horizontal and vertical effect as a transient effect dependent on respective coordinate. The vertical shear is defined in time by

$$V(z,t) = \begin{cases} V_{hub}\left(\frac{z}{z_{hub}}\right)^{\alpha} \pm \left(\frac{z-z_{hub}}{D}\right)\left(2,5 + 0,2\beta\sigma_1\left(\frac{D}{\Lambda_1}\right)^{1/4}\right)(1 - cos(2\pi t/T)) & \text{for } 0 \leqslant t \leqslant T \\ V_{hub}\left(\frac{z}{z_{hub}}\right)^{\alpha} & \text{otherwise} \end{cases} \tag{3.15}$$

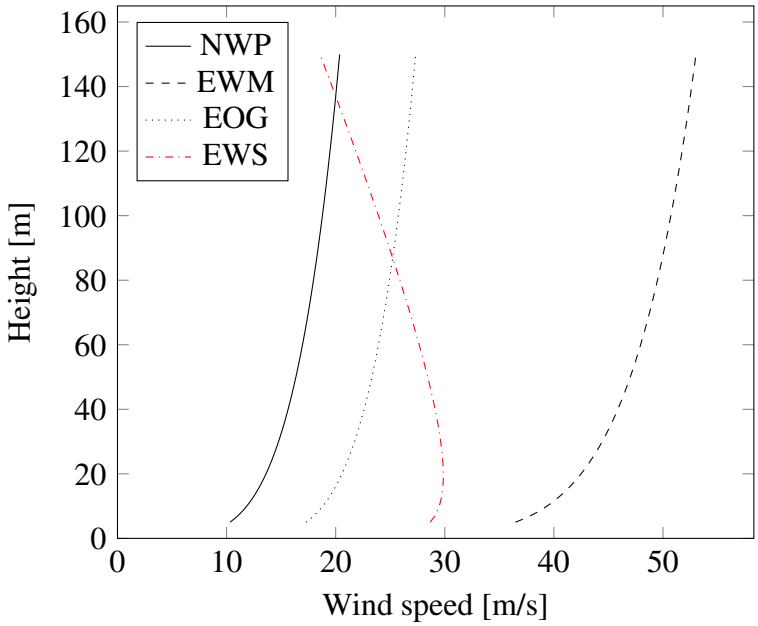

Figure 3.10: Different wind speed profiles from IEC

The horizontal shear is modelled as dependent of both y- and z-coordinates where y denotes the distance between the center of the tower and the investigated point measured perpendicular to the wind direction.

$$V(z,t) = \left\{ V_{hub}\left(\frac{z}{z_{hub}}\right)^{\alpha} \pm \left(\frac{y}{D}\right)\left(2,5+0,2\beta\sigma_1\left(\frac{D}{\Lambda_1}\right)^{1/4}\right)(1-cos(2\pi t/T)) \quad \text{for } 0 \leqslant t \leqslant T \right. \tag{3.16}$$

$\alpha = 0.2; \quad \beta = 6.4; \quad T = 12\,\text{s}$ for both vertical and horizontal shear. As was the case for EOG the wind profile for all other times, t, is defined using Equation (3.6).

The two different wind shears should not be applied simultaneously. The vertical wind shear for $t = 6\,\text{s}$ is shown in Figure 3.10 where it can be seen that the wind speed is at maximum approximately at the height 10 meters.

Extreme direction change (EDC)

The final extreme condition that will be introduced is extreme direction change which happens when the wind changes direction rapidly and the tower experiences extra stresses due to it. The angle, θ_e is calculated from

$$\theta_e = \pm 4 \arctan\left(\frac{\sigma_1}{V_{hub}\left(1+0,1\left(\frac{D}{\Lambda_1}\right)\right)}\right) \tag{3.17}$$

and is limited to $\pm 180°$. The change in direction has a duration of $T = 6\,\text{s}$ and is modelled over time with the following formula

$$V(z,t) = \begin{cases} 0° & \text{for } t < 0 \\ \pm 0,5\theta_e(1 - \cos(\pi t/T)) & \text{for } 0 \leqslant t \leqslant T \\ \theta_e a & \text{for } t > T \end{cases} \tag{3.18}$$

where the sign is chosen to give the maximum effect on the structure.

Design load cases

All of these different loads and models that are presented in previous sections are used for the design of the tower and supporting structures. There are a total of 17 different DLCs concerning ULS, for which a number of different wind speeds should be checked. The presentation of these are deemed to be superfluous and reference is made to Table 2 (IEC, 2005). Some of the important parameters that are of interest for the next section and define the wind speed at hub height are the following:

V_r is the rated wind speed. The minimum speed at which the towers rated power is achieved.
V_{out} is the highest wind speed that the tower is designed to produce power at.
V_{in} is the lowest wind speed that the tower is designed to produce power at.

3.4.2 Loads concerning fatigue

The loads used for the design with regard to fatigue are presented in a Table 2 in IEC (2005) and consists mainly of the load combinations for the normal conditions. A total of five different conditions are used for calculating fatigue loads:

DLC 1.2 Power production. Modelled using NTM for wind speeds of $V_{in} \leqslant V_{hub} \leqslant V_{out}$

DLC 2.4 Power production plus the occurence of fault. Modelled using NTM for $V_{in} \leqslant V_{hub} \leqslant V_{out}$

DLC 3.1 Start up. Modelled using NWP for $V_{in} \leqslant V_{hub} \leqslant V_{out}$

DLC 4.1 Normal shut down. Modelled using NWP for $V_{in} \leqslant V_{hub} \leqslant V_{out}$

DLC 6.4 Parked. Modelled using NWP for $V_{hub} < 0.7V_{ref}$

The number of each case refers to the DLC from IEC (2005). The different wind models are defined in the beginning of this section.

As can be seen in these different cases they represent the everyday life of the tower. The extreme cases presented in Section 3.4.1 are so infrequent that they are deemed uninteresting for the fatigue life of the structure.

From Figure 3.7 it can be seen that the wind speed and corresponding fatigue loads on the wind tower are not simple to interpret. Since the wind has stochastic variation there are different methods to transform these into loads that can be used in engineering situations. How this is done will be treated in Section 3.5.2

3.5 Additional aspects regarding wind loads

With the different models presented previously the loads acting on the structure can be calculated. Three different aspects of this will be treated briefly, namely:

- Design codes used for modelling
- Transforming time-loads from 20 to 50 years
- Design according to Eurocode and Fluid mechanics

3.5.1 Design codes used for modelling

The process of attaining the load effects is complicated and there are a number of different commercial design codes available of varying scope and detail. According to Ahlström (2005) there are three major ways to model these load effects in accordance with the structural dynamics condition described by IEC (2005). These are:

- Multiple Rigid Bodies (MRB)
- Assumed-Modes method
- Finite Element Method (FEM)

For each of these methods there are a number of design codes to be used. A more exact presentation of this can be found in Ahlström (2005). Halici and Mutingi (2016) make a study of three different models, namely FAST, ASHES and FOCUS6. The former consists of a modal analysis and the two latter of a FEM analysis. For more information about the specifics and the limitations of respective software reference is made to that study. One important aspect not introduced previously will however be discussed.

In order to model turbulence, IEC (2005) gives two different methods. Firstly, the Mann uniform shear turbulence model and, secondly, the Kaimal spectral model. The former consists of a large number of formulas and is too extensive to be described within the scope of this study. The latter is calculated from

$$f S_k(f) = \sigma_k^2 \frac{4 f L_k / V_{hub}}{(1 + 6 f L_k / V_{hub})^{5/3}} \tag{3.19}$$

where

f	is the frequency in hertz,
k	is the index indicating the component,
S_k	is the single-sided velocity component spectrum,
L_k	is the integral scale parameter,
σ_k	is the standard deviation of the wind,
V_{hub}	is the wind speed at hub height.

This is in turned based on the standard deviation and scale parameters defined in Equation (3.10) and Equation (3.13). For a more detailed description of the procedure see IEC (2005). One important thing to note is that several simplifications have been made in the model from IEC. This can lead to an overestimation of loads in some cases, e.g. as stated by Holtslag, Bierbooms, and van Bussel (2016), and in other cases the fatigue behaviour can be underestimated mainly because of the absence of surface roughness from the calculations (Holtslag et al., 2016). The surface roughness will be discussed in more detail in Section 3.5.3.

3.5.2 20 year loads to 50 year loads

One of the major focuses of this study was to investigate the effect of different life spans for the foundation. This is of main concern when it comes to the fatigue life but initially some comments will be made regarding the ULS.

As mentioned in Section 3.4.1 the load is calculated for a wind speed with a 50-year recurrence. Therefore, the ultimate load is already calculated for a 50-year life span despite the fact that most wind towers have a service life of 20 or 25 years. EN-1990 (2005) states that the life span of common structures is set to 50 years. Other types of structures like agricultural buildings and changeable parts of structures may have shorter life span. It is however hard to argue that a WPP foundation can be classified as a agricultural structure and therefore the life span should be set to 50 years. This influence the loads and certain concrete parameters, most notably creep and concrete cover.

The fatigue loads are often provided by the designer of the tower to the company designing the foundation. How well defined these loads are varies and can be problematic to use in combination with the partial safety factors. In order to provide a base for further discussion the methods used for representing loads in the reference project will be presented briefly. The two methods are the Rainflow matrix and Markov matrix which represents the same load in two different ways.

The most common way to calculate the loads is discussed by Ragan and Manuel (2007) from the University of Texas. The loads are produced from a time series similar to the one that can be seen in Figure 3.7. In order to provide the fatigue loads the Rainflow Cycle-Counting method is used (Ragan and Manuel, 2007). This process is described by Sutherland (1999) where the first step in this process is to identify local maxima and minima, often referred to as peaks and valleys, which are used to calculate ranges. For large batches of data this is done by computers using algorithms that often include range filters which remove the low variations in order to focus on the load ranges that cause damage. The next step is post-processing which takes these different ranges and put them into an appropriate cycle-count bin which has limits for ranges. The different load ranges in the time data is summed up within these bins and provide the fatigue loads of interest. The width of these bins can influence the fatigue loads in a significant manner. The final result is a Rainflow matrix which consists of stress ranges with associated number of cycles. Therefore the Rainflow matrix can be seen as a 1D representation of the load spectra (Sutherland, 1999). An example of a stress range matrix can be seen in Figure 3.12.

The Markov matrix is also described by Sutherland (1999). The main difference from the previous is that in addition to the ranges and cycles the mean level is also sampled. This is the preferred method by Sutherland since it also represents the mean stress levels in the structure. The Markov matrix is a 2D

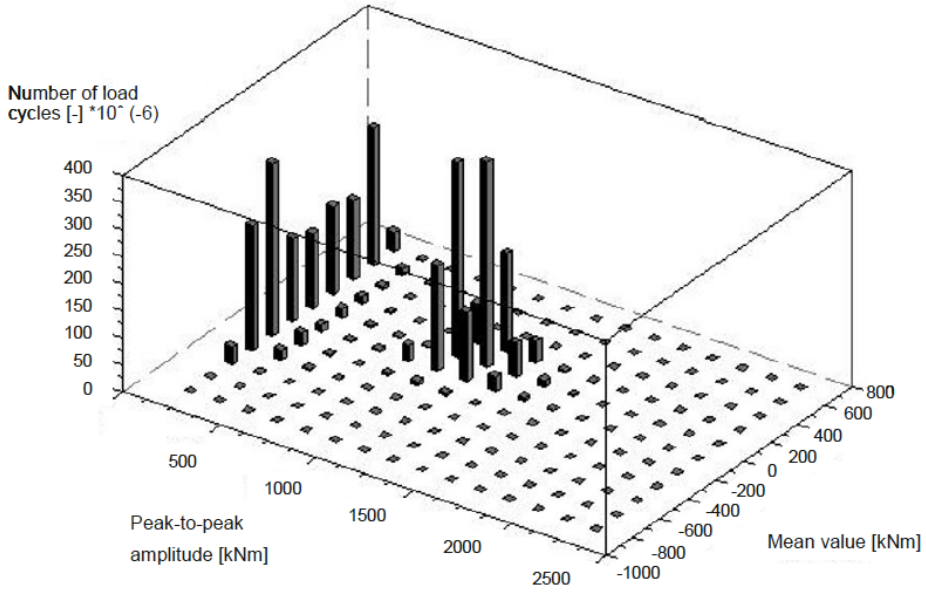

Figure 3.11: Example of a 2D representation of fatigue loads. Source: Gasch and Twele (2012)

representation of the loads as seen in Figure 3.11. Due to the difference between Rainflow and Markov representation specialized algorithms have to be used for each method. (Sutherland, 1999).

Since there is no realistic way to simulate the entire life span of a WPP there is always the problem of how loads can be represented in an accurate way. This problem is discussed by Sutherland (1999) where it is stated that as long as the values used for establishing the loads are representative, the amount of data does not increase for longer time spans. The same amount is needed for 30 years as for 60 years. The major problem then consists of defining a representative data, or in other words what is the minimum data required. This problem is also discussed in a report by Moriarty, Holley, and Butterfield (2004) where the effect of the extreme values on the loads are studied. The loads are calculated from 10-minute simulations for a certain wind condition. Moriarty et al. (2004) state that around 30 simulations is ideal for each loading condition whilst Sutherland (1999) gives a minimum value of around 19 but recommends more simulations depending on the sequencing of the samples. The number of cycles that each loading condition provides is then calculated by using a density function, e.g. the one presented in Equation (3.7), from which the extrapolated number of cycles is obtained (Sutherland, 1999). In IEC (2005) a minimum number of 6 simulations per mean hub wind speed is required, with the exception of three DLCs where 12 simulations are required. This number seems low but in their study Moriarty et al. (2004) used 9 simulations for each load bin and get satisfactory results (Moriarty et al., 2004). The conclusion drawn from this study is that due to the probabilistic way of acquiring the 20-year loads it is a sufficient to use a simple scaling of 2.5 to transform it to 50 years. The probable distribution of wind conditions is already accounted for in the original loads and it is seen as only increasing the amplitude of the distribution by a factor of 2.5.

The whole process of acquiring fatigue loads is summed visually using Figure 3.12 reprinted from Berglind and Wisniewski (2014). In this figure the load spectra is represented with a Rainflow matrix. It is deemed important to understand the process of acquiring these loads in order to better understand the

behaviour of the tower and to improve the cooperation with the tower manufacturer. The final part of the process, the fatigue life, and how this is calculated using existing norms will be the focus of Section 3.7 and Section 3.8.

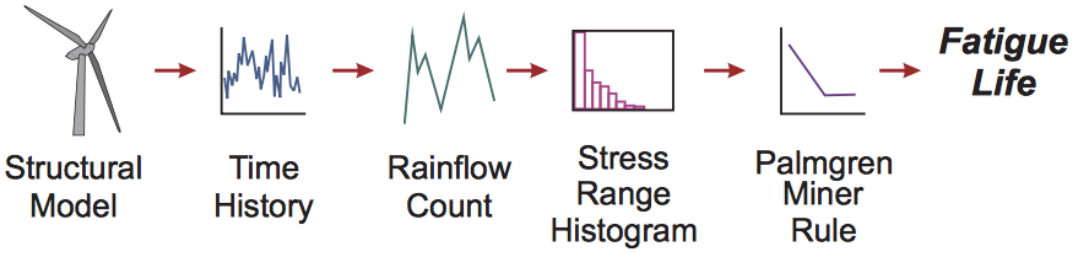

Figure 3.12: Visualization of fatigue load process. Source: Berglind and Wisniewski (2014)

3.5.3 Simplified wind calculations

When designing structures with regard to wind according to Eurocode the loads are normally determined using EN-1991-1-4 (2005). In order to get a more thorough grip on the magnitude of the load, this norm is used to calculate a reference load which is compared to the extreme load from Table 2.3. The load case most similar to the static case from Eurocode is DLC 6.1 which is the parked condition combined with EWM. This load case is very likely to occur during the service life since most towers stand still when the wind speed exceeds the cut-out wind speed V_{out}. It is also stated by Gasch and Twele (2012) that it is one of the two load cases that is likely to cause extreme stresses, the other being DLC 1.3 representing an extreme operating gust with an extreme direction change.

When designing according to Eurocode a different wind model is used, based on the boundary layer physics introduced by Prandtl (Gasch and Twele, 2012). The wind profile is calculated by combining equations (4.3)-(4.5) in EN-1991-1-4 (2005) resulting in

$$V(z) = 0.19 \ln\left(\frac{z_0}{z_{0,II}}\right)^{0.07} \ln\left(\frac{z}{z_0}\right) V_b \tag{3.20}$$

where

z_0 is the surface roughness dependent on the terrain,
$z_{0.II}$ is the surface roughness for terrain type II,
V_b is the characteristic wind speed according to equation 4.1 in EN-1991-1-4 (2005).

In order to calculate forces on a structure the following expressions are used to calculate forces at a reference height z_e. These are taken from equations (4.7) and (5.1) in EN-1991-1-4 (2005)

$$w_e = q_p(z) c_{Pe} = [1 + I_v(z)] \frac{1}{2} \rho V_m^2(z) c_{Pe} \tag{3.21}$$

$$I_v(z) = \frac{1}{\ln(z/z_0)}$$

where

z is the hub height,
c_{pe} is a shape factor dependent on the area studied,
w_e is the distributed force on the tower kN/m,
q_p is the characteristic distributed force kN/m,
I_v is the turbulence factor from EN-1991-1-4 (2005),
V_m is the mean wind speed at the highest point according to Equation (3.20).

There is no data within the norm specifically for wind towers but there are guidelines for circular cylinders which are used as an approximation. The width of the tower is assumed to vary linearly between 6 m at the bottom and 3 m at the top since there is no exact data. The pressure is assumed to be uniform over the whole height which is a simplification compared to section 7.2.2 in EN-1991-1-4 (2005). This is motivated by the fact that the width is significantly smaller than the height of the tower. The drag force (F_D) on the airfoil is calculated according to Gasch and Twele (2012), which states

$$F_D = c_d \frac{\rho}{2} V_{hub}^2 c L \tag{3.22}$$

where

c_d is a drag coefficient dependent on the attack angle,
ρ is the density of the air, typically 1.25 kg/m^3,
V is the mean wind speed over the rotor blade,
c is the cord length, the mean width of the rotor blade,
L is the length of the rotor blade.

The drag coefficient is determined from Figure 5-7 in Gasch and Twele (2012).

3.6 Theory regarding fatigue

The context in which the WPP is placed implies a very high number of loading cycles. During the whole life span the WPP is constantly subjected to the wind and in production to cyclic loads from the rotor blades. This can lead to fatigue problems in the structure and thus the ultimate limit state is not the only aspect that needs to be considered in the design process.

According to Thun (2006) fatigue is commonly divided into different categories, low-cycle and high-cycle fatigue, with the limit between the two at roughly 10^3 cycles. In recent years the concept of super-high cycle fatigue has been lifted for structures subjected to more than 10^7 cycles. This is however a quite uncommon situation (Thun, 2006). In Figure 3.13 the cycle spectra for different fatigue categories can be seen together with structures typically exposed to these kinds of loads. According to this WPPs falls within the high-cycle fatigue category. However, according to Gasch and Twele (2012) a WPP is subjected to more than 10^9 cycles during a 20 year life span (Gasch and Twele, 2012). This is also supported by Hau (2013) who places the number of cycles for a wind turbine between 10^7 and 10^8 (Hau, 2013). Therefore the foundation should probably be seen as a super-high cycle structure but there are no methods for accounting for that many cycles today.

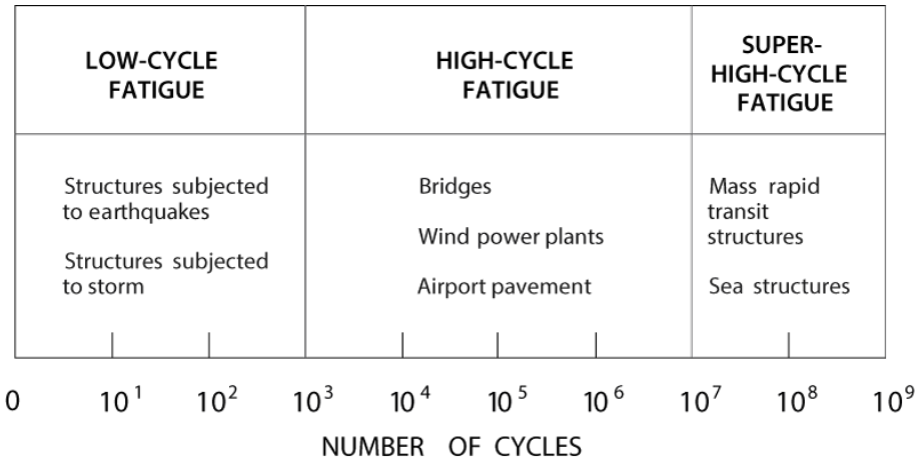

Figure 3.13: Cycle spectra for different classifications of fatigue life. Source: `http://www.structuremag.org/?p=10735`

A failure of a structure caused by a load lower than the design ultimate load is characterized as a fatigue failure. The failure is caused by a continuous decomposition of the material due to a high number of cycles. The progress of the decomposition is dependant on factors like the mean stress level, the amount of cycles and the stress range, which is the difference between maximum and minimum stress (Heffernan, 1997).

It is also important to note that the variation in results for similar fatigue analyses can vary significantly. In his report, Sutherland (1999) refers to a study by Veers of computed damage at failure which varies between 0.79 and 1.53, from which he concludes that a difference of factor 2 between damage prediction and life span is to be expected (Sutherland, 1999). This further points towards the difficulties of predicting fatigue resistance.

3.6.1 Fatigue in reinforcement

In a report written by Al-Emrani and Åkesson (2013), used as course literature at Chalmers University of Technology, the principles of fatigue in steel are introduced. They state that for most cases the fatigue cracks initiate in regions with high local stresses and often in combination with local defects, such as defects in the lattice structure of the metallic crystal. Repetitive loading accumulates these defects which induces the formation of slip bands that are susceptible to cracking. This is the first stage of the fatigue life, normally called *crack initiation*, and is concentrated to a few grains in the metal, with damage driven by shear stresses. In the second stage, *crack propagation*, some of the cracks have joined and formed larger cracks extending over several grains. These cracks do, contrary to the micro cracks, develop perpendicular to the main stress direction. These two stages can be seen in Figure 3.14.

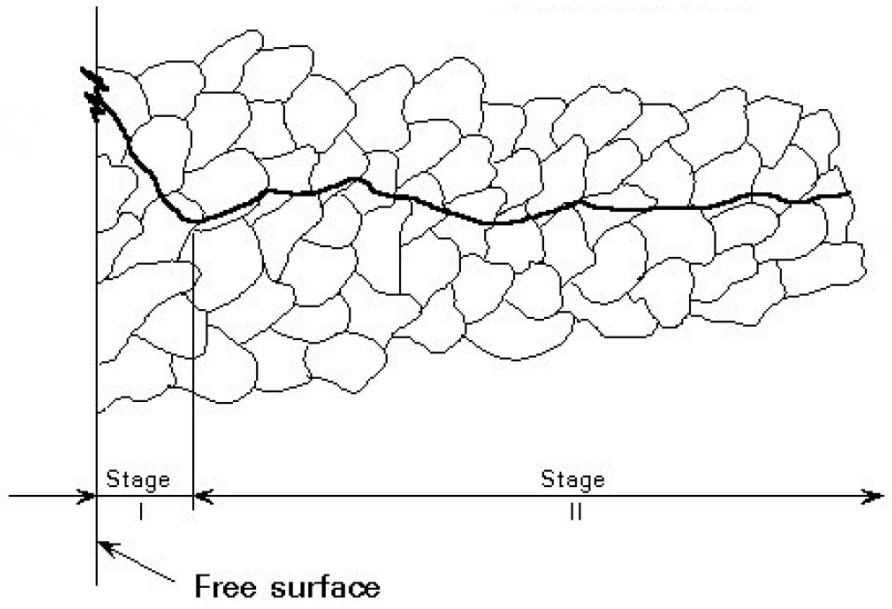

Figure 3.14: The crack development in a steel lattice. Source: Al-Emrani and Åkesson (2013)

There are a variety of factors affecting the fatigue life of steel. A higher static capacity, e.g., renders a more fatigue resistant steel. However, this is only valid to a certain point according to Heffernan (1997). For high strength steel this rule does not apply and higher steel classes do not increase the fatigue life significantly. Another aspect affecting the fatigue life are the geometry of the bar where plain bars have greater resistance than ribbed bars, with a difference of about 18%. In a similar way thicker bars have shorter fatigue life than thin bars (Heffernan, 1997).

A common way of evaluating fatigue, explained by Al-Emrani and Åkesson (2013), is the use of S-N curves which correlate the constant nominal stress range (S) to the resisting number of cycles (N). The curve is usually logarithmic and consists of two or three straight lines connected as shown in Figure 3.15. S-N curves are obtained by testing certain details until failure and noting the number of cycles. Different types of details, for example a plate without hole and a plate with a hole, will have different S-N curves. Thus every detail that is to be evaluated with the method requires an experimentally decided curve (Al-Emrani and Åkesson, 2013).

In order to use the curve, one has to know the load history, i.e. which stresses that have been applied and how many times. If this is known, the damage on the structure can be calculated which gives the remaining fatigue life. To assess the damage for a stress spectrum consisting of varying loads, Miner's rule can be used. It states that the damage (d) caused by a number of cycles with the same stress level is equal to the number of cycles (n) divided by the total amount of cycles required for failure (N) as shown in Equation (3.23). In reality the load intensity is quite random and therefore Miner's rule cannot be applied directly (Al-Emrani and Åkesson, 2013).

A way of considering a varying load history is by using Rainflow counting, a process discussed in Section 3.5.2 together with Rainflow or Markov matrix which is used to present the loads. The method

aims to convert a load spectrum into a relatively small number of load cycles with certain mean and range values. When this is done Miner's rule can be used to determine the resulting damage.

$$\sum_{i=1}^{k} \frac{n_i}{N_i} = d \tag{3.23}$$

3.6.2 Fatigue in concrete

According to Heffernan (1997) it is concluded that concrete has reduced strength for repetitive loading. The reason behind this phenomenon is micro cracks that are formed because of shrinkage occurring during the hardening process of the concrete. These cracks constitute a natural process in the concrete and cannot be prevented. The micro cracks propagate when the concrete member is subjected to loading and, if the number of load cycles is high enough, this will eventually lead to failure. The fatigue life of the concrete is not solely dependant on the number load cycles but also the humidity in the ambient air and what rate the load is applied. Also, there is a strong correlation between the static strength of the concrete and its fatigue resistance where higher strength concrete renders longer fatigue life (Heffernan, 1997).

3.6.3 Fatigue in reinforced concrete

The fatigue strength of composite members like reinforced concrete cannot be assessed solely on the fatigue strength of the individual components. This is because the individual components work together by interaction in order to form the member that resists the load. The strength of the member is thus highly dependant on the interaction and therefore this has to be included when assessing fatigue.

According to Heffernan (1997) the stress in the steel is higher near cracks in the concrete. This implies that these sections are more susceptible to fatigue damage and where a fatigue failure is expected. The fatigue life of a reinforced concrete member is mainly dependant on the fatigue life of the steel. On the other hand the serviceability is rather correlated to the fatigue characteristics of the concrete (Heffernan, 1997).

3.7 Norms concerning fatigue in reinforcement

As stated in previous sections this study will present the norms regarding fatigue according to different norms, both with regard to the reinforcement and the concrete. There are several different aspects to take into account for the different calculations and these will be discussed in connection with the corresponding case.

The design is made with S-N curves which has been created through extensive testing. One important aspect normally considered when designing steel with regard to fatigue is the fatigue limit. Beneath this stress level there can be an infinite amount of cycles (Al-Emrani and Åkesson, 2013). This is used when designing steel elements according to EN-1993-1-9 (2005). However, as can be seen in Figure 3.15

this limit is not present in the S-N curves for reinforcement, instead represented by limiting values in simplified approaches.

3.7.1 Design according to Eurocode

The rules for design with regard to fatigue can be found in section 6.8 in EN 1992-1-1 and concerns both reinforcement and concrete. The rules for concrete will be presented in Section 3.8. Another important thing to have in mind is that since there is no prestressing steel in the direction of the regular reinforcement the formulas that concern prestressing is omitted. For studies of this reference is made to EN-1992-1-1 (2005).

When calculating the effect on the structure from the cyclic load, the load combination presented in equation 6.69 in EN-1992-1-1 (2005) is used. This load combination is used for both concrete and reinforcement:

$$\sum_{i=1} G_{k,i} + \psi_{1,1} Q_{k,1} + \sum_{j=1} \psi_{k,j} Q_{k,j} + Q_{fat} \tag{3.24}$$

where

$G_{k,i}$ is the characteristic loads from permanent loads,
Q_{fat} is the relevant cyclic fatigue load presented by the designer of the WPP,
$Q_{k,i}$ are characteristic variable loads that the tower foundation is subjected to.

The verification of the reinforcement is made using the S-N curves presented in Figure 3.15 which shows the general form of the curve for reinforcement taken from EN-1992-1-1 (2005). The different parameters presented in the figure are:

$\Delta\sigma_{Rsk}$ Resisting stress range
N* Reference number of cycles

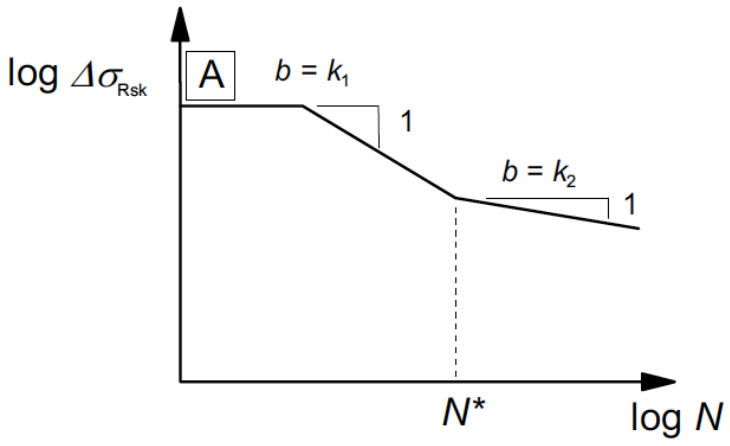

Figure 3.15: S-N curve from EN 1992-1-1

The values used differ between different reinforcements and are presented in Table 3.3. These values are again taken from EN-1992-1-1 (2005) and are valid in Sweden since no national choice has been made.

Table 3.3: Parameters for design of reinforcement in Eurocode

Type of reinforcement		stress exponent		$\Delta\sigma_{Rsk}$ [MPa]
	N*	k_1	k_2	at N* cycles
Straight and bent bars	10^6	5	9	162.5
Welded bars and wire fabrics	10^7	3	5	58.5
Splicing devices	10^7	3	5	35

The values presented in Table 3.3 are used directly for straight bars. In the case of bent bars, e.g. shear reinforcement, a reduction factor is used according to

$$\zeta = 0.35 + 0.026\frac{D}{\phi} \tag{3.25}$$

where

D is the diameter of the mandrel,
ϕ is the bar diameter.

There are almost no situations where the exact number of cycles is the same as the reference number and in order to transform this Equation (3.27) or Equation (3.28) may be used.

A common situation is that there are different stress ranges with varying number of cycles. Then the Palmgren-Miner rule can be used, see Equation (3.23), to sum the different contributions and fulfill the following condition,

$$D_{Ed} = \sum_{i=1}^{k} \frac{n(\Delta\sigma_i)}{N(\Delta\sigma_i)} \leqslant 1 \tag{3.26}$$

where

$n(\Delta\sigma_i)$ is the number of cycles applied for a given stress range,
$N(\Delta\sigma_i)$ is the resisting number of cycles for a given stress range.

The resisting number of cycles is calculated using the following expressions

$$N(\Delta\sigma_i) = N^* \left(\frac{\frac{\Delta\sigma_{Rsk}}{\gamma_{S,fat}}}{\gamma_{F,fat}\dot{\Delta}\sigma_i} \right)^{k_1} \quad \text{if} \quad \gamma_{F,fat}\dot{\Delta}\sigma_i(N^*) \leqslant \frac{\Delta\sigma_{Rsk}(N^*)}{\gamma_{s,fat}} \tag{3.27}$$

$$N(\Delta\sigma_i) = N^* \left(\frac{\frac{\Delta\sigma_{Rsk}}{\gamma_{S,fat}}}{\gamma_{F,fat}\dot{\Delta}\sigma_i} \right)^{k_2} \quad \text{if} \quad \gamma_{F,fat}\dot{\Delta}\sigma_i(N^*) \geqslant \frac{\Delta\sigma_{Rsk}(N^*)}{\gamma_{s,fat}} \tag{3.28}$$

where $\gamma_{F,fat}$ is a safety factor on the load effect with a recommended value in paragraph 6.8.4 in EN-1992-1-1 (2005) of 1.0. $\gamma_{S,fat}$ is a safety factor for uncertainties regarding the material. The value is defined in table 2.1N in EN-1992-1-1 (2005), with a recommended value of 1.15.

Simplified method in Eurocode

For the design of steel, a couple of alternative approaches are presented in EN-1992-1-1 (2005). Firstly, there are two limiting values recommended by Eurocode beneath which no check is required

$\Delta\sigma_S \leqslant 70\,\text{MPa}$	Valid for non-welded bars in tension
$\Delta\sigma_S \leqslant 35\,\text{MPa}$	Valid for welded bars in tension

$\Delta\sigma_S$ is the stress range independent of mean level. For this check the frequent load combination presented in Equation (3.24) is used.

The final method for verification presented in Eurocode is the *Damage equivalent method* where the full damage spectrum is represented by a single equivalent stress range $\Delta\sigma_{S,equ}$. This transformation needs to be done in a satisfactory way, one example is using guidelines for the transformation of loads for bridges presented in EN-1992-2 (2005). Another example is the method presented in Section 4.8. When this transformation is done the fatigue resistance can be verified using

$$\gamma_{F,fat}\dot{\Delta}\sigma_{S,equ}(N^*) \leqslant \frac{\Delta\sigma_{Rsk}(N^*)}{\gamma_{s,fat}} \tag{3.29}$$

where

$\Delta\sigma_{S,equ}(N^*)$	is the damage equivalent stress for a given number of cycles. This may be approximated on the safe side as the maximum stress range.
$\Delta\sigma_{Rsk}(N^*)$	is the resisting stress range for a given number of cycles.

If the equivalent stress range is calculated in a correct way the acquired result should be the same as when using Equation (3.26).

3.7.2 Design according to fib Model Code 2010

The design process according to fib (2013) is similar to the one from Eurocode and can be found in section 7.4.1 in fib (2013). Similar to the values presented in Table 3.3 there are values that correspond to the S-N curve presented in Figure 3.15. The values from table 7.4-1 in fib (2013) are presented in Table 3.4 in contracted form.

Table 3.4: Parameters for design of reinforcement in fib Model code

Type of reinforcement		stress exponent		$\Delta\sigma_{Rsk}$ [MPa]	
	N*	k_1	k_2	at N* cycles	at 10^8 cycles
Straight and bent bars $D > 25\phi$	10^6	5	9	210	125
$\phi \leqslant 16$ mm	10^6	5	9	160	95
$\phi > 16$ mm	10^6	5	9	-[1]	-[1]
Bent bars $D < 25\phi$	10^7	3	5	50	30
Welded bars including tick	10^7	3	5	65	40

As mentioned in Section 3.1.2 there are different levels of approximation in fib Model Code. For the design of reinforcement with regard to fatigue there are three different methods used, ranging from II to IV.

Level II approximation

The first level of approximation consists of a check of the maximum stress range for the frequent combination which should be below a limiting value. This value is calculated using

$$\gamma_{Ed}\Delta\sigma_{s,max} \leqslant \frac{\Delta\sigma_{Rsk}}{\gamma_{s,fat}} \tag{3.30}$$

where

$\Delta\sigma_{s,max}$ is the maximum stress range,
$\Delta\sigma_{Rsk}$ is the resistant stress range at 10^8 cycles,
$\gamma_{S,fat}$ is a safety factor for uncertainties regarding the material,
γ_{Ed} is a safety factor on the load. Either 1.1 or 1.0 depending on accuracy of loads.

Level III approximation

On the next level of accuracy the structure is verified using the following condition, see similarity with Equation (3.30).

$$\gamma_{Ed}\Delta\sigma_{s,max} \leqslant \frac{\Delta\sigma_{Rsk}(n)}{\gamma_{s,fat}} \tag{3.31}$$

The factors are the same as before and the values for calculating the resisting stress are taken from Table 3.4. The characteristic resistance for n cycles is calculated using

[1] these values are the same as the first line multiplied with the reduction factor Equation (3.25)

$$\Delta\sigma_{Rsk}(n) = \left(\frac{N^*}{n}\right)^{\frac{1}{k_1}} \Delta\sigma_{Rsk}(N^*) \qquad \text{if} \qquad n < N^* \tag{3.32}$$

$$\Delta\sigma_{Rsk}(n) = \left(\frac{N^*}{n}\right)^{\frac{1}{k_2}} \Delta\sigma_{Rsk}(N^*) \qquad \text{if} \qquad n > N^* \tag{3.33}$$

where

$\Delta\sigma_{Rsk}(N^*)$	the resisting stress range for N^* cycles,
k_1	is the slope of the S-N curve for $n < N^*$,
k_2	is the slope of the S-N curve for $n > N^*$.

Level IV approximation

The final level of approximation, i.e. the most accurate analysis, consists of using the Palmgren-Miner rule from Equation (3.26) where the whole load spectrum during the service life is used. When calculating the resisting number of cycles, N, the stress range is modified using $\gamma_{Ed}\gamma_{s,fat}\Delta\sigma_i$. The calculations are done with the relationships from Equation (3.32) and Equation (3.33).

One important note regarding D_{lim} is presented in fib (2013). This states that the limiting value of 1.0 can be an overestimation for decreasing stress ranges. This means that if the largest stress ranges occur in the beginning of the structures life cycle, the damage done may be extensive enough that the subsequent lower stress ranges can cause failure prematurely. Since there is no way to predict the wind during the WPP's life span this cannot be taken into account in a good way but it is important to keep in mind.

3.8 Norms concerning fatigue in concrete

As stated in Section 3.6.2 fatigue damage in concrete originates from micro cracks. There is no stress limit beneath which no fatigue damage can occur since the cracks are already there and the propagation phase is the only phase present.

3.8.1 Design according to Eurocode

The rules for the design of concrete can be found in section 6.8, EN-1992-1-1 (2005). In this section two different approaches for verification are presented for structures subjected to compression and shear. No guideline is given in EN-1992-1-1 (2005) for a design where the full load-cycle is considered similar to the Palmgren-Miner rule. There is however a possibility to use a method presented in EN-1992-2 (2005) which will be presented in this section as an alternative.

The first of these methods, in this study denoted EN1, consists of the following verification

$$S_{cd,max,equ} + 0,43\sqrt{1 - R_{equ}} \leqslant 1 \tag{3.34}$$

where

$$R_{equ} = \frac{S_{cd,min,equ}}{S_{cd,max,equ}} \tag{3.35}$$

$$S_{cd,min,equ} = \frac{\sigma_{cd,min,equ}}{f_{cd,fat}} \tag{3.36}$$

$$S_{cd,max,equ} = \frac{\sigma_{cd,max,equ}}{f_{cd,fat}} \tag{3.37}$$

and

R_{equ}	is the ratio between maximum and minimum stress,
$S_{cd,min,equ}$	is the minimum compressive stress level,
$S_{cd,max,equ}$	is the maximum compressive stress level,
$f_{cd,fat}$	is the fatigue strength according to Equation (3.38),
$\sigma_{cd,min,equ}$	is the minimum stress of the ultimate amplitude for N cycles,
$\sigma_{cd,max,equ}$	is the maximum stress of the ultimate amplitude for N cycles.

The design fatigue strength is calculated using the following formula, taken from EN-1992-1-1 (2005) equation (6.76)

$$f_{cd,fat} = k_1 \beta_{cc}\left(t_0\right) f_{cd}\left(1 - \frac{f_{ck}}{250}\right) \tag{3.38}$$

where

$\beta_{cc}(t_0)$	is a coefficient for the strength at the time of load application,
k_1	value defined in National Annex. Recommended value is 0.85 for $N = 10^6$.

The second alternative for verification, denoted EN2, is done using the following condition

$$\begin{aligned} \frac{\sigma_{c,max}}{f_{cd,fat}} &\leqslant 0.5 + 0.45\frac{\sigma_{c,min}}{f_{cd,fat}} \\ &\leqslant 0.9 \quad \text{for} \quad f_{ck} \leqslant 50\,\text{MPa} \\ &\leqslant 0.8 \quad \text{for} \quad f_{ck} > 50\,\text{MPa} \end{aligned} \tag{3.39}$$

where

$\sigma_{c,max}$	is the maximum compressive stress under the frequent load combinations,
$\sigma_{c,min}$	is the minimum compressive stress in the same fiber as $\sigma_{c,max}$. Has to be $\geqslant 0$ MPa.

There is also a section in EN-1992-1-1 (2005), section 6.8.7 (4), that gives guidelines regarding the design of structures without shear reinforcement. Since it is unrealistic to construct the foundation without shear reinforcement these are of no interest for this study.

Method according to EN 1992-2

The method presented in EN-1992-2 (2005), denoted EN3 in this study, is based on the Palmgren-Miner rule presented in Equation (3.26) where the resisting number of cycles is calculated using

$$N_i = 10^{14\left(\frac{1-S_{cd,max,i}}{\sqrt{1-R_i}}\right)} \tag{3.40}$$

where

R_i is the ratio between maximum and minimum stress,
$S_{cd,max,i}$ is the maximum compressive stress level according to Equation (3.37).

The fatigue capacity of the concrete is calculated using Equation (3.38). Since this method is mainly used for the design of bridges the results should be considered with some caution. However, for this study they are used for comparative reasons.

3.8.2 Design according to fib Model Code 2010

As for the design regarding reinforcement there are a number of levels of approximation. Contrary to the Eurocode there is a method presented which takes the full load cycle into account, similar to the method presented in Section 3.7.2.

Level II approximation

This verification is a check that a more detailed fatigue verification is not necessary if the maximum and minimum stresses are within a certain limit. This check can be made for both compression and tension. However, since there is no check for tension in Eurocode this will not be part of this study.

The verification for compression is done by comparing the maximum compressive stress under the frequent load combination against the fatigue strength

$$\gamma_{Ed}\sigma_{c,max}\eta_c \leqslant 0.45 f_{cd,fat} \tag{3.41}$$

where

$$\eta_c = \frac{1}{1.5 - 0.5|\sigma_{c1}|/|\sigma_{c2}|} \tag{3.42}$$

$$f_{cd,fat} = 0.85\beta_{cc}(t_0) f_{ck}\left(1 - \frac{f_{ck}}{400}\right)/\gamma_{c,fat} \tag{3.43}$$

and

$f_{cd,fat}$	is design fatigue strength according to Equation (3.43),
η_c	is the averaging factor for concrete stresses in the compression zone. The stress levels
$\lvert\sigma_{c1}\rvert$ and $\lvert\sigma_{c2}\rvert$	are determined in the same section and within 300 mm of the surface of the concrete.
$\beta_{cc}(t_0)$	is a coefficient that is determined according to section 5.1.9.1. in fib (2013) and takes into account the concrete age at first load application.
$\sigma_{c,max}$	is the maximum compressive stress.

Level III approximation

The next level of approximation in Model Code 2010 is based on maximum and minimum level of stress in both compression and tension. The verification is made by checking that

$$n \leqslant N$$

where N is the resisting number of cycles. The minimum and maximum stress levels are calculated from the following set of equations respectively

$$S_{cd,min} = \frac{\gamma_{Ed}\sigma_{c,min}\eta_c}{f_{cd,fat}} \tag{3.44}$$

$$S_{cd,max} = \frac{\gamma_{Ed}\sigma_{c,max}\eta_c}{f_{cd,fat}} \tag{3.45}$$

With these the resisting number of cycles can be calculated with the following equations. In fib (2013) there are methods for verifying both compression and tension. An important note is that $S_{cd,min} \leqslant 0.8$.

$$\log(N_1) = \frac{8}{Y-1}(S_{cd,max} - 1) \tag{3.46}$$

$$\log(N_2) = 8 + \frac{8\ln(10)}{Y-1}(Y - S_{cd,min})\log\left(\frac{S_{cd,max} - S_{cd,min}}{Y - S_{cd,min}}\right) \tag{3.47}$$

with:

$$Y = \frac{0.45 + 1.8S_{cd,min}}{1 + 1.8S_{cd,min} - 0.3S_{cd,min}^2} \tag{3.48}$$

where

(a) if $\log(N_1) \leqslant 8$ then $\log(N) = \log(N_1)$

(b) if $\log(N_1) > 8$ then $\log(N) = \log(N_2)$

As was the case for level II there are expressions for concrete in tension but they will not be expressed here since there are no equivalent in Eurocode.

Level IV approximation

The method on this level of approximation is the same as was presented in Section 3.7.2 where the Palmgren-Miner rule is used. The resisting number of cycles is calculated for each stress range as for level III approximation. The same problem exists when decreasing stress levels can be expected to limit the value allowed for D_{lim}.

4 Design method for wind tower foundations

The design method used for the case study is based around a method developed by Carl Eric Broms who is a professor at the Royal Institute of Technology. It is developed for square foundations with constant thickness and grid reinforcement.

An example of a calculation report for one of the towers can be seen in Appendix B, with all of the different verifications for the structure.

4.1 Loads

The outer loads are given from the manufacturer and act on the foundation as shown in Section 4.1. The most important loads are the moment and the vertical force. The horizontal force is relatively small and does not need major consideration. The moment and the vertical force from the tower are resisted by a distributed soil pressure. The moment causes an eccentricity and thus the soil pressure will be offset to one side of the foundation. The distributed pressure from the soil can be replaced by a resulting vertical point force with eccentricity *e* as indicated in Section 4.1.

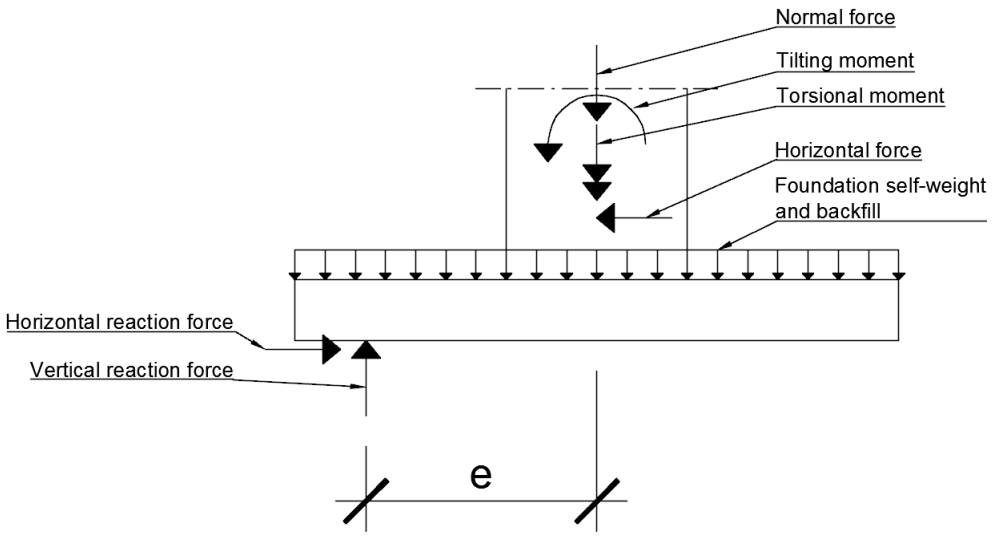

Figure 4.1: Loads acting on the foundation.

The load transfer to the tower and the bolt ring is assumed to be distributed between a force couple, one in tension and one in compression, due to the moment. The force transfer is also assumed to be concentrated to two quarter circles. This is motivated due to the stress distribution from Navier's formula where most

of the stress will be located in the parts farthest from the center. The lever arm, L_r, is calculated from center of gravity calculations according to

$$L_r = \frac{1}{A}\int_a^b f(x)xdx = \frac{2}{\pi r}\int_{-45^\circ}^{45^\circ} r\cos(\phi)rd\phi = \frac{\sqrt{8}r}{\pi} \approx 0.9r \tag{4.1}$$

which can be seen in Figure 4.2. From this the resulting force pair used for calculating section forces becomes

$$F_{t/c} = \frac{M}{1.8r} \tag{4.2}$$

where

M	is the bending moment in the tower,
$F_{t/c}$	is the resulting force from the moment,
r	is the radius of the bolt cage.

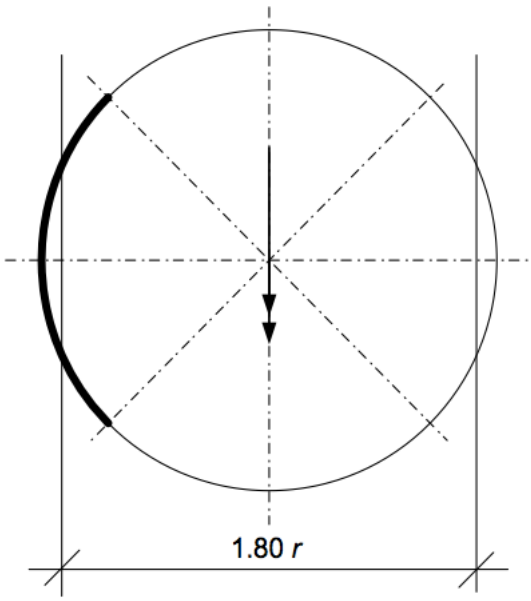

Figure 4.2: Visual representation of the reaction force from the tower.

4.2 Bearing capacity of the soil

The maximum capacity that the soil can withstand is calculated according to Eurocode 1997-1:2005. The check is made for drained conditions in accordance with the reference project, presented in Section 2.5. In order to perform the calculations the friction angle and the weight of the soil has to be known or

estimated in a satisfactory manor. The maximum capacity of the soil (q_p) is calculated according to Annex D in EN-1997-1-1 (2005) as

$$q_p = c' N_c b_c s_c i_c + q' N_q b_q s_q i_q + 0.5\gamma' N_\gamma b_\gamma s_\gamma i_\gamma \tag{4.3}$$

where a number of dimensionless parameters are divided into several categories.

- Bearing capacity

$$N_q = e^{\pi \tan(\phi')} \tan^2(45 + \phi'/2)$$
$$N_c = (N_q - 1)\cot\phi'$$
$$N_\gamma = 2(N_q - 1)\tan\phi'$$

- Inclination of the foundation

$$b_c = b_q - (1 - b_q)/(N_c \tan\phi')$$
$$b_q = b_\gamma = (1 - \alpha\tan\phi')^2$$

- Shape of the foundation

$$s_q = 1 + (B'/L')\sin\phi' \quad \text{for rectangular shape}$$
$$s_q = 1 + \sin\phi' \quad \text{for quadratic or circular shape}$$
$$s_\gamma = 1 - 0.3(B'/L') \quad \text{for rectangular shape}$$
$$s_\gamma = 0.7 \quad \text{for quadratic or circular shape}$$
$$s_c = (s_q N_q - 1)/(N_q - 1) \quad \text{for all shapes}$$

- Horizontal component of the load

$$i_c = i_q - (1 - i_c)(N_c \tan\phi')$$
$$i_q = [1 - H/(V + A'c'\cot\phi')]^m$$
$$i_\gamma = [1 - H/(V + A'c'\cot\phi')]^m$$

where

$$m = m_b = [2 + (B'/L')]/[1 + (B'/L')] \quad \text{when H has the same direction as B}$$
$$m = m_l = [2 + (L'/B')]/[1 + (L'/B')] \quad \text{when H has the same direction as L}$$

The parameters of interest in the formulas are

- c' is the apparent cohesion in the soil and typically assumed to be 0,
- γ' is the effective weight of the soil,
- q' is the pressure on the foundation from overhead loads,
- ϕ' is the inner friction angle,
- α is the angle of the foundation compared to the horizontal plane,
- B' is the effective width of the foundation,
- L' is the effective length of the foundation,
- H is the horizontal force on the foundation,
- V is the vertical force on the foundation.

The main parameters influencing the stability are the friction angle, ϕ', and the effective weight of the soil, γ'. Typical values for these parameters, taken from Bergdahl, Malmborg, and Ottosson (1993), can be seen in Table 4.1 and are chosen by the designer dependent on the given conditions at the site.

Table 4.1: Eurocode documents of interest for this thesis (EN-1990, 2005).

Soil type	Friction angle [°]	Weight [kN/m^3]
Sand	28-35	15-20
Gravel	30-37	15-20
Moraine	35-45	18-23

4.3 Resulting ground reaction and stability

The ground reactions in the soil are found by equilibrium calculations. These are necessary in order to find the design forces and moments acting on the slab and also to make sure that the foundation does not turn over. The foundation is checked in two directions, namely the wind direction parallel to the main axis of the foundation and the wind direction acting in a 45° angle from the main axis, see Figure 4.3. For both directions the load eccentricity is calculated using

$$e = \frac{M}{Q} \tag{4.4}$$

where

- e is the eccentricity, see Section 4.1,
- M is the moment acting at the bottom of the foundation,
- Q is the total vertical force.

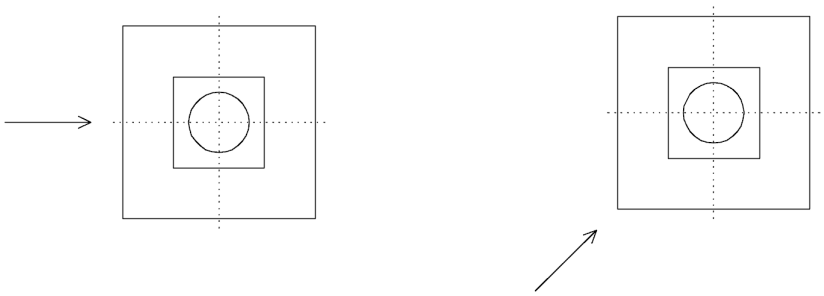

(a) (b)

Figure 4.3: (a) wind acting parallel to the main axis, (b) wind acting in a 45° angle from the main axis.

The calculations become problematic due to the soil pressure being triangularly distributed where the maximum value is at the edge. The first step is to find the distance L, see Figure 4.4. L is the part of the slab that is subjected to pressure from the soil due to the tilting moment, i.e. the required area in order for the soil to resist the overturning moment. A way of finding L is by performing a center of mass calculation.

Of course, the soil pressure is not a mass but varying distributed pressure. However, the analogy is a good way of understanding the calculations. In Figure 4.4b the pressure acting on the slab is shown in transparent and the soft layer which does not experience any pressure is represented by the solid grey. The calculations utilize the fact that the eccentricity, e, is known and coincides with the center of mass. This means that the distance, d, from the edge is known, see Figure 4.4a.

The calculation are simpler when the wind is acting parallel to the main direction because the width is constant, while for the wind acting in the diagonal direction the width is maximum in the middle and zero at the corner. For the main direction, the expressions for the pressure, denoted as h, and width for the main slab and softlayer become

$$
\begin{aligned}
b_{slab}(x) &= b_{found} \\
h_{slab}(x) &= (1 - x/L)h \\
b_{softlayer}(x) &= c \\
h_{softlayer}(x) &= (1 - \frac{x}{L-b})\frac{L-b}{L}h
\end{aligned}
$$

which are inserted into the expression for the center of gravity

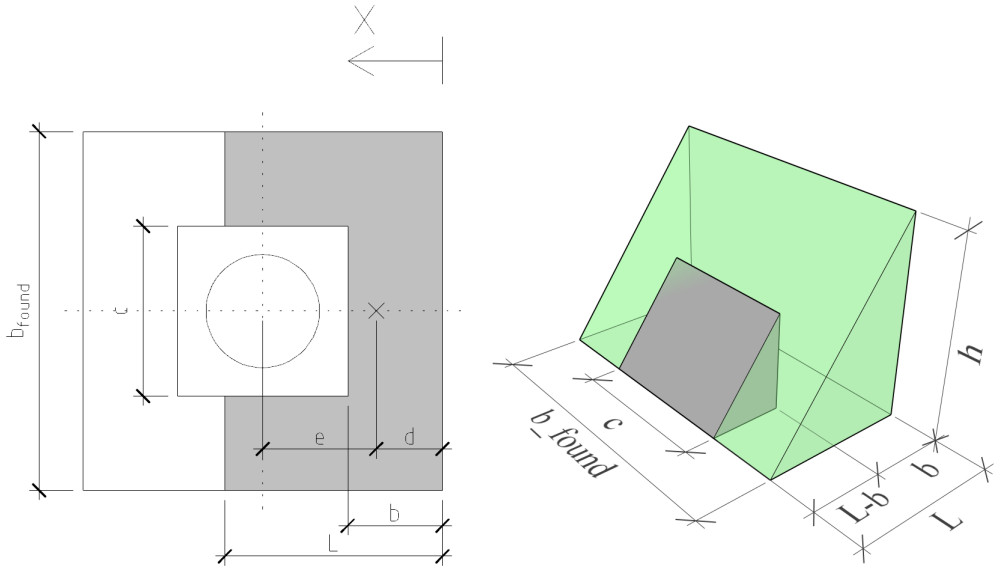

(a) (b)

Figure 4.4: Model used to find how big the pressured area is, (a) plane view showing the relation between the eccentricity, e and the distance, d from the edge to the center of mass, (b) visualization of the solution as a 3D-body center of mass calculation where the height indicates the magnitude of the soil pressure.

$$d = \frac{\int_0^L b_{slab}(x)h_{slab}(x)xdx - \int_0^{L-b} b_{softlayer}(x)h_{softlayer}(x)x}{\int_0^L b_{slab}(x)h_{slab}(x) - \int_0^{L-b} b_{softlayer}(x)h_{softlayer}(x)} \tag{4.5}$$

$$d = \frac{\frac{b_{found}hL^2}{6} - \frac{ch(b-L^2)(2b+L)}{6L}}{\frac{b_{found}hL}{2} - \frac{ch(b-L)^2}{2L}} \tag{4.6}$$

which can be solved for L since d is known. The result is relatively intuitive in the sense that it can be understood in terms of first areas of moment. Calculating the area of the main slab, e.g., resulted in the expression $\frac{b_{found}L}{2}$ and this is reasonable because the pressure varies from zero to the maximum. The lever arm can be understood using the same analogy where the resultant of the linearly varying pressure should be at one third from the edge which is $\frac{L}{3}$. The same applies for the area with the soft layer, however here the area is reduced by the factor $\frac{L-b}{L}$ since the area does not stretch to the edge and therefore does not experience the maximum soil pressure. The lever arm is a summation of the distance to the edge of the soft layer and a third of the negatively pressured area, $b - \frac{L-b}{3}$.

Furthermore, the next step is to find the maximum pressure at the edge. This is done by integrating the soil pressure over the slab area and putting it equal to the vertical force from the tower, Q. Then the only unknown is the maximum stress at the edge, σ_{max}. Note that the variable x now starts where the pressure is zero, contrary to the previous case, so that expression for the slab becomes

$$\sigma_{slab}(x) = \sigma_{max}\frac{x}{L}$$
$$b_{slab}(x) = b_{found}$$
$$\sigma_{softlayer}(x) = \sigma_{max}\frac{x}{L}$$
$$b_{softlayer}(x) = c$$

and by integrating these expressions over the lengths L, for the slab, and L-b, for the soft layer, results in

$$Q = \int_0^L \sigma_{slab}(x)b_{slab}(x)dx - \int_0^{L-b} \sigma_{softlayer}(x)b_{softlayer}(x)dx \tag{4.7}$$

$$Q = \sigma_{max}\left(\frac{b_{found}L}{2} - \frac{c}{2L}(L-b)^2\right) \tag{4.8}$$

where Q is the total vertical force from the tower.

The diagonal case is solved in the same manner as described above. However, in this case the width of the pressured area varies triangularly, see Figure 4.5, and thus complicates the expressions.

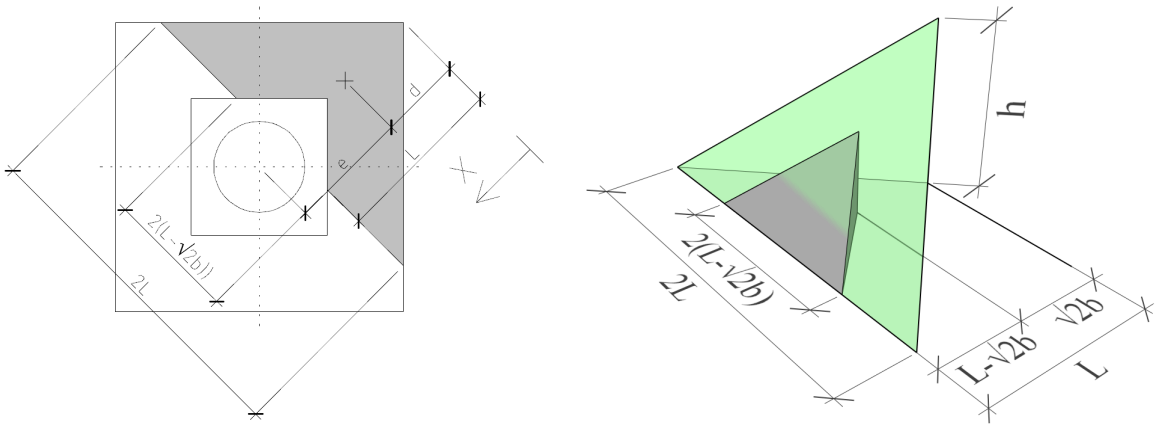

(a) (b)

Figure 4.5: Model used to find how big the pressured area is, (a) plane view showing the relation between the eccentricity, e and the distance, d from the edge to the center of mass, (b) visualization of the solution as a 3D-body center of mass calculation where the height indicates the magnitude of the soil pressure.

The expressions for the triangular shaped bodies are

$$
\begin{aligned}
h_{slab}(x) &= \left(1 - \frac{x}{L}\right) h \\
b_{slab}(x) &= 2x \\
h_{softlayer}(x) &= \left(1 - \frac{x}{L - \sqrt{2}b}\right) \frac{L - \sqrt{2}b}{L} \\
b_{softlayer}(x) &= 2x
\end{aligned}
$$

which are inserted into the expression for the center of gravity

$$
\begin{aligned}
d &= \frac{\int_0^L b_{slab}(x) h_{slab}(x) x dx - \int_0^{L-b} b_{softlayer}(x) h_{softlayer}(x) x}{\int_0^L b_{slab}(x) h_{slab}(x) - \int_0^{L-b} b_{softlayer}(x) h_{softlayer}(x)} \\
d &= \frac{\frac{hL^3}{6} - \frac{1}{6L}(L - \sqrt{2}b)^4}{\frac{hL^2}{2} - \frac{1}{3L}(L - \sqrt{2}b)^3}
\end{aligned}
$$

which can be solved for the length, L. These expressions can be understood using the same analogy as explained previously, i.e. by seeing the problem as different first areas of moment where the linearly varying pressure shifts the center of mass.

As explained previously, when the pressured area is solved, the only unknown is the maximum pressure at the edge, σ_{max}, which is found by integrating the pressure over the area and putting it equal to the weight from the tower. The expression for the soil pressure becomes a variable dependant on x, where x starts from where the soil pressure is zero and not the corner,

$$
\begin{aligned}
\sigma_{slab}(x) &= \sigma_{max} \frac{x}{L} \\
b_{slab}(x) &= L - x \\
\sigma_{softlayer}(x) &= \sigma_{max} \frac{x}{L} \\
b_{softlayer}(x) &= 2(L - \sqrt{2}b - x)
\end{aligned}
$$

and, once again, by integrating over the lengths L and L-b respectively the total reaction force is expressed as

$$Q = \int_0^L \sigma_{slab}(x) b_{slab}(x) dx - \int_0^{L-b} \sigma_{softlayer}(x) b_{softlayer}(x) dx \tag{4.9}$$

$$Q = \frac{\sigma_{max}}{3} \left(L^2 - \frac{1}{L} \left(L - \sqrt{2} b \right)^3 \right) \tag{4.10}$$

which is equal to the total vertical reaction and thus σ_{max} can be solved.

The resulting stress from the soil is compared to the limiting value calculated according to Section 4.2. No limiting value for the eccentricity is given in the calculations. In the Swedish handbook *Plattgrundläggning* a limiting value of $e \leqslant b_{found}/6$ is given which is also used for calculations for slender buildings. Section 6.5.4, EN-1997-1-1 (2005), states that special care should be taken if the eccentricity exceeds $1/3$ of the width of a rectangular base plate.

In order to verify that the behaviour is satisfactory in serviceability limit state, Navier's formula is used to verify that the whole foundation is in compression according to

$$\sigma_{main} = \frac{Q}{A_{found}} \pm \frac{M_{found}}{I_{found}} \frac{b_{found}}{2} < 0\,\text{MPa} \tag{4.11}$$

$$\sigma_{diagonal} = \frac{Q}{A_{found}} \pm \frac{M_{found}}{I_{found}} \frac{\sqrt{2} b_{found}}{2} < 0\,\text{MPa} \tag{4.12}$$

This is done for both the main direction and for 45° where the latter is normally the most severe case. As is mentioned by Broms (2013) the foundation should be placed with the main axis parallel to the main direction of the wind to lessen this risk. This check in combination with the limiting value presented previously verifies a good interaction between the foundation and the soil.

4.4 Bending capacity

The sectional moments in the foundation are calculated in two sections, one on the tension side and one on the compression side. In this model the foundation is seen as two dimensional. The moment on the tension side causes tension in the upper part of the slab and on the compression side the upper part is in compression. According to these moments the bending reinforcement is designed. It should be mentioned that the required top reinforcement always is lower than the bottom reinforcement due to the effect of the weight of the tower, which causes tension on the bottom and compression on the top of the foundation.

The soil stress is assumed to be triangular with a maximum at the edge. The soft layer will also influence the length of the soil reaction. The resulting moment in the foundation can be seen in Figure 4.6.

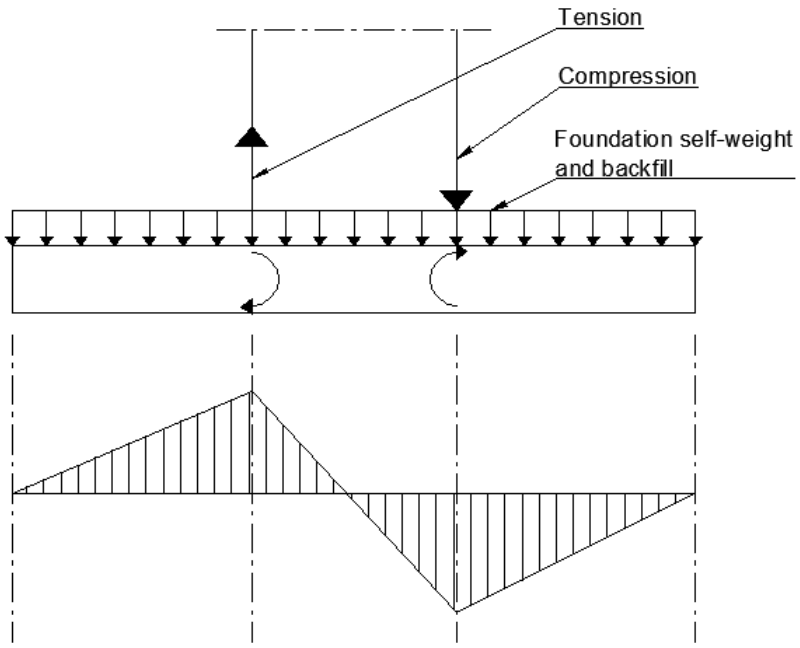

Figure 4.6: Moment distribution in the foundation due to the tilting moment.

For the bottom part the required reinforcement is calculated with the following formulas for single reinforced members, i.e. the effect of top reinforcement is not taken into account.

$$m = \frac{M_{max}}{2d_c^2 r_{tow} f_{cd}} \tag{4.13}$$

$$\omega = 1 - \sqrt{1 - 2m} \tag{4.14}$$

$$A_{s.bottom} = \frac{M_{max}}{d_c \left(1 - \frac{\omega}{2}\right) f_{yd}} \tag{4.15}$$

where

m	is the relative moment in the section,
d_c	is the effective depth of the concrete section,
r_{tow}	is the radius of the tower,
f_{cd}	is the design compressive strength of the concrete,
ω	is the reinforcement ratio in the section,
f_{yd}	is the design yield stress of the reinforcement.

These formulas hold true if the ratio calculated in Equation (4.14) is below the value for a balanced reinforcement, ω_{bal}, which is calculated from

$$\omega_{bal} = 0.8 \frac{\epsilon_{cu} E_s}{f_{yd} + \epsilon_{cu} E_s} \tag{4.16}$$

where

ϵ_{cu} is the ultimate strain of the concrete,
E_s is the elasticity modulus of the reinforcement steel.

It represents the case when the reinforcement starts to yield at the same moment as the concrete collapses. If the value calculated in Equation (4.14) is higher than the one calculated in Equation (4.16) another expression is used for calculating the reinforcement needed. This is however not a desirable situation since it means that the concrete fails before the reinforcement yields resulting in a brittle failure.

For the top reinforcement the same formulas are used as before. As mentioned previously the needed amount in the top of the foundation is lower. Therefore, the minimum required reinforcement needed to avoid cracks in the concrete has to be checked. This amount is calculated according to equation (9.1) in EN-1992-1-1 (2005) as

$$A_{s.min} = 0.26\frac{f_{ctm}}{f_{yk}} b_{found} d_c \tag{4.17}$$

where

f_{ctm} is the mean tensile strength of the concrete class,
f_{yk} is the characteristic yield strength of the reinforcement,
b_{found} is the width of the foundation,
d_c is the effective depth of the concrete section.

In order to improve the behaviour in the serviceability state the reinforcement is arranged in a way that two thirds of the reinforcement is placed in a column strip with a width of half the foundation. This process is in accordance with the strip method presented in Engström (2014). The reinforcement can be placed with different configurations as the designer chooses as long as certain guidelines are followed (Engström, 2014).

4.5 Shear capacity outside the perimeter of the tower

The shear force is assumed to be transferred along one quarter of the tower perimeter. First a check is performed to see if the concrete alone can withstand the shear force using equations (6.2a) and (6.2b) from EN-1992-1-1 (2005). The shear capacity of the section per meter is set to the lowest of

$$V_{Rd.c} = C_{Rd.c} k (100 \rho_l f_{ck})^{1/3} d_c \tag{4.18}$$
$$V_{Rd.c} = \upsilon_{min} d_c \tag{4.19}$$

where

k $= 1 + \sqrt{\frac{200}{d}} \leqslant 2.0$,
ρ_l $= \frac{A_{sl}}{b_w d}$,
A_{sl} is the flexural reinforcement in the studied section,
$C_{Rd.c}$ $= \frac{0.18}{\gamma_c}$
v_{min}, $= 0.035 k_1^{3/2} f_{ck}^{1/2}$: $k_1 = 0.15$.

Due to the very large forces acting on the foundation shear reinforcement is almost always needed. The amount of shear reinforcement is calculated assuming that the reinforcement should carry the whole shear force. The necessary reinforcement area is calculated according to

$$A_{sv} = \frac{V_{Ed}}{f_{yd}} \tag{4.20}$$

where

V_{Ed} is the design shear force in section,
f_{yd} is the design yield stress of the reinforcement.

Thereafter, the required amount is placed within circles with certain radius from the center depending on the effective area of the stirrups. The amount is expressed as a portion of the total area (ρ_i) according to

$$\rho_i = \frac{A_{sv}}{A_i} \tag{4.21}$$

Similar to the case for the moment the shear reinforcement is mainly placed in the centre of the foundation but still reaching outside the column strip mentioned in the previous section. In the design used by WSP the reinforcement is arranged in three circles of increasing diameter where half of the required reinforcement area is placed within each circle. This results in a total reinforcement amount that is 50 % higher than the limiting amount. The motivation behind this is assumed to be increased behaviour with regard to cracking and to avoid cumbersome calculations regarding capacity in different sections.

4.6 Bolts and bolt ring

When designing the anchor cage and its components it is important to ensure that concrete is never in tension. This implies that the prestress force in the bolts is high enough and that the splitting forces can be handled. Consideration is needed for relaxation in the bolts but also for shrinkage and creep in the concrete. The bolts are placed in a circle under the tower, and the amount of bolts needed depends on how high the tensile force from the tower is.

The stress in the bolts is chosen so that the concrete is in compression whilst the maximum tensile stress in the bolts is below the 0.1% proof stress. This stress depends on the type of bolts used and will not be discussed.

In order to calculate the stress in the concrete and the bolts, the respective stiffness, EA, is calculated from

$$(EA)_{bolt} = E_s n_{bolt} A_{bolt} \tag{4.22}$$
$$(EA)_c = E_{cd}(b_{anchor} + 0.25h)\pi 2r_{tow} \tag{4.23}$$
$$\tag{4.24}$$

and the proportional stiffness from the bolts and concrete are expressed as

$$k_i = \frac{(EA)_i}{\sum(EA)} \tag{4.25}$$

where

i	is index for either concrete, c, or bolts,
E_s	is the elasticity modulus of the bolts,
E_{cd}	is the elasticity modulus of concrete,
n_{bolt}	is the number of bolts in the bolt cage,
A_{bolt}	is the area an individual bolt,
b_{anchor}	is the width of the anchor plate.

The maximum force per meter acting on the concrete is then a combination of the prestress force and the force from the tower according to

$$F_{max} = -\frac{G_{tower}}{A_{cyl}} + \frac{M_d}{W_{cyl}} + \frac{n_{bolt}F_{bolt}}{\pi 2r_{tow}} \tag{4.26}$$

where

M_d	is the design moment according to Table 2.3,
A_{cyl}	is the area of the anchor plate,
W_{cyl}	section modulus of the anchor plate,
n_{bolt}	is the number of bolts in the bolt cage,
F_{bolt}	is the prestress force of one bolt,
r_{tow}	is the radius of the tower at foundation height.

In order to determine the long term effect on the bolts the stress relaxation, creep and shrinkage must be taken into account. The stress relaxation factor, χ, in the bars is calculated from section 3.3.2 in EN-1992-1-1 (2005) with different values used depending on the type of prestressing bars used. The creep is estimated using the initial stress, σ_{init}, from the prestressing bolts which represents the average stress the concrete is exposed to during the lifetime. This is calculated according to

$$\sigma_{init} = \frac{n_{bolt}F_{bolt}}{\pi 2r_{tow}(b_{cyl} + 0.25h)} \tag{4.27}$$

where

h	is the height of the foundation,
b_{cyl}	is the width of the anchor plate.

The creep factor, ϕ, is estimated from the method in Section 3.1.4 in EN-1992-1-1 (2005). In the same section the method for estimating the shrinkage of the concrete, ϵ_{cs}, can be found. The total shrinkage is a combination of drying shrinkage and autogenous shrinkage. In section 5.10.6 in EN-1992-1-1 (2005) it is stated that due to the interaction between the three effects the stress relaxation factor can be lessened with a factor of 0.8. The total prestress loss can then be calculated as

$$\Delta\sigma_s = E_s\epsilon_{cs} + \phi\frac{E_s}{E_{cd}}\sigma_{init} + 0.8\chi\sigma_{init} \tag{4.28}$$

where

ϵ_{cs} is the total shrinkage of the concrete,
σ_{init} is the initial prestress level in the bolts,
E_s is the elasticity modulus of the bolts,
E_{cd} is the elasticity modulus of concrete.

In order to verify the behaviour of the connection two checks are made. The first of these is to ensure that there is no gap between the tower and foundation under normal conditions. The force that needs to be resisted for this is calculated from

$$F_{nor,t} = -\frac{G_{tower}}{A_{cyl}} + \frac{M_{nor}}{W_{cyl}} \tag{4.29}$$

This is then verified by controlling that

$$F_{nor.t} \leqslant \frac{F_{pre,\infty}}{k_c} \tag{4.30}$$

where

$F_{pre,\infty}$ is the prestressing force after long term losses according to Equation (4.28),
k_c is the relative stiffness of concrete according to Equation (4.24).

The second control is done by controlling the relative eccentricity between the moment in the tower and the compressive reaction force. The vertical force is calculated by integration over the circle in Figure 4.7 according to

$$\begin{aligned}\sigma &= \frac{\sigma_{max}(\cos\phi - \cos\alpha)}{1-\cos\alpha} \\ V &= \int_{-\alpha}^{\alpha} \sigma r_{tow} d\phi = \frac{\sigma_{max} r_{tow}}{1-\cos\alpha}\int_{-\alpha}^{\alpha}(\cos\phi - \cos\alpha)d\phi = \frac{\sigma_{max} r_{tow}}{1-\cos\alpha}2(\sin\alpha - \alpha\cos\alpha)\end{aligned} \tag{4.31}$$

where

α is the angle according to Figure 4.7,
σ_{max} is the stress at the edge of the circle, see Figure 4.7.

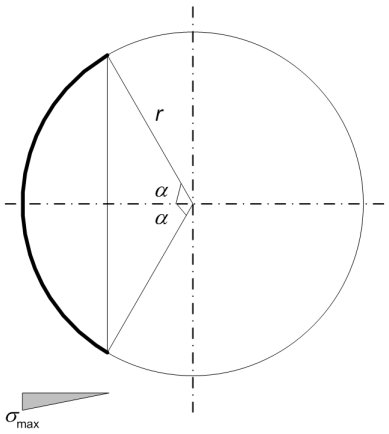

Figure 4.7: Example of stress distribution in foundation in ULS.

The moment is calculated in a similar way using

$$M = \int_{-\alpha}^{\alpha} \sigma r_{tow}^2 \cos\phi d\phi = \frac{\sigma_{max} r_{tow}^2}{1-\cos\alpha} \int_{-\alpha}^{\alpha} \cos\phi(\cos\phi - \cos\alpha) d\phi = \frac{\sigma_{max} r_{tow}^2}{1-\cos\alpha}(\alpha - \sin\alpha\cos\alpha) \quad (4.32)$$

With this a relative eccentricity, e_r, can be calculated by dividing the design moment with the reaction force times the radius

$$e_r = \frac{M}{V r_{tow}} = \frac{1}{2}\frac{\alpha - \sin\alpha\cos\alpha}{\sin\alpha - \alpha\cos\alpha} \quad (4.33)$$

$$e_r = \frac{M_d}{G_{tower} + n_{bolt} F_{bolt}} \quad (4.34)$$

This relative eccentricity is calculated for both the initial prestressing force and the force after prestress loss calculated from Equation (4.28). For the initial case the maximum stress in the bolts is compared to the design resistance of the bolts. In the second case the maximum compressive reaction on the concrete and the angle (α) are calculated by combining Equation (4.33) and Equation (4.34). The stress from this compressive force is then checked against the design capacity of the grout and concrete.

The maximum compressive stress can also be expressed in regards of the average stress from the reaction force as seen in Figure 4.10 according to

$$k_\sigma = \frac{\sigma_{max}}{\left(\frac{G_{tower} + n_{bolt} F_{bolt}}{2\pi r}\right)} \quad (4.35)$$

Anchor plate and distribution ring

The anchor plate is designed using a structural model according to Figure 4.8 where the force is distributed over the width of the anchor plate. This results in a sectional moment which is calculated from

$$M_{plate} = \sigma_{plate} \frac{(b_{anchor} - b_{dist})^2}{8} \tag{4.36}$$

where

σ_{plate} is the stress in concrete from the bolt force,
b_{anchor} is the width of the anchor plate,
b_{dist} is the distance between the bolts.

This gives a distributed moment per meter and the resisting moment is calculated from the plastic section of the plate in accordance with equation (6.7) in EN-1993-1-1 (2005) where it is stated that the strength in a section with holes can be based around the ultimate stress instead of the yeild stress. The plastic resistance thus becomes

$$M_R = \frac{0.9 f_u}{1.25} \frac{t_{anchor}^2}{4} \frac{d_{bolt} - d_{hole}}{d_{bolt}} \tag{4.37}$$

where

f_u is the ultimate stress in the plate,
d_{bolt} is the distance between the bolts,
d_{hole} is the diameter of bolt holes,
t_{anchor} is the thickness of the anchor plate.

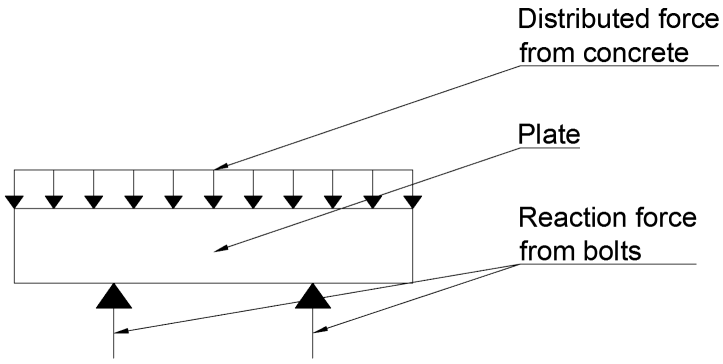

Figure 4.8: Model used for calculating stresses in the anchor plate.

Another check that has to be made is the splitting force from the prestressing. This is controlled using a strut-and-tie model, seen in Figure 4.9, according to section 6.5 in EN-1992-1-1 (2005) where the

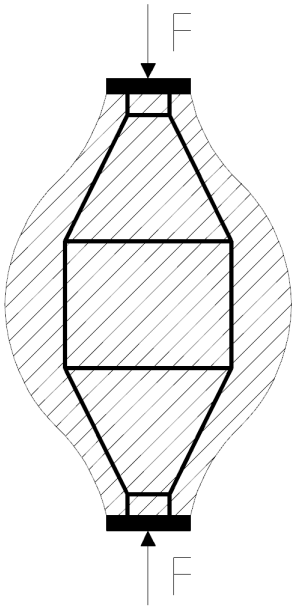

Figure 4.9: Strut and tie model used to calculate the splitting forces in the concrete under the anchor plate.

section is treated as a full discontinuity region. The tie force, T, is calculated using the initial prestressing force distributed over the anchor plate according to

$$T = \frac{1}{4}\left(1 - 0.7\frac{b_{anchor}}{0.5h_{cage}}\right)F_{init} \tag{4.38}$$

where

b_{anchor} is the width of anchor plate,
h_{cage} is the height of the anchor cage,
F_{init} is the initial prestressing force.

This tie force is resisted primarily by the flexural reinforcement. However, is this not satisfactory, splitting reinforcement can be placed radially in the middle part of the foundation to avoid splitting of the concrete.

The final part of the connection that is designed is the distribution ring which is placed under the concrete grout, see Section 2.5. This is designed in a similar way to the anchor plate described above. The difference is that there are two conditions for the concrete. The first is taken from equation (5.42) in EN-1992-1-1 (2005) and states that the concrete stress, σ_c, is lower than $0.6f_{ck}$ at all times. The second condition is that the concrete stress is below the limiting value f_{cd}. Due to the effect of bending the concrete is in a triaxial state of compression and the verification becomes

$$\sigma_c \leqslant \frac{3f_{ck}}{\gamma_c} \tag{4.39}$$

in accordance with section 6.5.3 in EN-1992-1-1 (2005) where it is stated that a triaxially compressed node can be verified using equations (3.24) and (3.25) from EN-1992-1-1 (2005).

4.7 Shear capacity within the perimeter of the tower

The shear force within the tower have to be considered as well. The shear force is calculated according using the stress distribution as in Equation (4.32) and Equation (4.31) with the angle α in Figure 4.7 as $\frac{\pi}{2}$, i.e. an elastic stress distribution. Using this gives

$$V = \frac{\sigma_{max} r_{tow}}{1 - \cos\alpha} 2(\sin\alpha - \alpha\cos\alpha) = \sigma_{max} r_{tow} 2 \tag{4.40}$$

$$M = \frac{\sigma_{max} r^2}{1 - \cos\alpha}(\alpha - \sin\alpha\cos\alpha) = \frac{\sigma_{max} r_{tow}^2 \pi}{2}. \tag{4.41}$$

where

σ_{max} is the maximum stress in the stress distribution,
r_{tow} is the radius of the tower.

By then expressing the maximum stress from Equation (4.41) the shear force can be calculated as

$$V_M = \frac{2M_{Ed}}{r_{tow}^2 \pi} r_{tow} 2 = \frac{4M_{Ed}}{\pi r_{tow}} \tag{4.42}$$

and the total shear force inside the tower then becomes

$$V_{M,tot} = \frac{4M_{Ed}}{\pi r_{tow}} - 0.5G_{tower} \tag{4.43}$$

An important note here is that in previous calculations provided by WSP and controlled by Carl-Erik Broms, professor at the Royal Institute of Technology, the force is expressed as

$$V_{M,CE} = \frac{M_{ed}}{r_{tow}^2 \pi} r_{tow} 2 = \frac{2M_d}{\pi r_{tow}} \tag{4.44}$$

and the ratio between these results is 2:1. No feasible reason behind this difference has been found and for the calculations to be verifiable against previous work done by WSP the force is calculated using Equation (4.44).

This shear force is checked against the criteria expressed in equations (6.5) and (6.6) from EN-1992-1-1 (2005) where the maximum allowed shear stress in a section is calculated using

$$0.5 \cdot 0.6 \frac{f_{ck}}{\gamma_c} \left[1 - \frac{f_{ck}}{250\,\text{MPa}}\right] d_c 2 r_{tow} \tag{4.45}$$

where

f_{ck} is the characteristic compressive stress of the concrete,
d_c is the effective depth of the concrete section,
r_{tow} is the radius of the tower.

The anchor bolts that are not used for anchoring, i.e. outside the area illustrated in Figure 4.2, are utilized as shear reinforcement since they are deemed more efficient than regular stirrups. The anchor bolts are active as shear reinforcement within an effective region where they are in tension but not utilized for anchoring the moment. This region is indicated in Figure 4.10. The stirrups are fully effective between angles β and $\frac{\pi}{4}$, and increase in efficiency from 0% to 100% effectiveness between α and β.

The stress is calculated in the same way as in Section 4.6 with the effect of stress loss accounted for. With α according to Equation (4.33) and Equation (4.34) and k_σ according to Equation (4.35) the angle for the start of the effective section (β) is calculated from the relation

$$\frac{1-\cos\beta}{1-\cos\alpha} = \frac{k_\sigma - 1}{k_\sigma} \tag{4.46}$$

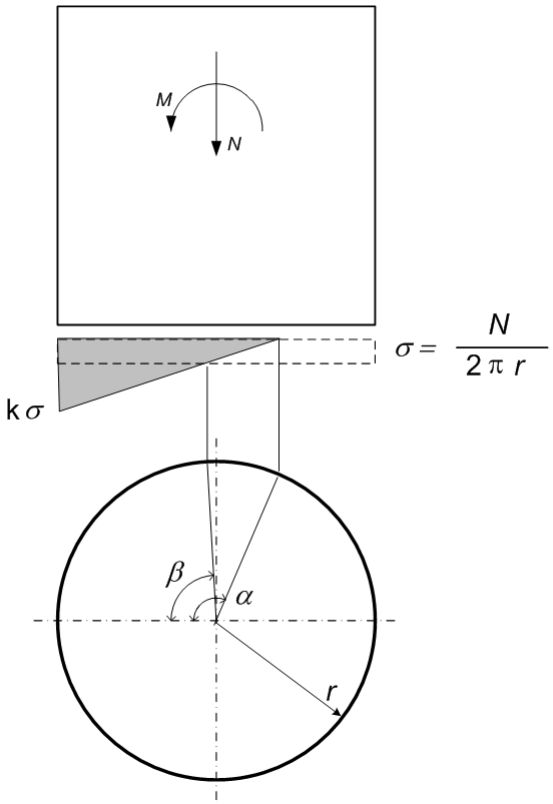

Figure 4.10: Average stress and stress distribution for the bolts in ULS.

The total shear capacity of the anchor bolts can then be calculated from

$$F_R = \left(\frac{0.5(\alpha - \beta)}{\pi} + \frac{(\beta - \pi/4))}{\pi} \right) n_{bolt} F_{bolt,\infty} \tag{4.47}$$

where

$F_{bolt,\infty}$ is the prestress force after stress loss,
n_{bolt} is the number of bolts in the bolt cage.

If the calculated capacity is higher than the shear force calculated in Equation (4.43) then there is no need for additional shear reinforcement. However, due to the risk of the bending moment causing vertical cracks within the tower perimeter, vertical stirrups should be added to compensate for the reduced effectiveness. With the assumption that the shear force is taken by an inclined strut with a slope of roughly 1:2 the reinforcement ratio becomes

$$\rho_w = \frac{1}{2} \frac{f_{ctm}}{f_{yk} \sin^2 \alpha} \tag{4.48}$$

where

f_{ctm} is the mean tensile strength of the concrete,
f_{yk} is the characteristic strength of the reinforcement,
α is the the angle of the strut, ≈ 1.11 rad.

4.8 Fatigue assessment

Several checks regarding fatigue have to be conducted when designing a WPP. The parts that have to be checked include the bottom and top flexural reinforcement, the prestressed bolts, the shear reinforcement and the concrete under the distribution ring.

For most cases, the load is treated using an equivalent moment range which is calculated using Miner's rule, seen in Equation (3.23). This equivalent moment will represent the entire Markov matrix and is calculated using a trial-and-error approach where the representative damage from each entry in the Markov matrix is calculated using Equation (4.49). For the right equivalent moment the sum of the damages from each entry will be equal to 1.0. The equivalent moment is chosen to represent a strategic number of cycles, e.g. 10^6 cycles for reinforcement steel in accordance with Figure 3.15, which is indicated with N^*.

$$d_i = \begin{cases} \frac{n_i}{N^*} \left(\frac{M_i}{M_0} \right)^{k_1} & \text{if } M_i \leqslant M_0 \\ \frac{n_i}{N^*} \left(\frac{M_i}{M_0} \right)^{k_2} & \text{if } M_i > M_0 \end{cases} \tag{4.49}$$

where

n_i is the applied number of cycles for the moment range,
N^* is the resisting number of cycles for the equivalent moment range,
M_i is the applied moment range,
M_0 is the equivalent moment range,
k_1 is the slope of the curve for a moment range lesser than the equivalent moment range,
k_2 is the slope of the curve for a moment range greater than the equivalent moment range.

The reason for using this equivalent method is to simplify the calculations. By using a equivalent moment range that represents the whole load range it limits the number of calculations needed, e.g. it is enough to calculate the required reinforcement from only this single moment range, as seen in Section 4.8.1. This will most likely have an effect on the result and another method could potentially result in different requirements. However, the effect of this is not included in this study.

There is one additional aspect that should be noted before the checks for each structural element is introduced. The loads provided by Vestas correspond to a life span of 20 years whilst Eurocode states that the life span should be 50 years. This is treated by multiplying the damage with a factor of 2.5, i.e. $d_{50} = 2.5d_{20}$.

4.8.1 Flexural reinforcement

The fatigue calculations for the flexural reinforcement are based on bending moments that are equivalent to a 50 year life span. The design fatigue strength for 10^6 cycles can be calculated by using the fatigue class for reinforcement where the different values can be seen in Table 3.3. With this value a design stress range can be calculated according to

$$\Delta\sigma_{rd,fat} = \frac{\Delta\sigma_{Rsk}}{\gamma_s.} \tag{4.50}$$

where

$\Delta\sigma_{rd,fat}$ is the design stress range for the reinforcement steel,
$\Delta\sigma_{Rsk}$ is the stress range from Table 3.3,
γ_s is a safety factor for the material.

Then the needed reinforcement area can be estimated using

$$A_{s,fat} = \frac{M_{equ}}{0.9d_c\sigma_{rd,fat}} \tag{4.51}$$

where

$A_{s,fat}$ is the needed reinforcement area for fatigue,
M_{equ} is the equivalent moment in accordance with previous Section,
d_c is the effective depth of the concrete section

By comparing this value to the values calculated from Equation (4.15) and Equation (4.17) the governing factor for the flexural reinforcement can be found.

4.8.2 Bolts

A similar process as for the flexural reinforcement is used for calculating the fatigue life of the bolts. An equivalent stress range is found by using the equivalent fatigue moment range. The parameters used for calculating the resistance are listed in Table 6.4N in EN-1992-1-1 (2005) and can be seen in Table 4.2. The shape of the S-N curve used can be seen in Figure 3.15. Since the type of bolt used for anchoring is not explicitly stated in the norm, the lowest values are used to get a value on the safe side. The resisting stress range is calculated using Equation (4.50).

Table 4.2: Parameters for design of prestressing steel in Eurocode

Type of reinforcement		stress exponent		$\Delta\sigma_{Rsk}$ [MPa]
	N*	k_1	k_2	at N* cycles
pre-tensioning	10^6	5	9	185
post-tensioning				
Single strands in plastic ducts	10^6	5	9	185
Straight or curved tendons in plastic ducts	10^6	5	10	150
Curved tendons in steel ducts	10^6	5	7	120
Splicing devices	10^6	5	5	80

The acting stress range in the bolt is calculated using the section modulus of the foundation connection, calculated from

$$W_{cyl} = \pi \frac{(2r_{tow})^2}{4} \tag{4.52}$$

which gives the force per meter of the circle. With the assumption that this force is acting on the whole circle the stress range can be divided over the total number of bolts. Thus the acting stress range, with due regard to the stress distribution according to Equation (4.24), becomes

$$\Delta\sigma_{Ed} = \frac{M_{equ}}{W_{cyl}} \frac{2\pi r_{tow}}{A_{bolt} n_{bolt}} k_{bolt} = \frac{2M_{equ} k_{bolt}}{n_{bolt} r_{tow} A_{bolt}} \tag{4.53}$$

where

M_{equ} is the equivalent moment for the steel,
r_{tow} is the radius of the tower,
A_{bolt} is the area of a single bolt,
n_{bolt} is the total number of bolts in the connection.

The control of the connection is then done by checking this stress against the resisting stress range.

4.8.3 Shear reinforcement

As in Section 4.8.2 the equivalent stress range is based on the equivalent moment range and from this an equivalent shear force is calculated. The allowed stress range for the shear reinforcement uses the same values as the flexural reinforcement, but is modified with regard to anchorage, i.e. bending around the flexural reinforcement, according to Equation (3.25).

Both the shear reinforcement outside and inside the tower perimeter need to be checked. The dimensioning shear force outside the tower is calculated by assuming that the earth pressure varies linearly over the slab. By using Navier's formula, the pressure at the edge of the foundation is found as

$$\Delta\sigma_{edge} = \frac{M_{equ}}{I_{found}} \frac{b_{found}}{2} \tag{4.54}$$
$$I_{found} = \frac{b_{found}^4}{12}.$$

The shear force range is found by integrating the pressure which varies from maximum at the edge to zero in the middle. The pressure is integrated over one quarter of the slab, with the width increasing from zero at the center to the full width at the edge. The reason for integrating over this area is that the shear force is assumed to only be transferred along this part. The shear force range then becomes

$$\Delta V_{equ} = \int_0^{\frac{b_{found}}{2}} b(x)\sigma(x)dx = \frac{\Delta\sigma_{edge} b_{found}^2}{6} \tag{4.55}$$
$$b(x) = b_{found} - 2x$$
$$\sigma(x) = \Delta\sigma_{edge} \frac{\frac{b_{found}}{2} - x}{\frac{b_{found}}{2}}.$$

This shear force can then be used along with a design stress range in order to find the required amount of shear reinforcement. The design stress range is found using Equation (4.50) from Section 4.8.1, adjusted according to Equation (3.25), as

$$A_{s,fat} = \frac{\Delta V_{equ}}{\sigma_{rd,fat}}. \tag{4.56}$$

4.8.4 Concrete

The fatigue in the high performance concrete, i.e. the grout, that is used between the anchor plate and the distribution ring is not checked for fatigue since there is little knowledge about its behaviour in this regard.

The concrete under the distribution ring has to be checked with regard to FLS because of the maximum and minimum bending moments, the prestress force from the bolts and the gravity load from the tower. The fatigue damage can be evaluated using a Markov matrix provided by the manufacturer. In contrast to the previous cases in this section there is no equivalent moment, instead the damage from each load is added to the total damage. If the total damage is less than 1.0 the design is considered to be adequate. The fatigue strength of concrete is calculated from equation (6.76) in EN-1992-1-1 (2005) and states that

$$f_{fat} = 0.85\frac{f_{ck}}{1.5}\left(1 - \frac{f_{ck}}{250\text{MPa}}\right). \tag{4.57}$$

In EN-1992-1-1 (2005) the capacity for concrete with regard to fatigue is verified using equation (6.72). This is expressed as

$$E_{cd,max} + 0.43\sqrt{1 - R_{equ}} \leqslant 1.0 \tag{4.58}$$

where

$E_{cd,max}$ is the maximum stress level,
R_{equ} is the ratio between maximum and minimum stress level.

The terms in Equation (4.58) are calculated according to equations (6.73)-(6.75) in EN-1992-1-1 (2005). The verification is valid for 10^6 cycles and there is no guideline for how a potential S-N curve is shaped. The assumption is made that the curve varies linearly in a log-log scale between f_{fat} for 1 cycle and σ_{max} for 10^6 cycles. For each entry in the Markov matrix the value of σ_{max} is calculated from

$$\sigma_{max,i} = f_{fat}\left(1 - 0.43\left(\sqrt{1 - R_{equ}}\right)\right) \tag{4.59}$$

which is a rewritten version of Equation (4.58). The slope of this curve for R_{equ}=0 becomes

$$\text{m} = \frac{\log\left(\frac{10^6}{1}\right)}{\log\left(\frac{1}{0.57}\right)} \approx 24.6 \tag{4.60}$$

and using this the maximum stress for 10^9 cycles becomes

$$f_{max,9} = f_{fat} \cdot 0.57\left(\frac{10^6}{10^9}\right)^{1/24} \approx 0.43 f_{fat} \tag{4.61}$$

The corresponding curve for this method can be seen in Figure 4.11

Recent research conducted has shown that confinement increases the fatigue life of concrete. This confinement effect is considered using equation (3.25) from EN-1992-1-1 (2005) which states that

$$1.5 f_{cd,c} = f_{ck} \left(1.125 + 2.5 \frac{\sigma_2}{f_{ck}} \right) \tag{4.62}$$

where

$f_{cd.c}$ is the confined concrete compressive strength,
f_{ck} is the characteristic compressive strength,
σ_2 is the lateral stress in the concrete.

For the compression side the confinement factor, c, becomes 3 due to active confinement, similar to Equation (4.39), whereas the confinement factor on the tensile side comes from passive confinement caused by the reinforcement. With a Poisson's ratio of 0.2 the lateral stress becomes $0.2 f_{ck}$ and the confinement factor can be expressed by rewriting Equation (4.62) as

$$1.5 f_{cd,c} = (1.125 + 2.5 \cdot 0.2) f_{ck} \Rightarrow \frac{1.675}{1.5} f_{ck} \tag{4.63}$$

and therefore the confinement factor can be said to vary between ≈ 1.5 and 3. In a conservative way the values 1.0 and 3.0 are used. It is assumed that the confinement effect has disappeared for 10^9 cycles for R_{equ}=0. The fatigue capacity at this number of cycles is calculated from

$$f_{fat,9} = f_{fat} \left(c - (c - 0.43) \sqrt{1 - R_{equ}} \right) \tag{4.64}$$

where

f_{fat} is the fatigue strenght according to Equation (4.57),
0.43 is the relative strength in accordance with Equation (4.61),
R_{equ} is the ratio between minimum and maximum stress.

With these values a S-N curve dependent on the the confinement level, c, and stress ratio, R_{equ}, can be constructed. Examples of curves for different ratios can be seen in Figure 4.11. With the slope of the curve, m, the resisting number of cycles for each entry can be calculated as

$$N_i = 10^9 \left(\frac{\sigma_{max,i}}{f_{fat,9}} \right)^{m_i} \tag{4.65}$$

and the total damage can be calculated using Miner's rule from Equation (3.23).

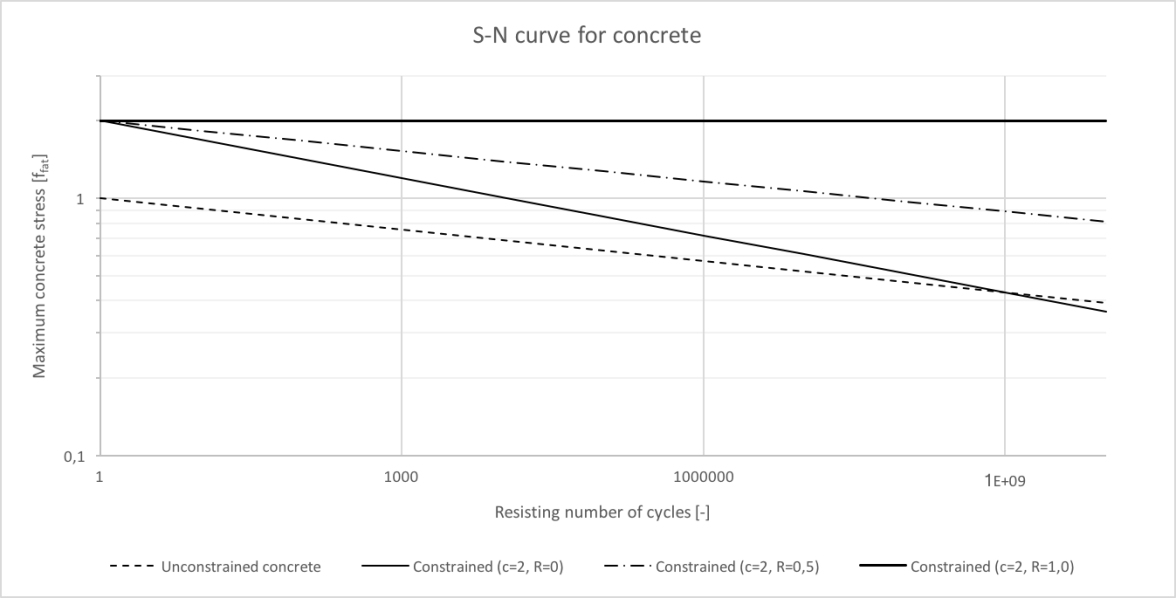

Figure 4.11: S-N curve for concrete stress according to method by Carl-Erik Broms.

This method is questioned by the Norwegian company Det Norske Veritas, today DNV-GL, in their third party review. Their main objection is against the confinement factor since there is no mention of it connected to fatigue in Eurocode. The difference in results between the method presented in Broms (2013) and the used norms will be discussed in Section 6.3.2.

5 Results

In Section 2.5 the three different case studies were introduced together with the dimensions of the towers. The results in this section is calculated with the method presented in Chapter 4 and will be discussed in Chapter 6

5.1 Case study 1 - Influence of tower height

For each tower a set of normal loads and a set of abnormal loads is used which are presented in Table 5.1.

Table 5.1: Characteristic moments for normal and abnormal cases.

Parameter	V126-3.3 MW ™	V112-3.0 MW ™	V100-1.8 MW ™
Normal moment	104 900 kN m	82 800 kN m	65 700 kN m
Abnormal moment	132 800 kN m	92 260 kN m	80 700 kN m
Normal horizontal force	850 kN	724 kN	708 kN
Abnormal horizontal force	1055 kN	748 kN	842 kN

Using the partial safety factors from Eurocode, see Table 3.2, gives design forces presented in Table 5.2. The relationship between the height of the tower and the design forces can be seen in Figure 5.1 and Figure 5.2.

Table 5.2: Design moments for the different towers.

Parameter	V126-3.3 MW ™	V112-3.0 MW ™	V100-1.8 MW ™
Design moment	159 360 kN m	124 320 kN m	98 550 kN m
Design horizontal force	1276 kN	1122 kN	1062 kN

The resulting dimensions can be seen in Table 5.3 together with the total weight of the foundation and the towers. The foundations are quadratic in shape. A graphic showing the relation between the values in Table 5.3 and the height of the tower can be seen in Figure 5.3 and Figure 5.4.

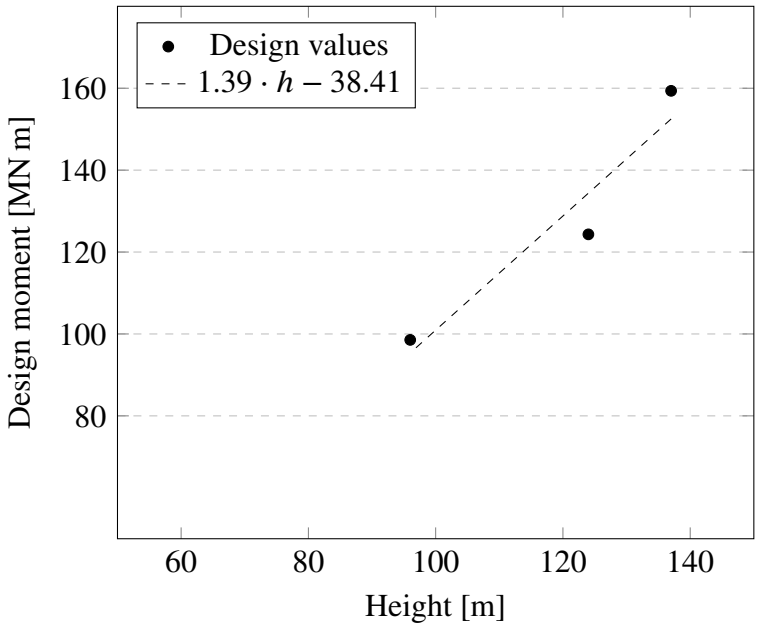

Figure 5.1: Relationship between height and design moment with linear trendline. Data taken from Table 5.2

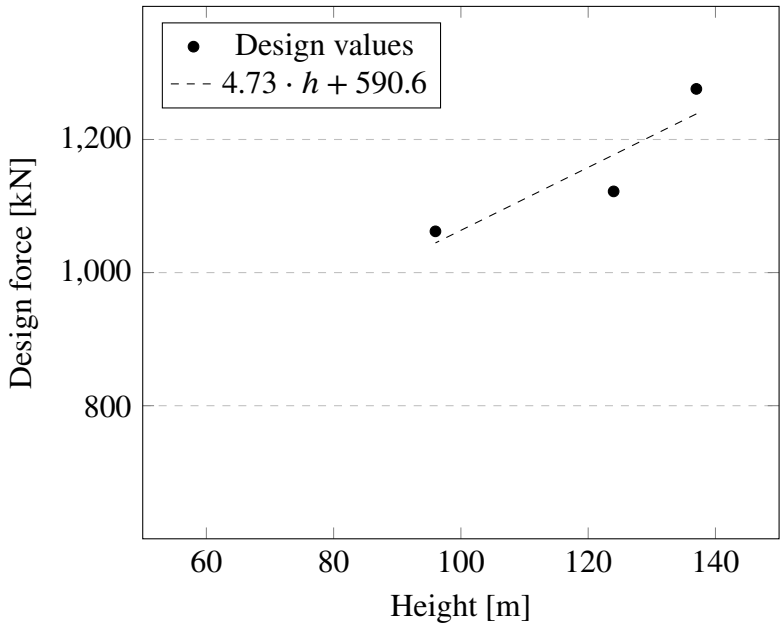

Figure 5.2: Relationship between height and design horizontal force with linear trendline. Data taken from Table 5.2

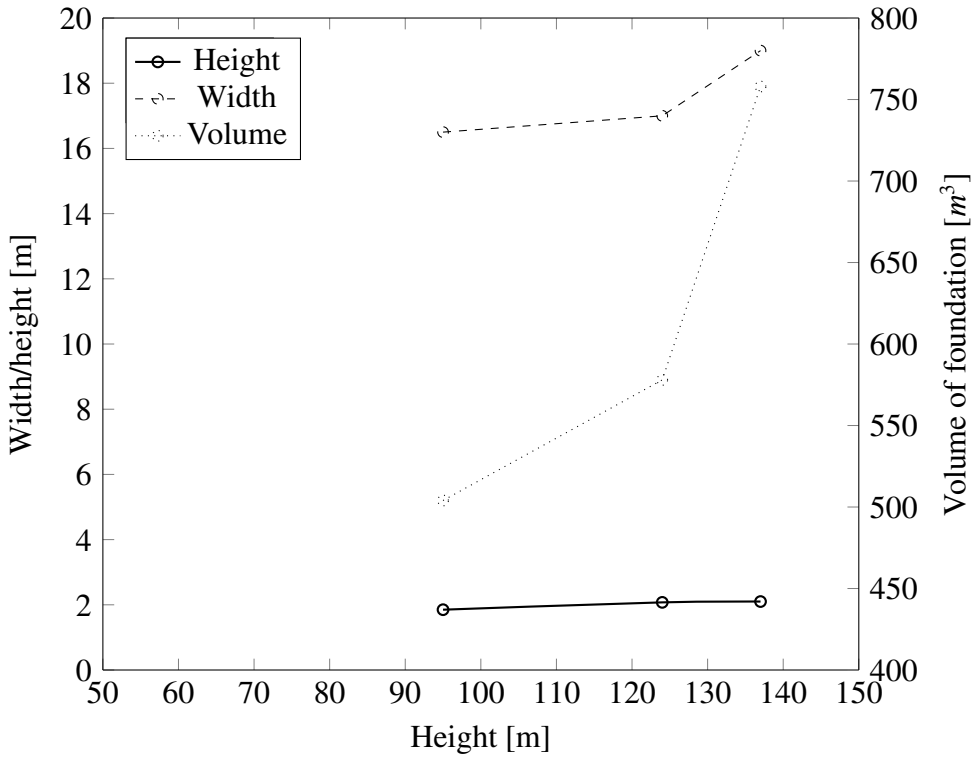

Figure 5.3: Height, width and volume of the three different towers

Table 5.3: Design dimensions and weights for the different towers.

Parameter	V126-3.3 MW ™	V112-3.0 MW ™	V100-1.8 MW ™
Foundation width	19 m	17 m	16.5 m
Height	2.1 m	2.075 m	1.85 m
Volume	758 m^3	578 m^3	504 m^3
Total weight	24 569 kN	19 734 kN	15 952 kN
Tower radius	3 m	2.095 m	1.95 m

From the resulting internal section forces the needed reinforcement areas are calculated. These areas can be seen in Table 5.4. A comparison between the different reinforcement amounts can be seen in Figure 5.5

In a similar way the reinforcement area with regard to fatigue can be seen in Table 5.5. No area for shear reinforcement is calculated since it is only verified whether fatigue is governing or not.

Finally, the fatigue damage for the reinforcement is presented in Table 5.6. The damage is calculated using the maximum reinforcement amount from Table 5.4 and Table 5.5. Therefore the damage is 1.0 for the cases when fatigue is limiting

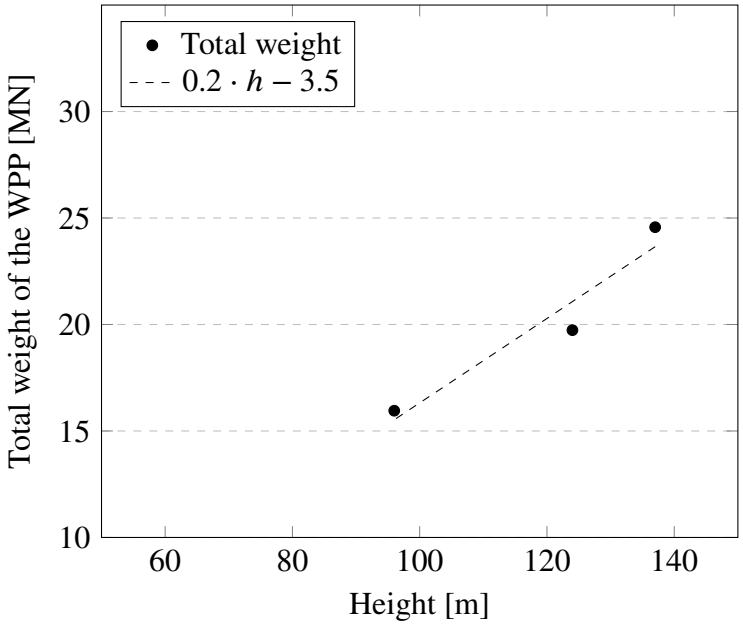

Figure 5.4: Relationship between height and design weight with linear trendline. Data taken from Table 5.2

Table 5.4: Resulting reinforcement area for extreme loads.

Parameter	V126-3.3 MW ™	V112-3.0 MW ™	V100-1.8 MW ™
Bottom reinforcement	88 893 mm^2	98 973 mm^2	79 012 mm^2
Top reinforcement	51 004 mm^2	42 127 mm^2	40 027 mm^2
Shear reinforcement	43 583 mm^2	39 035 mm^2	31 397 mm^2

Table 5.5: Resulting reinforcement area for fatigue loads.

Parameter	V126-3.3 MW ™	V112-3.0 MW ™	V100-1.8 MW ™
Bottom reinforcement	63 957 mm^2	65 628 mm^2	50 286 mm^2
Top reinforcement	56 115 mm^2	60 414 mm^2	34 294 mm^2

Table 5.6: Damage from fatigue calculations for reinforcement.

Parameter	V126-3.3 MW ™	V112-3.0 MW ™	V100-1.8 MW ™
Bottom reinforcement	0.05	0.02	0.01
Top reinforcement	1.0	1.0	0.14

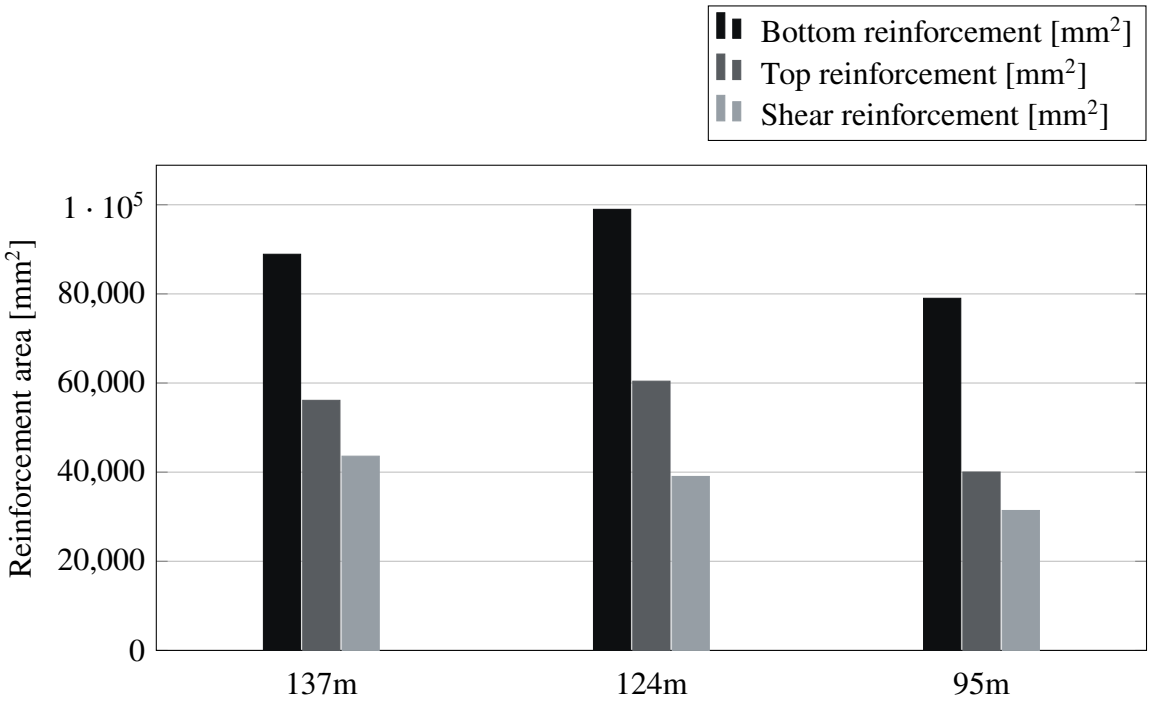

Figure 5.5: Governing reinforcement amounts for the three different towers

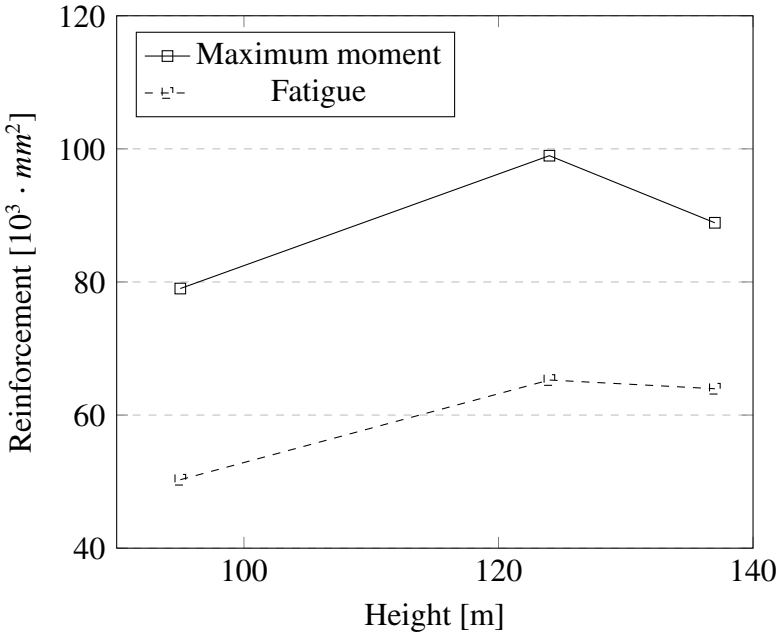

Figure 5.6: Amount of bottom reinforcement required with regard to the maximum bending moment and fatigue loading.

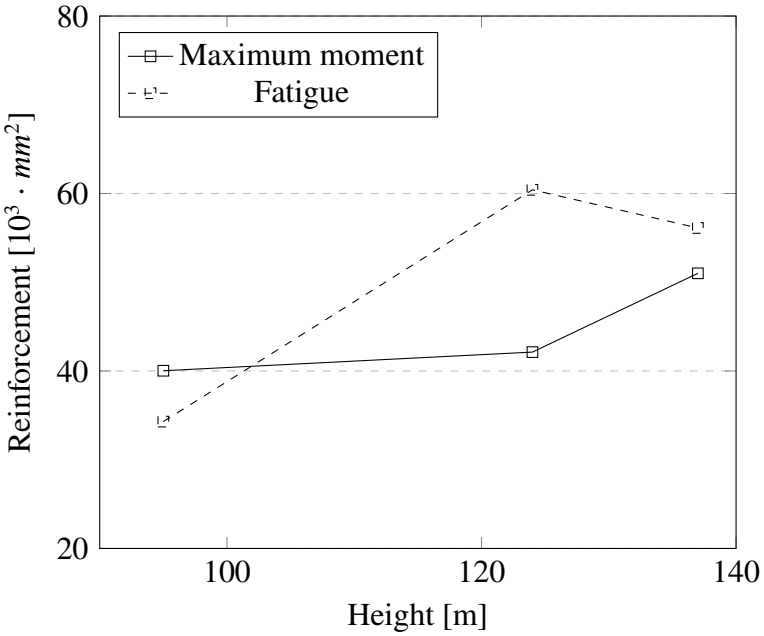

Figure 5.7: Amount of top reinforcement required with regard to the maximum bending moment and fatigue loading.

5.2 Case study 2 - Designing for 20 years instead of 50 years

For the comparison, the two interesting parameters are the reinforcement amounts and the equivalent moments. The equivalent moments can be seen in Tables 5.7 and 5.8 and shows a slight decrease with around 10% for each equivalent moment, except for steel which shows a decrease of around 20%. This is to be expected since the applied number of cycles is only 40 % of the previous and the damage has to be increased for each entry in the Markov matrix. The different notations in Tables 5.7 and 5.8 corresponds to:

Tower	equivalent moment for the anchoring bolts
BR	equivalent moment for bottom reinforcement
TR	equivalent moment for top reinforcement
Steel	equivalent moment for the distribution plate

In Table 5.9 the reinforcement amount for the design with regard to fatigue can be seen. This amount is compared to the results from the previous section, and the changes in reinforcment amount can be seen in Table 5.10 for bottom reinforcement and in Table 5.11 for top reinforcement. This shows no change in the amount for bottom reinforcement and a slight change for two of the towers for the top reinforcement. These results are shown graphically in Figure 5.8 and Figure 5.9

The results from this case study will be discussed in Section 6.1.2

Table 5.7: Equivalent fatigue loads for 50 years

Moment	V100-1.8 MW ™	V112-3.0 MW ™	V126-3.3 MW ™
M_{Tower} [kN m]	32391	44591	53736
M_{BR} [kN m]	10407	14883	15397
M_{TR} [kN m]	7366	14196	13837
M_{Steel} [kN m]	25199	36291	45885

Table 5.8: Equivalent fatigue loads for 20 years

Moment	V100-1.8 MW ™	V112-3.0 MW ™	V126-3.3 MW ™
M_{Tower} [kN m]	27942	39317	47568
M_{BR} [kN m]	9138	13132	13631
M_{TR} [kN m]	6568	12548	12339
M_{Steel} [kN m]	20190	29465	36903

Table 5.9: Resulting reinforcement area for fatigue loads using 20 years.

Parameter	V126-3.3 MW ™	V112-3.0 MW ™	V100-1.8 MW ™
Bottom reinforcement	56 623 mm^2	57 590 mm^2	43 733 mm^2
Top reinforcement	50 037 mm^2	53 653 mm^2	30 579 mm^2

Table 5.10: Resulting reinforcement change for bottom reinforcement.

Parameter	V126-3.3 MW ™	V112-3.0 MW ™	V100-1.8 MW ™
50 year	88 893 mm^2	98 973 mm^2	79 012 mm^2
20 year	88 893 mm^2	98 973 mm^2	79 012 mm^2
Change [mm^2]	0	0	0
Change [%]	0	0	0

Table 5.11: Resulting reinforcement change for top reinforcement.

Parameter	V126-3.3 MW ™	V112-3.0 MW ™	V100-1.8 MW ™
50 year	56 115 mm^2	60 414 mm^2	40 027 mm^2
20 year	51 004 mm^2	53 653 mm^2	40 027 mm^2
Change [mm^2]	5111	6761	0
Change [%]	9.1	11.1	0

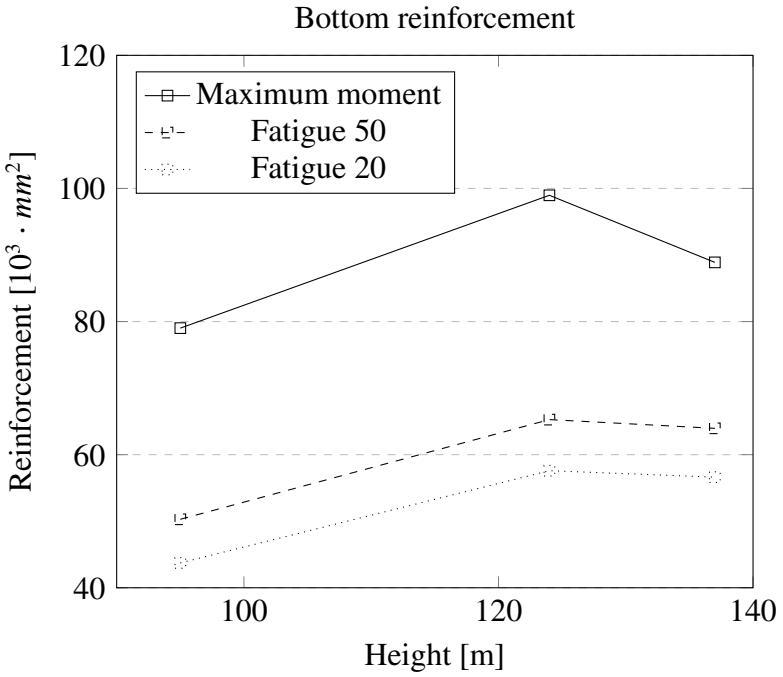

Figure 5.8: Amount of bottom reinforcement required with regard to the maximum bending moment and fatigue loading for both 20 and 50 years.

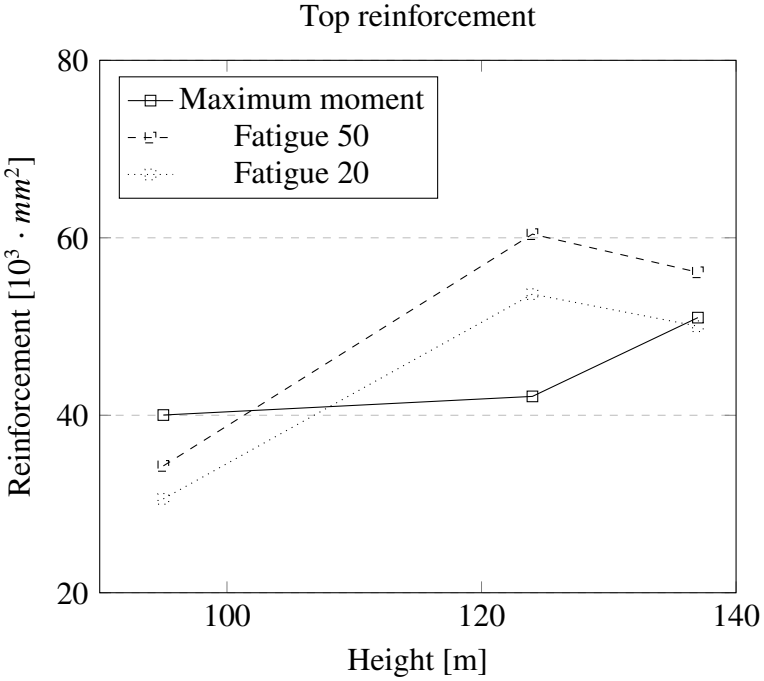

Figure 5.9: Amount of top reinforcement required with regard to the maximum bending moment and fatigue loading for both 20 and 50 years.

5.3 Case study 3 - Conflicts between norms

In case study 3 a comparison between Eurocode and IEC was performed. The aim was to find any differences that might change the amount of required reinforcement, preferably less since that gives the designer the option to create a cheaper foundation with less material.

The expected result was that the material usage would decrease since IEC provides smaller load partial factors than Eurocode, see Table 3.2. This was true in some situations, sometimes it did not matter and in one case it actually increased the amount as can be seen in Table 5.12.

For the shear reinforcement, IEC rendered less reinforcement in all three towers, see Figure 5.12. This is explained by the fact that the tilting moment is reduced which, in turn, reduces the eccentricity. This implies that a larger area of the foundation will be used to resist the tilting moment. The shear force that is dimensioning is located at the edge of the tower. If a large part of the slab beyond this section is compressed, the shear force will be lower.

The amount of bottom reinforcement was lower in two towers and slightly larger in one, see Figure 5.10. The two cases where it was larger is due to the tilting moment being smaller which causes less pressure from the soil and smaller moment in the foundation. The larger amount of reinforcement when using IEC's partial factors is because one of the favourable forces was reduced and thus the total strain reduced.

The top reinforcement was not affected by the change of partial factors, see Figure 5.11. The reason is that the dimensioning factor was either the minimum reinforcement or the amount with regards to fatigue, both of which are independent of the load partial factors.

Table 5.12: Resulting reinforcement amounts from case study 3.

	V126-3.3 MW ™		V112-3.0 MW ™		V100-1.8 MW ™	
Parameter	Eurocode	IEC	Eurocode	IEC	Eurocode	IEC
Bottom rein.	88 893 mm^2	80 808 mm^2	98 973 mm^2	99 301 mm^2	79 012 mm^2	69 156 mm^2
Top rein.	51 004 mm^2	51 004 mm^2	42 127 mm^2	42 127 mm^2	40 027 mm^2	40 027 mm^2
Shear rein.	43 583 mm^2	41 239 mm^2	39 035 mm^2	36 401 mm^2	31 397 mm^2	29 529 mm^2

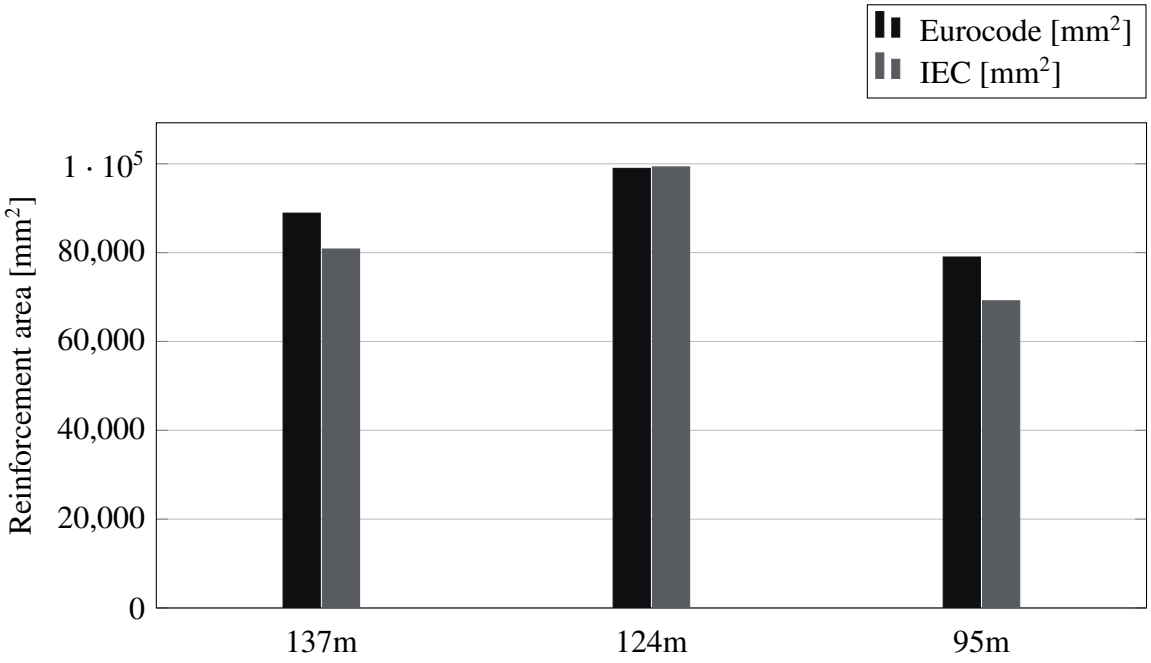

Figure 5.10: Relation between Eurocode and IEC with regards to bottom reinforcement

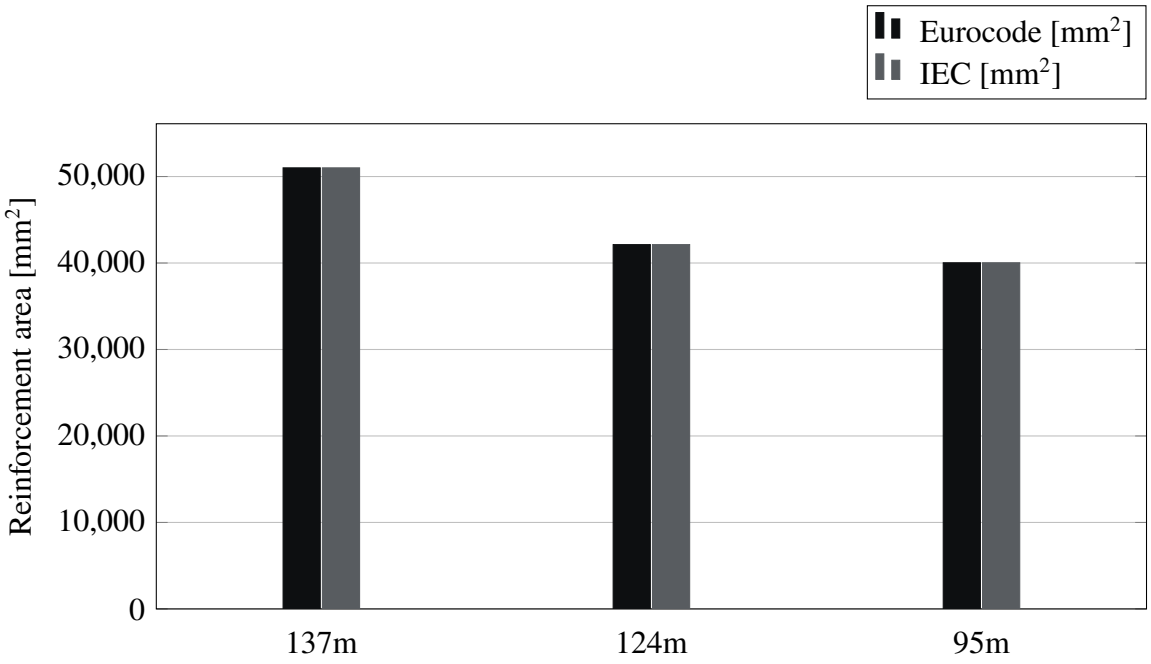

Figure 5.11: Relation between Eurocode and IEC with regards to top reinforcement

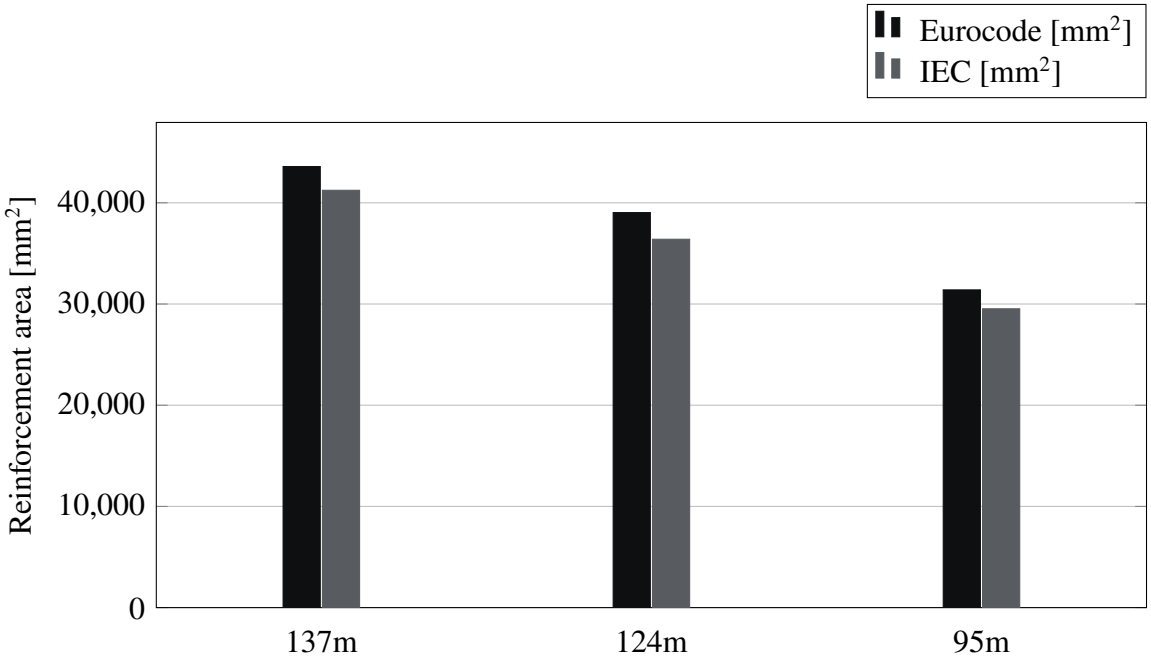

Figure 5.12: Relation between Eurocode and IEC with regards to shear reinforcement

6 Discussion

The discussion in this Chapter is based on the results in Chapter 5 and previously introduced theory. In order to support the discussion and conclusions, drawn references are introduced to present alternative views to the raised problems.

6.1 Observations from Case Studies

At the initiation of this study there were a number of questions that were raised and which were introduced in the Objectives, see Section 1.3.1. Based on the results observations have been made which is the basis recommendations were made on how to treat this problems.

6.1.1 Case Study 1 - Influence of height

Before going into discussion of the results it should be noted that one of the towers, the one that is 124 m high, has a different wind class than the others and is therefore designed for a V_{ref} of 42.5 m/s. This may have an influence on the results and will be mentioned in more detail where it is of interest.

One of the aims in conducting this study was to investigate relationships to support a preliminary sizing, when the information surrounding the tower is limited. In Figure 5.1 and Figure 5.2 linear trendlines for both design moment and horizontal forces can be seen. Despite the limited sample size the curves show clear trends which supports the idea of using it in an initial stage of production. Examples of design forces using those trends can be seen in Table 6.1. If there is an interest to find a more detailed curve more towers can be checked; however the potential improvement is deemed to be of little magnitude. An interesting note is that the tower with a higher wind class has a force that lies below the curve which at first seems contradictory. The probable reason for this is that the higher wind speed lessens the size of the rotor blades and results in lower forces in total.

Table 6.1: Approximated design forces for different tower heights.

Height [m]	Design moment [kN m]	Design horizontal force [kN]
80	73	969
90	87	1017
100	101	1064
110	115	1111
120	129	1159
130	143	1206
140	157	1253

No clear relationships can be seen for the dimension of the foundation when it comes to tower height. This has some to do with the fact that the ratio between width and height is chosen by the designer during

the process. Therefore the volume and total weight is more interesting to look at. In a similar fashion to the design moment the volume seen in Figure 5.3 is lower for the second tower. This is obviously due to the fact that the design moment is lower. However, since the weight of that tower is proportionately higher, the effect is lesser for the weight as can be seen in Figure 5.4.

The bottom reinforcement amounts can be seen in Table 5.4 and Table 5.5 and shows that the extreme moment is governing for all heights. The top reinforcement can also be seen and it shows that for the higher towers fatigue is governing whilst for the lowest tower the maximum moment results in the highest reinforcement amount. A summary of this can be seen in Table 6.2. It should also be noted that the minimum reinforcement for cracking according to Equation (4.17) is governing in some of the cases. However, for the discussion with regard to height this is not considered since those values are independent on the height, instead dependent on the concrete class.

Table 6.2: Governing factor for the different reinforcement amounts

	V126-3.3 MW ™		V112-3.0 MW ™		V100-1.8 MW ™	
Governing factor	Extreme	Fatigue	Extreme	Fatigue	Extreme	Fatigue
Bottom reinforcement	✓		✓		✓	
Top reinforcement		✓		✓	✓	
Shear reinforcement	✓		✓		✓	

That the required bottom reinforcement is higher than the required top reinforcement is expected since the permanent loads, i.e. the self-weight, gives tension in the bottom part of the foundation and raises the maximum load level in the reinforcement. Therefore, it is only natural that the governing phenomena for the bottom reinforcement is the maximum moment since it will give the highest stress levels. This becomes more interesting when looking at the top reinforcement which is governed by fatigue for all cases except for the lowest tower. The explanation behind this is that the maximum stress level is lowered due to compression from the weight of the tower. However, the moment ranges from the Markov matrix is the same as for the bottom reinforcement and, since the fatigue design for reinforcement is only dependent on the ranges, the values become roughly the same. This is further verified by checking the average ratio between bottom and top reinforcement which is ≈ 2.0 for extreme moment and ≈ 1.2 for fatigue. The relation between the different reinforcement amount can be seen in Figure 5.5 which shows that the ratio between the different reinforcement amounts is quite constant for the different tower heights.

When it comes to fatigue damage it appears that the damage increases with height. This is true for both top and bottom reinforcement which can be seen in Table 5.6 where the damage for bottom reinforcement increases with height in addition to the previously raised points. The data is however to limited to find a threshold height when fatigue becomes governing for the top reinforcement. By calculating some more towers a clearer pattern may be found. It is however quite safe to state that the bottom reinforcement will be determined from the extreme moment, regardless of height, since the minimum ratio between fatigue and extreme reinforcement is 1.57.

From the results in the study it has become clear that there is one other parameter that seems to have a significant influence on the amount of reinforcement needed. The radius of the tower will influence

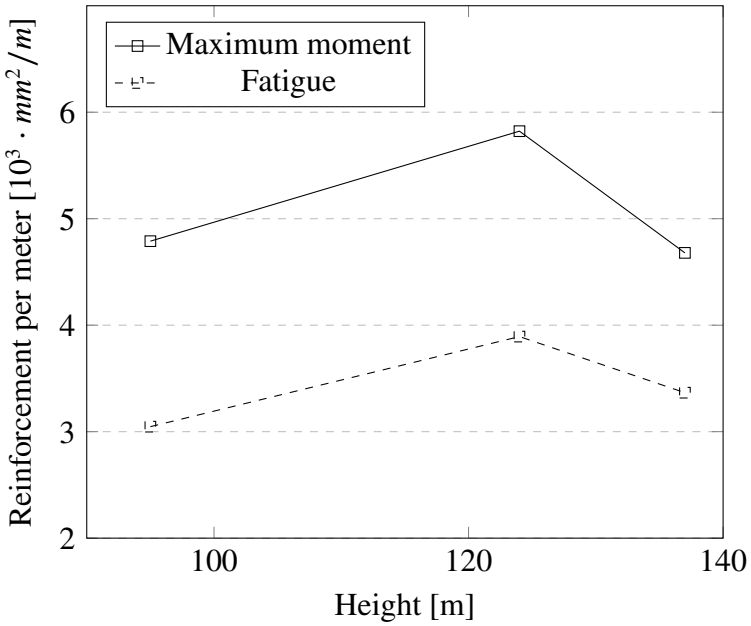

Figure 6.1: Amount of bottom reinforcement required with regard to the maximum bending moment and fatigue loading.

the size of the sectional forces, or more precisely the magnitude of the force component calculated in Equation (4.2). With a small radius this force becomes significantly larger and results in higher sectional forces. This effect is lesser when it comes to the dimensions since this is more dependent on the eccentricity of the reaction force which is independent of the radius. This effect is further accentuated by Figure 6.1 where the reinforcement amount per meter is presented, which shows a clear increase for the middle tower and quite similar values for the other two. This is probably due to the relatively small radius.

6.1.2 Case Study 2 - Designing for 20 years instead of 50 years

Another parameter that was studied was the influence of using a shorter life span for the foundation. Since there was major doubts within the company that there would be a possibility to replace the tower and use another, thus almost reaching the prescribed 50 year life-time, the potential gain of designing for 20 years was of interest.

In Table 5.9 the reinforcement amount for fatigue loading can be seen when 20 years is used. The change in reinforcement amount can be seen in Table 5.10 and Table 5.11. From this it can be seen that the change is marginal on the reinforcement amount needed in the foundations. The largest difference is 11% for the middle tower which is a marginal financial gain compared to the total cost of the foundation.

It should also be noted that for a 20 year span only the top reinforcement in the middle tower is governed by fatigue. From this it can be argued that the effect of fatigue is not as severe as thought. This is also supported by Hau (2013) who does not put fatigue as one of the design drivers for foundations. While it is unreasonable to not check the fatigue behaviour, it is clear that the maximum moment is the major

concern in design. Since there is no mention in Eurocode of a lower partial safety factor when designing for a shorter life span, a decrease in service life will not affect the dimension of the foundation since it is mainly designed to withstand overturning.

In addition to what has been mentioned the other main parameter influenced by a shorter life span is the concrete cover which could potentially be decreased since the environment cannot do as much damage in a shorter span. However, there is no mention of this in EN-1992-1-1 (2005) or the Swedish National annex. And since the difference would be in the span of 10 – 20 mm on each side of a foundation slab that is around 2 m thick the potential gain is very little, even with regard to a increased lever arm for the reinforcement.

Since the method for transforming the fatigue loads to a 50 year life span is simple and the potential gain in reinforcement amounts is low, the recommendation is not to design for 20 years, instead using the more common 50 years. This also opens for the possibility to change the tower after it has been used for its intended lifetime. The chance of this happening is however deemed to be very small due to the fast advancements for new Wind towers, especially off-shore. These will most likely make the wind towers used today uneconomic.

6.1.3 Case Study 3 - Conflicts between norms

One of the studied aspects was what influence Eurocode and the international standard, IEC, have on the design. This is of interest since the two norms propose different partial factors for the loads which, intuitively, suggests that the resulting design will be different.

The expected result from the case study was that the use of lower partial load factors would put less stress on the structure and thus reduce the required amount of material. However, some of the design aspects were not affected and in one case the required amount of reinforcement was increased.

The outcome of these results are explained quite easily. In two of three cases the bottom reinforcement was affected positively by the reduced partial factors due to its direct correlation with the tilting moment from the wind. Lower partial factors rendered lower design moment and thus reduced the reinforcement area.

However, for the accidental load case the amount of bottom reinforcement was increased. The reason being that a favourable force was reduced when the lower partial factors were introduced, which increased the stress on the foundation. Another contributing factor was that in this case the unfavourable force from the wind was not correlated with the partial factors, and was thus unaffected when using lower factors.

Furthermore, for the top reinforcement the results were not dependant on the partial factors. This is explained by the fact that the decisive factor was either the requirements with regards to minimum reinforcement or fatigue, which are both independent of the partial factors.

In summary, even in those cases where the biggest gains could be made, the differences were relatively small and it can therefore be questioned whether it is of any interest to apply other norms in the design process. This is, of course, a very subjective matter and the outcome might be greater in other projects regarding design of WPP's, e.g. a piled foundation. Therefore, it is up to every designer to make the judgement whether to apply any other norms.

It should also be mentioned that a more thorough investigation of partial factors could have been done. In Eurocode probabilistic methods are provided which are based on safety indexes, what type of failure that is of interest and the life span. This in combination with statistical data, e.g. of material strengths and load spectra, can be used to determine partial factors. This was not included simply because that kind of study would be too complex and thus the study was limited to only using the values stated by the norms.

6.2 Simplified wind-model

From the different sections in Chapter 3 the modelling of wind loads is introduced in order to increase the knowledge. As mentioned in Section 3.5.3 one of the load cases in IEC (2005) can be approximated using simplified methods. For this comparison two different wind profiles from Eurocode is used. The first wind model from Eurocode (EC I) has a reference wind speed of 23 m/s and terrain type I, the other (EC II) has a reference wind speed of 25 m/s and terrain type II. The parameters are also presented in Table 6.3 and are chosen to give a similar speed at hub height to the one from IEC.

A comparison of the wind profile used in IEC, see Equation (3.6), and the one used in Eurocode, see Equation (3.20), can be seen in Figure 6.2 where the two different wind profiles from Eurocode are used. One of the major questions regarding the wind models from IEC is the absence of the surface roughness. The terrain is instead accounted for with the turbulence intensity which is verified from field measurements (IEC, 2005). The difference between these two methods could be interesting to investigate further since it will probably influence wind shear and other factors in calculations. It is however outside the scope of this study.

Table 6.3: Wind parameters for Figure 6.2

Case	v_b	Terrain type
EC I	23 m/s	I
EC II	25 m/s	II

The resulting loads can be seen in Table 6.4 together with the characteristic loads from Vestas also seen in Table 2.3. All calculations are made on the wind tower with a height of 137 m.

Table 6.4: Characteristic loads from Eurocode and IEC

Case	H_{car}[kN]	M_{car}[MN m]
EC I	731	44.6
EC II	814	49.6
IEC	850.4	104.9

As can be seen in the table the horizontal loads are fairly similar while the moment differs a lot between IEC and Eurocode. The assumption is that the difference comes from the neglect of the wind load on the

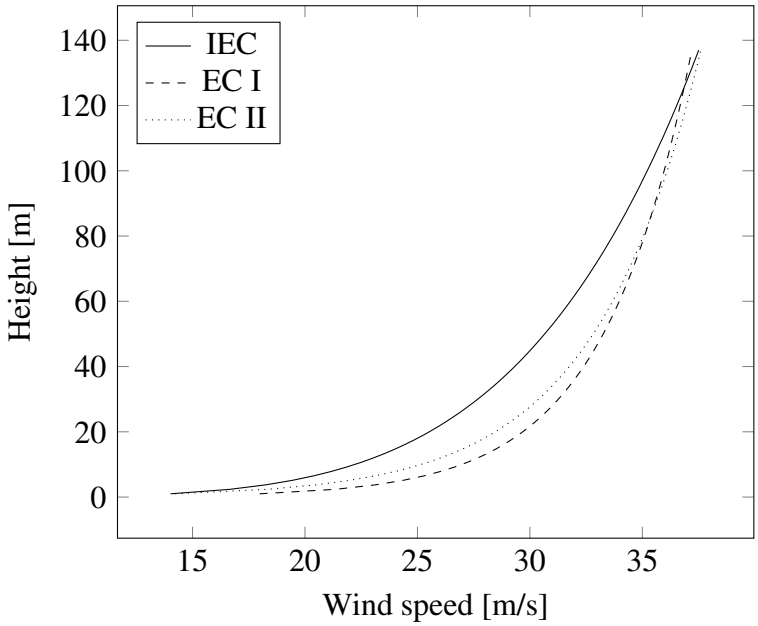

Figure 6.2: Wind speed profiles for Eurocode and IEC

rotor blades which provides a large moment due to their large distance from the foundation. Therefore, the forces on the rotor blades are calculated according to Equation (3.22). The forces on the blades are treated as three point loads acting on the tower at hub height in the principal wind direction. The value of C_d is set to 1.0. This is motivated due to the fact that the pitch angle of the blades at high wind speed is $\approx 85°$ according to Gasch and Twele (2012).

The resulting forces can be seen in Table 6.5. The horizontal force changes from a 9% underestimation to a 67% overestimation. In a similar way the moment at the foundation is increased from a 55% underestimation to a 29% overestimation. These results still are significantly different from the loads provided by the manufacturer. It is clear that Equation (3.22) overestimates the forces on the airfoil and the simplified model with three point loads at hub height does not capture the complexity of the loading situation.

Table 6.5: Characteristic loads for Eurocode with added drag forces on rotor blades

Case	H_{car}[kN]	M_{car}[MN m]
EC I	1369	132.0
EC II	1467	139.1
IEC	850.4	104.9

The difference between the simplified calculations and the provided moment can be explained by the complexity of the loading. Some of the factors that can be assumed to influence the accurate forces are:

- eccentricity of self-weight.
- loads from the nacelle and other parts with high eccentricity.
- effect of yaw misalignment and wind shear.
- the effect of turbulence.
- the shape of the rotor blades.

The conclusion here is that it is not recommended to use Eurocode when designing structures supporting wind towers. The method presented is to simplistic to model the complicated loading situation on a wind tower. However, for some older towers where a more detailed load calculation has not been done this is the only alternative available. For more modern towers the more appropriate way is either to use the loads provided by the designer or in an early stage use the relationship discussed in Section 6.1.1. For calculations in this section see Appendix A.

6.3 Additional aspects regarding fatigue

The design with regard to fatigue is still in development and new facts change the methods used. In Figure 6.3 the difference between values for design of concrete for Model code 90 and 2010 can be seen. The main difference regards the strength for a high number of cycles, $N > 10^8$, where the strength is lower for the new code. However, the opposite holds true for moderate number of cycles that are most common where the updated code gives a higher capacity.

6.3.1 Comparison between Modal Code and Eurocode

For the different verification methods presented in Section 3.8 there are four factors that influence the fatigue capacity of concrete. These are maximum and minimum stress levels, the full loading history and the ratio between maximum and minimum stress. These are listed in Table 6.6 where it can be seen that two of the methods take all of these into account. The naming of the different methods derives from

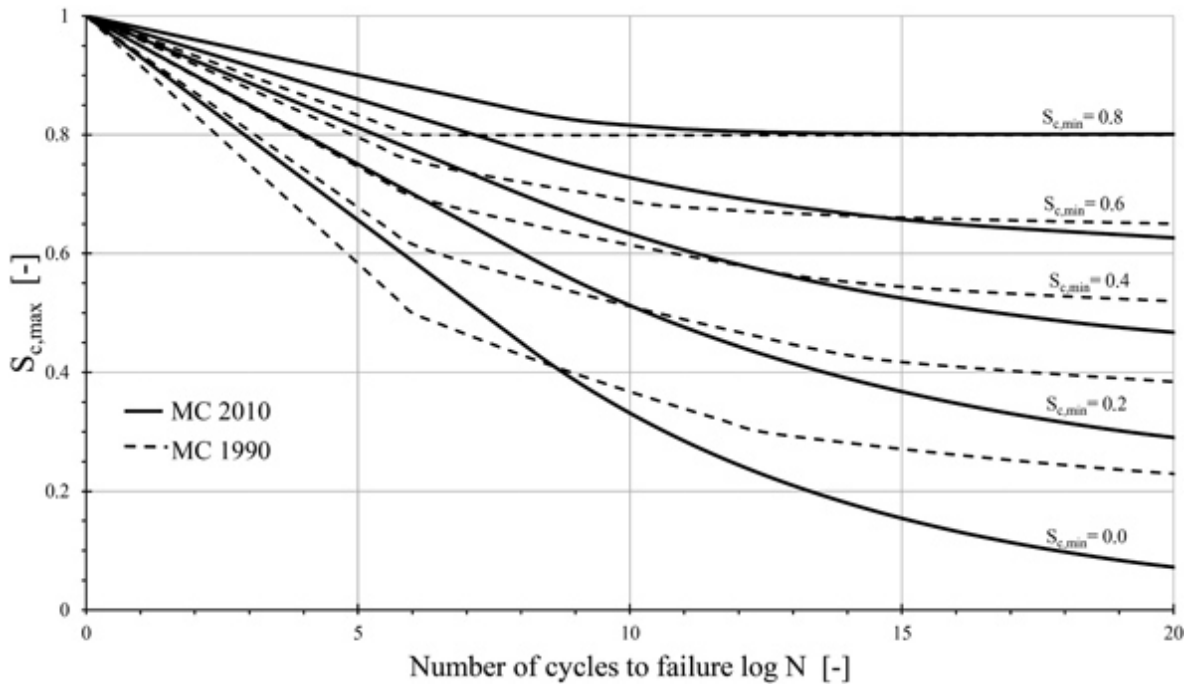

Figure 6.3: Difference between Model Code 90 and 2010 for different minimum stress levels. Source: Urban, Strauss, Schütz, Bergmeister, and Dehlinger (2014)

Section 3.8 where the notations from the different methods are introduced. The methods from fib (2013) is denoted using fib and its level of approximation as presented in Section 3.8.2. The concept of level of approximation was introduced in Section 3.1.2.

A Doctoral Thesis Thun (2006) discusses the influencing factors for fatigue life. Four factors are named where the maximum and minimum stress levels already have introduced. The third one mentioned is the stress amplitude, i.e. the difference between maximum and minimum stresses, which is accounted for in several of the verification methods. The last one is the stress frequency which is not accounted for in current norms. Due to the uncertainties in the wind loads it would not have been realistic to account for stress frequency when designing a WPP regardless.

Table 6.6: Parameters influencing the different design checks

Parameter	fib II	fib III	fib IV	EN 1	EN 2	EN 3
Maximum stress level	✓	✓	✓	✓	✓	✓
Minimum stress level		✓	✓	✓	✓	✓
Loading history			✓	✓		✓
Ratio between maximum and minimum stress				✓		✓

By doing a similar figure as Figure 6.3 with the method from EN-1992-2 (2005), seen in Equation (3.40), and the method presented in fib (2013), seen in Equations (3.46) to (3.48), the differences between the two methods can be studied. A couple of observations can be made from this. The first being that for the

number of cycles that the wind tower is exposed to, $\approx 10^9$ according to Gasch and Twele (2012), the equation from Eurocode gives lower values than Model Code. This means Eurocode is on the safe side. The exception is for $S_{cd.min} = 0.8$ where the positions are reversed. By comparing Figures 6.3 and 6.4 it can be seen that the two figures are similar and it is clear that EN-1992-2 (2005) was written using Model Code 1990 as a reference.

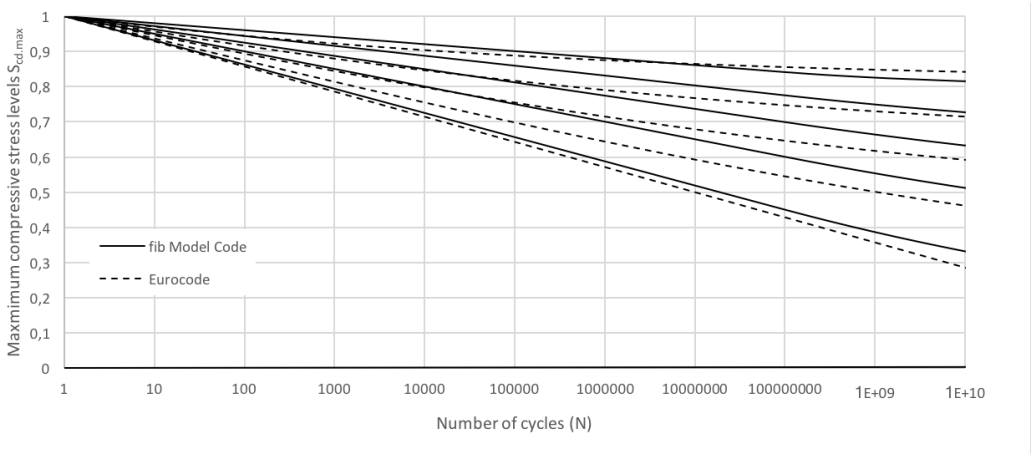

Figure 6.4: Graph showing the difference between Model Code 2010 and Eurocode.

Another point of interest is the different equations for the fatigue strength of concrete, namely Equations (3.38) and (3.43). The values for the different concrete classes can be seen in Figure 6.5 where it is noted that the fatigue strength for Model Code 2010 is significantly higher than for Eurocode with an increasing effect for higher compressive strength. For the concrete class C35/45 the difference is 6% between the two methods.

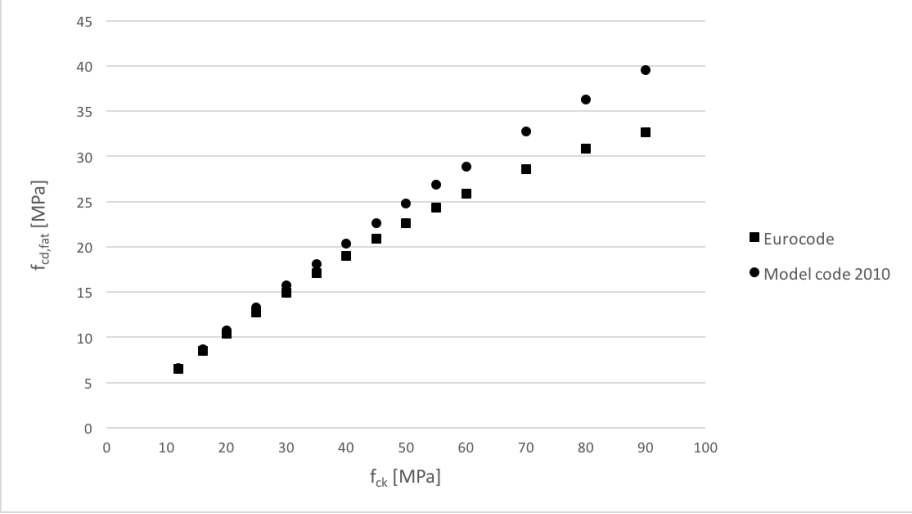

Figure 6.5: Fatigue strength of different concrete classes for Model Code 2010 and Eurocode.

These two effects combined indicate that there is a lot more capacity in the concrete when using Model Code 2010 compared to Eurocode which is natural since the former represents the latest in research

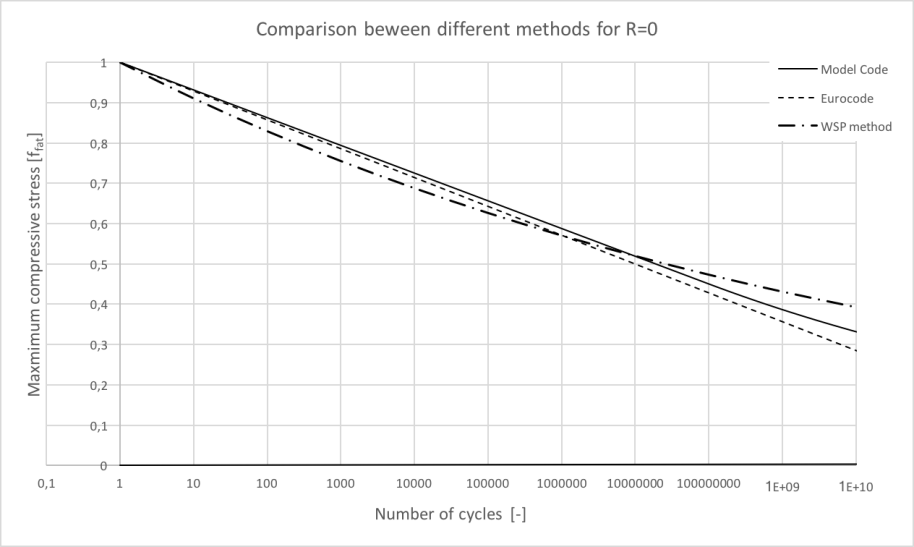

Figure 6.6: Maximum stress level for $\sigma_{min} = 0$ for the three discussed methods.

whilst the latter is based on previous recommendation. It will interesting to see if the next revision of Eurocode is closer in results to Model Code.

6.3.2 Comparison with the method from Carl-Erik Broms

In a report made by Broms (2013) he argues that the method used in Section 4.8.4 is more severe than the formula presented in EN-1992-2 (2005), presented here in Equation (3.40). His argument is that for cycles above 10^6 the results from the formula presented in Eurocode become unrealistic (Broms, 2013). In Figure 6.6 the three different curves can be seen for a case when the minimum stress is zero, representing a pulsating load. Here it can be seen that the curve presented by Carl-Erik is below both of the curves presented in the norms. Note that this is without any adjustment for confinement. It is also clear that for a high number of cycles, $> 10^7$, the method presented by Carl-Erik gives a higher capacity than the others. Therefore this method should probably be used with some caution for a high number of cycles. An attempt to calculate the damage from the different methods was found inconclusive with results that varied significantly. This is explained mainly due to the very high mean compressive stress in the concrete due to the prestressing and the self-weight of the tower. This led to maximum stresses that exceeded the fatigue strength of the concrete and gave unreasonable results, with damages in the range 10^{24}.

The second part of the argumentation that needs to be addressed is the confinement factor presented in Equations (4.39) and (4.63). There is no mentioning of how this effect should be accounted for in neither Eurocode or Modal Code with regard to fatigue. Therefore there is no set method to verify the method presented by Broms (2013). It is also clear from correspondence between WSP and the Norwegian company Det Norske Veritas, today DNV-GL, that this is one of the major uncertainties in the design methodology used. A full investigation of this is beyond the scope of this study; however a short introduction to the problem is provided.

The effect of confinement is discussed in a technical paper by Lü, Li, and Song (2007) and also in an article by Wang and Song (2011). Both of these present analytical expressions for S-N curves where the effect of lateral constraints are considered (Lü et al., 2007). In their article Wang and Song (2011) show that the confinement effect lessens with an increased number of cycles and has almost disappeared for cycles in the range of 10^8, as seen in Figure 6.7. They are also of the opinion that it leads to a waste of material when concrete structures subjected to confinement are designed for values attained for uniaxail compression (Wang and Song, 2011). From Figure 6.7 it seems that the value of 3.0 proposed in Section 4.8.4 is a bit high, and some caution should be used when designing according to it. It will be interesting to see if this effect will be considered in future revisions of norms in order to utilize the material more efficiently while still providing structures of satisfactory safety.

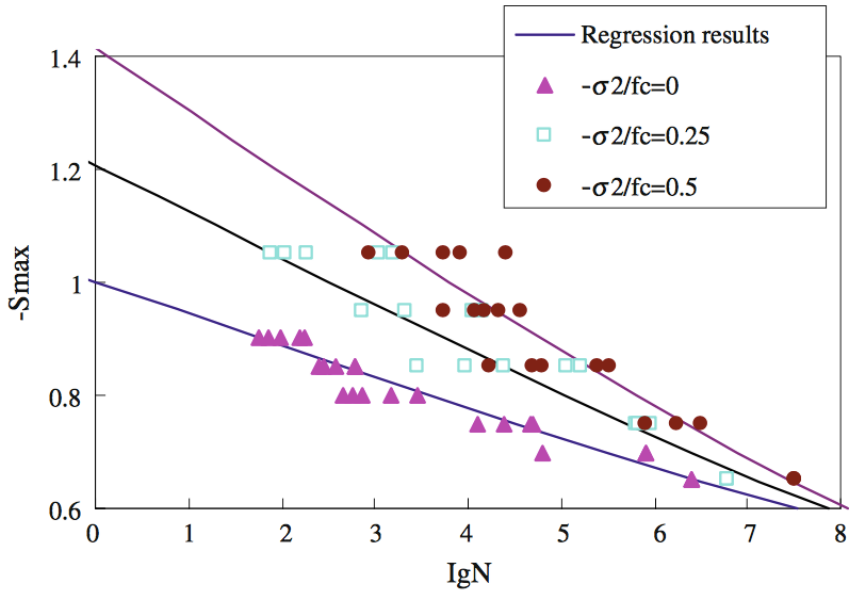

Figure 6.7: The effect of confinement on fatigue strength in concrete. Source: Wang and Song, 2011

7 Conclusions

The aim of this study was to investigate the design methodology of wind power plant foundations used at WSP, the underlying theory and the major issues surrounding it. This was the main objective along with increasing the knowledge within the subject. In addition tools have been developed to use WSP's method more efficiently. However, there is a problem with transparency in the tools developed and there are still parts of the design process that are a bit unclear.

The major cause for concern is the fatigue loading where the view is that all of the issues raised have not been answered in a satisfying way. Regarding the influence Eurocode and Model code 2010 the main conclusion is that for reinforcement the methods agree in general and feels reliable. However, for concrete the methods differ significantly and feels volatile. When an attempt was made to study the difference between the results using one of the wind towers, the results were inconclusive since some of the resulting damage were in the range of 10^{24}. The reason behind this is the compression from the anchor ring which raises the compressive stress above the fatigue strength in the concrete. This automatically results in severe damage regardless of the range of the loads.

This leads back to the effect of confinement which is a concept with a lot of uncertainty. The method proposed by Carl-Erik Broms account for the confinement, but is not based on any of the governing norms and therefore has to be verified by a third party company. It will be of great interest to see if future revisions of Model Code 2010 and Eurocode will take this effect into account and bring clarity to the question of confinement for fatigue loaded structures. The work surrounding this study has not been enough to bring clarity to the issue. It is highly recommended that anyone who is involved in the design of wind power plant foundations gets acquainted with the problems surrounding confinement.

The case studies gave several of the sought answers. This has given an improvement in regard to preliminary sizing. A relatively clear relationship between height and design loads have been established which can be helpful in early stages. This, combined with the results showing that extreme loads is the governing factor for the final design of the foundation, means that preliminary dimensions can be calculated in a matter of minutes from only the outer dimensions of the tower. For the initial stages when a lot of data is unknown this is a major gain. The developed calculation document also greatly improve the speed and decrease the effort surrounding the calculations in the detailed phase. However, it was also discovered that other factors can have major impact on the final design. One of these was the diameter of the tower where a smaller tower resulted in more reinforcement in the foundation. A smaller diameter means that the force couple that resist the tilting moment from the tower has a smaller leverarm. This, in turn, means that the magnitude of the force couple has to be bigger to compensate which renders a higher moment in the slab and therefore more reinforcement is required.

In addition, the results show no severe disadvantage when designing for 50 years which is stated by Eurocode instead of 20 years proposed by IEC. The only positive effect is a slight decrease in the top reinforcement, in the range of 10%, which is minor and therefore it is recommended to use the 50 year life span suggested by Eurocode.

Finally, the difference between using partial safety factors from IEC instead of Eurocode is minor. The difference in reinforcement amounts and outer dimensions are small. Therefore there is no apparent reason to use the less safe method proposed by IEC and take the risk of a potential legal feud concerning this, since Eurocode is the governing norm according to Swedish law.

7.1 Suggestions for future research

There are still a number of uncertainties when it comes to the design of wind power plant foundations. The different choices made influence the design in a major way and in order to improve the design process further, the background to these choices is needed. From the work on this study the following issues are suggested for further studies surrounding wind power plant foundations.

- Implement this method on a circular or octagonal foundation.
- How long term loading affects the soil properties and how this, in turn, affects the tower. For example does constant tilting cause electricity losses due to less stiffness in the foundation.
- A deeper investigation into the effect of fatigue with focus on the effect of confinement for concrete.
- The moments provided by the manufacturer are often simplified. How large difference is it between these moments and a more accurate method.
- Investigate the effect of the ratio between the width of the foundation and radius of the tower.
- A more thorough economic study connected to the design of foundations.

References

EN-1990. (2005). *Eurocode - basis of structural design*. European Committee for Standardization. (Cited on pages 18, 19, 22, 23, 33, 52).

EN-1991-1-4. (2005). *Eurocode 1 - actions on structures – part 4: General actions - wind actions*. European Committee for Standardization. (Cited on pages 35, 36).

EN-1992-1-1. (2005). *Eurocode 2 - design of concrete structures – part 1-1: General rules and rules for buildings*. European Committee for Standardization. (Cited on pages 40–42, 44, 45, 59, 61, 62, 64–66, 70, 72, 73, 89).

EN-1992-2. (2005). *Eurocode 2 - design of concrete structures – part 2: Bridges*. European Committee for Standardization. (Cited on pages 42, 44, 46, 93–95).

EN-1993-1-1. (2005). *Eurocode 3 - design of steel structures – part 1-1: General rules and rules for buildings*. European Committee for Standardization. (Cited on page 64).

EN-1993-1-9. (2005). *Eurocode 3 - design of steel structures – part 1-9: Fatigue*. European Committee for Standardization. (Cited on page 39).

EN-1997-1-1. (2005). *Eurocode 7 - geotechnical design – part 1: General rules*. European Committee for Standardization. (Cited on pages 51, 57).

Ahlström, A. (2005). *Aeroelastic simulation of wind turbine dynamics* (Doctoral dissertation, Royal Institute of Technology). (Cited on page 32).

Bergdahl, U., Malmborg, B., & Ottosson, E. (1993). *Plattgrundläggning*. AB Svensk Byggtjänst. (Cited on page 52).

Berglind, J. B. & Wisniewski, R. (2014). Behavior of concrete under nonproportional biaxial fatigue stresses with one constant. *Wind Energy*. (Cited on pages 34, 35).

Broms, C.-E. (2013). *V100 hh95m structural calculations*. Report regarding the structural calculations for a square gravity foundation. (Cited on pages 57, 74, 95).

Burton, T. (2011). *Wind energy handbook* (2nd edition). John Wiley and Sons, Ltd. (Cited on pages 7, 8, 10).

Campbell, S. (2016). 10 of the biggest turbines. Retrieved April 11, 2016, from http://www.windpowermonthly.com/10-biggest-turbines. (Cited on page 6)

Al-Emrani, M. & Åkesson, B. (2013). *Steel structures (course literature - vsm 191)*. Department of Civil and Environmental Engineering. (Cited on pages 37–39).

Engström, B. (2014). *Design and analysis of slabs and flat slabs*. Department of Civil and Environmental Engineering. (Cited on page 59).

fib. (2013). *Fib model code for concrete structures 2010*. International Federation for Structural Concrete. (Cited on pages 20, 23, 42, 44, 47, 93).

Gasch, R. & Twele, J. (2012). *Wind power plants: Fundamentals, design, construction and operation* (2nd edition). Springer-Verlag Berlin Heidelberg. (Cited on pages 5, 6, 10, 11, 18, 23–27, 34–36, 91, 94).

Gulvanessian, H., Calgaro, J., & Holický, M. (2012). *Designers' guide to eurocode: Basis of structural design, en 1990*. ICE Publishing. (Cited on page 17).

Halici, Ö. F. & Mutingi, H. (2016). *Assessment of simulation codes for offshore wind turbine foundations* (Master's thesis, Chalmers University of Technology, Division of Structural Engineering). (Cited on page 32).

Hanser Verlag, C. (2014). *Understanding wind power technology* (A. Schaffarczyk, Editor). John Wiley and Sons, Ltd. (Cited on pages 6, 7, 9).

Hau, E. (2013). *Wind turbines: Fundamentals, technologies, application, economics* (2nd edition). Springer. (Cited on pages 23–26, 36, 88).

Heffernan, P. (1997). *Fatigue behaviour of reinforced concrete beams with cfrp laminates* (Doctoral dissertation, Royal Military College of Canada). (Cited on pages 37–39).

Holtslag, M. C., Bierbooms, W. A. A. M., & van Bussel, G. J. W. (2016). Wind turbine fatigue loads as a function of atmospheric conditions offshore. *Wind Energy*. Retrieved March 14, 2017, from http://www.lr.tudelft.nl/fileadmin/Faculteit/LR/Organisatie/Afdelingen_en_Leerstoelen/Afdeling_AEWE/Wind_Energy/Research/Publications/Publications_2016/Holtslag_et_al-2016-Wind_Energy.pdf. (Cited on page 33)

IEC. (2005). *Iec 61400-1 wind turbines - part 1: Design requirements*. International Electrotechnical Commission. (Cited on pages 15, 26, 27, 31–34, 90).

IEC. (2017). About the iec. Retrieved February 10, 2017, from http://www.iec.ch/about/?ref=menu. (Cited on page 20)

Johansson, M. (2015, August 18). Vindkraft i sverige. Retrieved April 10, 2017, from http://www.energimyndigheten.se/fornybart/vindkraft/marknadsstatistik/ny-sida/. (Cited on page 1)

Knappett, J. & Craig, R. (2012). *Craig's soil mechanics* (8th edition). Spon Press. (Cited on page 9).

Lin, S. & Huang, Z. (2016). *Comparative design of structures*. Springer Berlin Heidelberg. (Cited on page 16).

Lü, P., Li, Q., & Song, Y. (2007). Behavior of concrete under nonproportional biaxial fatigue stresses with one constant. *ACI MATERIALS JOURNAL*. (Cited on page 96).

Moriarty, P., Holley, W., & Butterfield, S. (2004). *Extrapolation of extreme and fatigue loads using probabilistic methods*. Office of Energy Efficiency and Renewable Energy. (Cited on page 34).

Ragan, P. & Manuel, L. (2007). Comparing estimates of wind turbine fatigue loads using time-domain and spectral methods. *Wind Engineering*. Retrieved April 7, 2017, from http://www.ce.utexas.edu/prof/Manuel/Papers/RaganManuel_WindEngineering.PDF. (Cited on page 33)

Sutherland, H. J. (1999). *On the fatigue analysis of wind turbines*. Sandia National Laboratories. (Cited on pages 33, 34, 37).

Svensk Energi. (2016). Vindkraft. Retrieved February 9, 2017, from http://www.svenskenergi.se/Elfakta/Elproduktion/Vindkraft/. (Cited on pages 1, 5)

Thun, H. (2006). *Assessment of fatigue resistance and strength in existing concrete structures* (Doctoral dissertation, Luleå University of Technology). (Cited on pages 36, 93).

Urban, S., Strauss, A., Schütz, R., Bergmeister, K., & Dehlinger, C. (2014). Dynamically loaded concrete structures – monitoring-based assessment of the real degree of fatigue deterioration. *Structural concrete*, *15*. (Cited on page 93).

Wang, H. J. & Song, Y. P. (2011). Fatigue capacity of plain concrete under fatigue loading with constant confined stress. *Materials and Structures*. (Cited on page 96).

A Wind forces according to Eurocode

Design moment from Eurocode

Case I

Input

	Value	*Unit*	
b_1	3		Width of tower at hub height
b	6	m	Width of tower at foundation
z	137	m	Height of the tower
vref	23	m/s	Reference wind speed acc. to 1991-1-4
Terrain type	I		Terrain type acc. to 1991-1-4
c	4	m	Maximum chord length
l_{blade}	61,6	m	Lenght of a rotor blade
$c_{d,blade}$	1		Drag coefficent for the rotor blade according to Fig 5-7 in Gasch and Twele (2012)
ρ	1,25	kg/m^3	Density of air
k_r	0,17		Terrain factor according to EN 1991-1-4 (4.5)
c_r	1,62		Rawness factor according to EN 1991-1-4 (4.4)
v_{hub}	37,19	m/s	Wind speed at hub height
q_p	1,50	kn/m^2	Pressure according to EN 1991-1-4 (4.8)
Re	9,80E+06		Reynolds number
I_v	0,105		Turbulence intensity according to EN-1991-1-4 (4.7)
c_{pe}	7,91E-01		Coefficient of external pressure

Results

H_{blades}	638,98814	kN	Horizontal force on the blades
H_{tower}	730,96	kN	Horizontal force on the tower
H_{tot}	*1369,95*	kN	Total force at foundation level
M_{tower}	44507,61	kNm	Moment from the forces on the tower
M_{blade}	87541,3752	kNm	Moment from the forces on the blades
M_{tot}	*132048,98*	kNm	Total moment at foundation level

Case II

Input

	Value	*Unit*	
b_1	3		Width of tower at hub height
b	6	m	Width of tower at foundation
z	137	m	Height of the tower
vref	25	m/s	Reference wind speed acc. to 1991-1-4
Terrain type	II		Terrain type acc. to 1991-1-4
c	4	m	Maximum chord length
l_{blade}	61,6	m	Lenght of a rotor blade
$c_{d,blade}$	1		Drag coefficent for the rotor blade according to Fig 5-7 in Gasch and Twele (2012)
ρ	1,25	kg/m^3	Density of air
k_r	0,19		Terrain factor according to EN 1991-1-4 (4.5)
c_r	1,50398551		Rawness factor according to EN 1991-1-4 (4.4)
v_{hub}	37,60	m/s	Wind speed at hub height
q_p	1,66	kn/m^2	Pressure according to EN 1991-1-4 (4.8)
Re	1,03E+07		Reynolds number
I_v	0,126		Turbulence intensity according to EN-1991-1-4 (4.7)
c_{pe}	7,93E-01		Coefficient of external pressure

Results

H_{blades}	653,144533	kN	Horizontal force on the blades
H_{tower}	814,22	kN	Horizontal force on the tower
H_{tot}	*1467,37*		Total force at foundation level
M_{tower}	49577,14	kNm	Moment from the forces on the tower
M_{blade}	89480,801	kNm	Moment from the forces on the blades
M_{tot}	*139057,94*	kNm	Total moment at foundation level

B Calculation report for Vestas V126-3.3MW™

Complementary document for Excel

The aim of this document is to be a complement to the Excel calculations. The purpose is to create understanding for the calculations as well as the underlying theory and assumptions that they are based on.

1. Preconditions

The values that might occur for certain parameter are specifically for a project including a wind power plant of type *Vestas V126 3,3 MW*. These values are thus not general but may vary from different projects.

The wind loads are calculated in accordance to IEC 61400-1 Edition 3 and Wind turbine generator systems-Part 1: safety requirements.

The loads are given in the load document supplied by the tower manufacturer.

Norms

These handbooks and codes have been used for design of the square gravity foundation.

- IEC 61400-1 Wind turbines – Part 1
- Foundation Loads, *document from the manufacturer*
- BFS 2015:6 – EKS10
- Eurocde 1, 1991-1
- Eurocode 2, 1992-1-1, 1992-2
- Eurocode 3, 1993-1
- Eurocode 7, 1997-1
- Handboken Bygg Geoteknik (Swedish handbook for geotechnical design)
- Plattgrundläggning (Swedish handbook for slab/foundation design)

Material properties

Concrete class: 35/45

Grout: Masterflow 800

Reinforcement class: K500C-T

Geometry

Abbreviation	Value	Unit	Description
h	2,1	m	Height of the foundation
$h_{backfill}$	0,4	m	Height of the topping
b_{found}	19	m	Width of the foundation
d_{found}	1,9	m	Distance from edge to reinforcement
r_{tow}	3	m	Radius of the tower
c_{sl}	9	m	Size of soft layer
h_{hor}	2,3	m	Height of the horizontal force

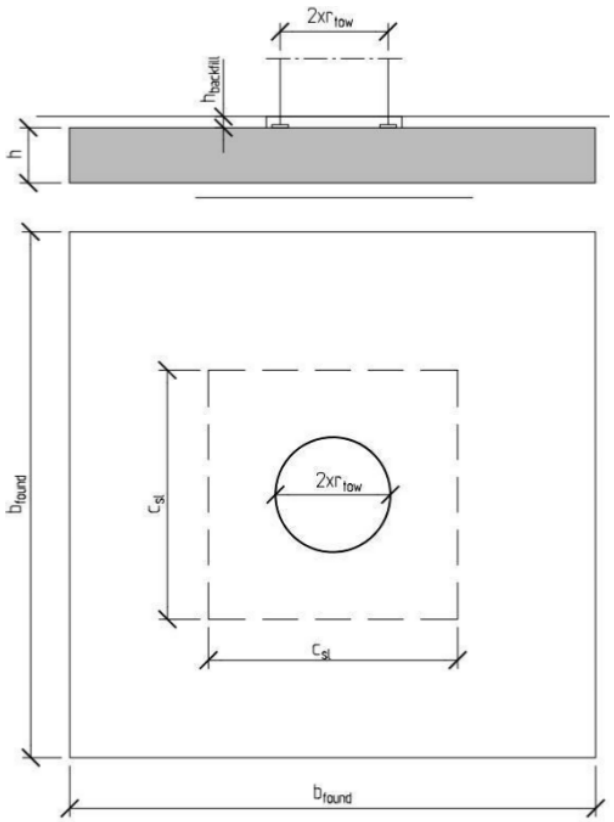

2. Loads

In this chapter the loads from the self-weight and the wind are presented.

Gravity loads

The gravity loads from are presented in the table below and consist of the self-weight from the concrete and backfill.

Density		
Material	Weight [kN/ m^3]	Abbrevation
Concrete	25	$\rho_{concrete}$
Backfill	18	$\rho_{backfill}$

The weight from the tower is given from the manufacturer as:

$$G_{tower} =$$

The total weight of the foundation is calculated as:

$$G_{found} = \rho_{concrete} b_{found}^2 h$$

The total weight from the backfill is calculated as:

$$G_{backfill} = \rho_{backfill} h_{backfill} \left(b_{found}^2 - \pi r_{tow}^2 \right)$$

Additional loads are the live load:

$$q_{LL} = 5kN/m^2$$

In the calculation document the sum of the gravity loads except the live load is referred to as:

$$Q = G_{tower} + G_{found} + G_{backfill}$$

Extreme horizontal loads

The follow loads are acting at the bottom of the tower.

Abbreviation	Value	Unit	Description
$M_{ex.characteristic}$	132800	kNm	Bending moment
$H_{ex.characteristic}$	1055	kN	Horizontal force
$M_{ex.characteristic.alternatively}$	104900	kNm	Bending moment
$H_{ex.characteristic.alternatively}$	850.4	kN	Horizontal force
$M_{tor.characteristic.alternatively}$	6429	kNm	Torsional moment

Normal operation (serviceability load)

Abbreviation	Value	Unit	Description
$M_{normal.characteristic}$	104898.93	kNm	Bending moment
$H_{normal.characteristic}$	850.43	kN	Horizontal force
$M_{normal99.characteristic}$	69611.92	kNm	Bending moment, 99% fraction value
$H_{normal99.characteristic}$	553.27	kN	Horizontal force, 99% fraction value

Fatigue loading

Markov matrices and S-N curves…

Have to explain how the Markov matrix functions when it translates the load spectrum into an equivalent load.

Abbreviation	Value [kNm]	Description
$M_{fat.tower}$	53 800	Anchor bolts
$M_{fat.BR}$	15 450	Top reinforcement
$M_{fat.TR}$	13 900	Bottom reinforcement
$M_{fat.steel}$	46 000	Anchor plate

3. Foundation stability

The resulting eccentricity due to bending moment and horizontal force is calculated as:

$$e = \frac{M_{found}}{Q}$$

Where:

$$M_{found} = M_{ex.d} + H_{ex.d} * h_{hor}$$

Figure of this, describing the original load case and the equivalent.

Wind direction parallel to the main axis

If evenly divided soil pressure and the soft layer is neglected the soil pressure can be calculated as:

$$\sigma = \frac{Q}{2\left(\frac{1}{2}b_{found} - e\right)b_{found}}$$

Figure for better understanding why these dimensions are used in this particular way

When the soft layer is included the calculations become slightly more complicated. In order to find the pressure from the soil the total compressed area needs to be known which is done by center of mass calculations.

The distance between the edge and the eccentricity is:

$$d = \frac{b_{found}}{2} - e$$

The distance between the edge and the soft layer is defined as:

$$b_{sl} = \frac{b_{found}}{2} - \frac{c_{sl}}{2}$$

The soil that is pressured can then be calculated by solving the equation:

$$d = \frac{b_{found}\frac{L^2}{2} - c_{sl}(L - b_{sl})\left(b_{sl} + \frac{L - b_{sl}}{2}\right)}{b_{found}L - c_{sl}(L - b_{sl})}$$

Where L is unknown.

When L is known the soil pressure is calculated as:

$$\sigma = \frac{Q}{b_{found}L - c_{sl}(L - b_{sl})}$$

Do we need to explain this more in detail? Add figure of course….

Wind in diagonal direction

In a similar fashion the resulting soil pressure can be found when the wind is acting diagonally. For the case when the soft layer is neglected the soil pressure is calculated as:

$$\sigma = \frac{Q}{\left(\frac{3}{2}\right)^2 \left(\sqrt{2}\frac{b_{found}}{2} - e\right)^2}$$

Where the distance d between the resultant and the corner of the foundation is expressed as:

$$d = \sqrt{2}\frac{b_{found}}{2} - e$$

d is acting at a distance one third from the bottom of the pressured triangular area meaning that the total height of the pressured area is expressed as:

$$\left(\frac{3}{2}\right) d = Height\ of\ pressure\ triangel$$

Thus the above expression for the soil stress.

If the soft layer is included the calculations become more cumbersome. The distance between the corner of the foundation and resultant is:

$$d = \sqrt{2}\frac{b_{found}}{2} - e$$

The distance between the corner of the foundation and the soft layer is expressed as:

$$b_{sl} = \sqrt{2}(\frac{b_{found}}{2} - \frac{c_{sl}}{2})$$

The equation for solving L thus becomes:

$$d = \frac{\frac{2}{3}L^3 - (L - b_{sl})^2\left(L - \frac{1}{3}(L - b_{sl})\right)}{L^2 - (L - b_{sl})^2}$$

The soil stress is then calculated as:

$$\sigma = \frac{Q}{L^2 - (L - b_{sl})^2}$$

Add figure with all dimensions to make the calculations clear

Accidental load case

In the accidental load case the water level is assumed to be at the top of the foundation and thus providing buoyancy. This reduces the vertical pressure on the soil as shown in the following equation:

$$Q = G_{tow} + G_{found} - b_{found}^2 h\rho_{water} + G_{backfill}$$

In all other aspects the equations to find the soil pressure are exactly the same as in the previous chapter.

Bearing capacity of the soil

The bearing capacity of the soil is calculated according to SS-EN 1997-1-1:2005, appendix D.4 using the following equations.

$$\sigma = c'N_c b_c s_c i_c + qN_q b_q s_q i_q + 0.5\gamma B N_\gamma b_\gamma s_\gamma i_\gamma$$

However for cohesion soil during undrained conditions it is often assumed that $\phi = 0$ leading to:

$$\sigma = c'N_c b_c s_c i_c + qN_q b_q s_q i_q;\ (N_q = 1)$$

And for friction soil it is often assumed that $c = 0$ leading to:

$$\sigma = qN_q b_q s_q i_q + 0.5\gamma B N_\gamma b_\gamma s_\gamma i_\gamma$$

The N-values account for the bearing capacity of the soil, the b-values for the inclination of the slab surface, the s-values for the shape of the slab and the i-values for the inclination of the load due to the horizontal load components.

$$N_q = e^{\pi \tan \phi'} \tan^2\left[45 + \frac{\phi'}{2}\right]$$

$$N_c = \left(N_q - 1\right)\cot \phi'$$

$N_\gamma = 2\left(N_q - 1\right)\tan \phi'$, where $\delta \geq \frac{\phi'}{2}$ and δ is the friction angle in the contact area

$$i_c = i_q - \frac{1 - i_q}{N_c tan\phi'}$$

$$i_q = \left[1 - \frac{H}{V + A'c'cot\phi'}\right]^m$$

$$i_\gamma = \left[1 - \frac{H}{V + A'c'cot\phi'}\right]^{m+1}$$

$$b_c = b_q - \frac{1 - b_q}{N_c tan\phi'}$$

$$b_q = b_\gamma = (1 - \alpha tan\phi')^2$$

$s_q = 1 + \frac{B'}{L'} sin\phi'$, for rectangular shape

$s_q = 1 + sin\phi'$, for circular shape

$s_\gamma = 1 - 0{,}3\frac{B'}{L'}$, for circular shape

$s_\gamma = 0.7$, for quadratic or circular shape

$$s_c = \frac{s_q N_q - 1}{N_q - 1}$$

$m = m_B = \frac{2+\frac{B'}{L'}}{1+\frac{B'}{L'}}$, when the horizontal force, H, is acting parallel to the side B

$m = m_B = \frac{2+\frac{L'}{B'}}{1+\frac{L'}{B'}}$, when the horizontal force, H, is acting parallel to the side L

4. Ground reaction in serviceability limit state

In order to ensure proper stiffness of the foundation no gap between the subsoil and the foundation should occur during normal conditions. This is evaluated by calculating the stresses in the in the soil, if the stresses are negative on the "tension side" the whole soil area under the foundation is compressed.

$$A_{found} = b_{found}^2 - c_{sl}^2$$

$$I_{found} = \frac{b_{found}^4}{12} - \frac{c_{sl}^4}{12}$$

$$\sigma = -\frac{Q}{A_{found}} + \frac{M}{I_{found}} \frac{b_{found}}{2}$$

5. Reaction from tower

Elastic behavior

$$A_{cylinder} = 2 r_{tower} \pi$$

$$W_{cylinder} = \pi \frac{(2 r_{tow})^2}{4}$$

$$F_{compression} = -\frac{1.35 G_{tow}}{A_{cylinder}} - \frac{M}{W_{cylinder}}$$

$$F_{tension} = -\frac{G_{tow}}{A_{cylinder}} + \frac{M}{W_{cylinder}}$$

6. Overall structural behavior

In this chapter the moments and shear forces are calculated based on the results from

Wind in main axis direction

The calculations in this chapter aim to find the sectional shear forces and moments in the foundation in section 1-1 as shown in figure … In these calculations the soil pressure is assumed to have a triangular distribution which makes the procedure slightly more cumbersome. Except for that difference the calculations basically follow the same procedure described in the previous chapters. It starts with a calculation of the eccentricity performed exactly as before which is followed by a center of mass calculation and when this is known the maximum soil stress at the edge of the foundation, the shear force and moment at section 1-1 can be calculated.

$$e = \frac{M}{Q}$$

$$d = \frac{\frac{b_{found} * L^2}{6} - \frac{c_{sl}}{2 * L} * (L - b)^2 * \left(b + \frac{L - b}{3}\right)}{\frac{b_{found} * L}{2} - \frac{c_{sl}}{2 * L} * (L - b)^2}$$

$$\sigma = \frac{Q}{\frac{b_{found} * L}{2} - \frac{c_{sl}}{2 * L} * (L - b)^2}$$

When the soil stress is known the moment and shear force can be calculated in section 1-1 as shown in figure …

The moment causing tension in the bottom of the slab is calculated as:

$$M_{bottom} = Q(e - 0.9r_{tower}) + \sigma_{11} b_{found} c_{sl} \frac{x_{11}^2}{6} - G_{found+backfill} b_{found} \frac{\left(\frac{b_{found}}{2} - 0.9r_{tower}\right)^2}{2} - H_{ex} 0.9 d_{found}$$

$$M_{top} = (q_{imposed} + G_{found+backfill}) \frac{\left(\frac{b_{found}}{2} - 0.9r_{tower}\right)^2}{2}$$

For the shear force the calculation becomes as follows. Q is the resultant from the soil pressure which has to be reduced with the soil pressure acting before the section in question. Only one fourth of the self-weight of the slab is assumed to be carried through this section and thus the dividing four in the last term.

$$V = Q - \sigma\left(b_{found} - c_{sl}\right)\frac{x}{2} - \frac{G_{found} + G_{backfill}}{4}$$

Wind in 45 degree direction

The calculations follow the same procedure as in the previous chapter, however, the dimensions needs to be slightly redefined because of the 45 degree direction. The same eccentricity is used so that:

$$e = \frac{M}{Q}$$

$$d = \frac{\frac{L^3}{2} - \left(L - \sqrt{2} * b\right)^3 \frac{1}{L}\left(\sqrt{2}b + \frac{L - \sqrt{2}b}{2}\right)}{L^2 - \left(L - \sqrt{2}b\right)^3 \frac{1}{L}}$$

$$\sigma = \frac{Q}{\frac{1}{3}\left(L^2 - \left(\left(L - \sqrt{2}b\right)^2 \frac{1}{L}\right)\right)}$$

The last equation can be derived by using integration techniques and expressions for the soil pressure depending on the length variable x. For the large triangle we have the expressions:

$$\sigma(x) = \sigma_{max} \frac{x}{L}$$

$$b(x) = 2L - 2x$$

Into the integral:

$$\int_0^L b(x)\sigma(x)\, dx = \int_0^L (2L - 2x)\, \sigma_{max} \frac{x}{L}\, dx$$

$$\frac{2\,\sigma_{max}}{L} \int_0^L (L - x)x\, dx = \frac{2\,\sigma_{max}}{L} * \left[\frac{Lx^2}{2} - \frac{x^3}{3}\right]_0^L = \frac{\sigma_{max}}{3} L^2$$

For the smaller triangle the same procedure is performed but with other expressions for the stress and the width:

$$\sigma(x) = \sigma_{max} \frac{x}{L}$$

$$b(x) = 2(L - \sqrt{2}b) - 2x$$

$$\int_0^{L-\sqrt{2}*b} b(x)\sigma(x)\, dx = \int_0^{L-\sqrt{2}*b} \left(2(L - \sqrt{2}b) - 2x\right)\, \sigma_{max} \frac{x}{L}\, dx$$

$$\frac{2\,\sigma_{max}}{L} \int_0^{L-\sqrt{2}b} \left(L - \sqrt{2}b - x\right) * x\, dx = \frac{2\,\sigma_{max}}{L}\left[L\frac{x^2}{2} - \sqrt{2}bx - \frac{x^3}{3}\right]_0^{L-\sqrt{2}*b}$$

$$\frac{2\,\sigma_{max}}{L}\left(\frac{1}{6}\left(L^3 - 3\sqrt{2}L^2 + 6b^2L - 2\sqrt{2}b^3\right)\right) = \frac{\sigma_{max}}{3}\frac{1}{L}\left(L - \sqrt{2}b\right)^3$$

Thus the resulting expression for both the big and small triangle becomes:

$$\frac{\sigma_{max}}{3}\left(L^2 - \frac{1}{L}\left(L - \sqrt{2}b\right)^3\right)$$

The moment and shear force and shear force in section 1-1 and 2-2 can be found by using the same type of integration techniques described in the previous chapters. For the shear force the expression become:

$$b(x) = 2\frac{b_{found}}{4\sqrt{2}} - 2x$$

$\sigma(x) = \sigma$, for the part with constant pressure

$\sigma(x) = \sigma_{max}\frac{x}{\frac{b_{found}}{4\sqrt{2}}}$, for the part with triangularly distributed pressure

$$V = \int_0^{\frac{b_{found}}{4\sqrt{2}}} \sigma\left(2\frac{b_{found}}{4\sqrt{2}} - 2x\right)dx = 2\sigma\left[\frac{b_{found}}{4\sqrt{2}}x - \frac{x^2}{2}\right]_0^{\frac{b_{found}}{4\sqrt{2}}} = 2\sigma\frac{\left(\frac{b_{found}}{4\sqrt{2}}\right)^2}{2} = \sigma\frac{\left(\frac{b_{found}}{4}\right)^2}{2}$$

$$V = \int_0^{\frac{b_{found}}{4\sqrt{2}}} \sigma_{max}\frac{x}{\frac{b_{found}}{4\sqrt{2}}}\left(2\frac{b_{found}}{4\sqrt{2}} - 2x\right)dx = \frac{2\sigma_{max}}{\frac{b_{found}}{4\sqrt{2}}}\left[\frac{b_{found}}{4\sqrt{2}}\frac{x^2}{2} - \frac{x^3}{3}\right]_0^{\frac{b_{found}}{4\sqrt{2}}}$$

$$\frac{2\sigma_{max}}{\frac{b_{found}}{4\sqrt{2}}}\left(\frac{\left(\frac{b_{found}}{4\sqrt{2}}\right)^3}{2} - \frac{\left(\frac{b_{found}}{4\sqrt{2}}\right)^3}{3}\right) = 2\sigma_{max}\frac{\left(\frac{b_{found}}{4\sqrt{2}}\right)^2}{6} = \sigma_{max}\frac{\left(\frac{b_{found}}{4}\right)^2}{6}$$

The moment on the other hand can be expressed as:

$$b(x) = 2\frac{b_{found}}{4\sqrt{2}} - 2x$$

$\sigma(x) = \sigma$, for the part with constant pressure

$\sigma(x) = \sigma_{max}\frac{x}{\frac{b_{found}}{4\sqrt{2}}}$, for the part with triangularly distributed pressure

$$leverarm = x$$

$$M = \int_0^{\frac{b_{found}}{4\sqrt{2}}} \sigma b(x)x = 2\sigma_{max}\int_0^{\frac{b_{found}}{4\sqrt{2}}} x\left(\frac{b_{found}}{4\sqrt{2}} - x\right)\,dx = 2\sigma_{max}\left[\frac{b_{found}}{4\sqrt{2}}\frac{x^2}{2} - \frac{x^3}{3}\right]_0^{\frac{b_{found}}{4\sqrt{2}}}$$

$$2\sigma_{max}\frac{\left(\frac{b_{found}}{4\sqrt{2}}\right)^3}{6} = \sigma_{max}\frac{\left(\frac{b_{found}}{4}\right)^3}{6\sqrt{2}}$$

$$M = \int_0^{\frac{b_{found}}{4\sqrt{2}}} \sigma b(x) x \, dx = \frac{2\sigma_{max}}{\frac{b_{found}}{4\sqrt{2}}} \int_0^{\frac{b_{found}}{4\sqrt{2}}} x\left(\frac{b_{found}}{4\sqrt{2}} - x\right) x \, dx = \frac{2\sigma_{max}}{\frac{b_{found}}{4\sqrt{2}}} \left[\frac{b_{found}}{4\sqrt{2}} \frac{x^3}{3} - \frac{x^4}{4}\right]_0^{\frac{b_{found}}{4\sqrt{2}}}$$

$$\frac{2\sigma_{max}}{\frac{b_{found}}{4\sqrt{2}}} \left(\frac{b_{found}}{4\sqrt{2}} \frac{\left(\frac{b_{found}}{4\sqrt{2}}\right)^3}{3} - \frac{\left(\frac{b_{found}}{4\sqrt{2}}\right)^3}{4} \right) = 2\sigma_{max} \frac{\left(\frac{b_{found}}{4\sqrt{2}}\right)^3}{12} = \sigma_{max} \frac{\left(\frac{b_{found}}{4}\right)^3}{6\sqrt{2}}$$

The moment is calculated as follows and is increased by the shear force times the effective depth:

$$M = \sigma_{max} \frac{\left(\frac{b}{4}\right)^2}{2} \left(\frac{\frac{b}{4}}{3\sqrt{2}} + d_{found} \right) +$$

7. Moments and reinforcement at foundation edge

Depending on what dimensions the reinforcement bars can be delivered in to the building site, slicing of the bars might be required. However, since the moment at the edges is lower than near the tower and thus a lower amount of reinforcement is appropriate. The design moment is calculated in same fashion for both the top and bottom reinforcement.

$$M_{edge} = \frac{\frac{l_{splice} M}{\frac{b_{found}}{2} - 0.9 r_{tow}}}{b_{found}}$$

And the required reinforcement is calculated as:

$$A_s = \frac{M_{edge}}{d_{found} f_{yd}}$$

8. Flexural reinforcement

The required reinforcement is calculated according to the book *Byggkonstruktion* (Isaksson, Mårtensson and Thelandersson, 2008) . Depending on if the section is normally reinforced or over reinforced different equations are used to find the amount of reinforcement.

The relative moment is calculated as:

$$m = \frac{M}{2 r_{tower} d^2 f_{cd}}$$

And the limit between normally reinforced concrete and over reinforced concrete is defined as:

$$\omega_{bal} = 0.8 \frac{\epsilon_{cu} E_s}{f_{yd} + \epsilon_{cu} E_s}$$

Which should be compared to:

$$\omega = 1 - \sqrt{1 - 2m}$$

$$A_s = \frac{M}{f_{yd} d\left(1 - \frac{\omega}{2}\right)}, \qquad \text{if } \omega \leq \omega_{bal}$$

$$A_s = \frac{M}{\sigma_s d\left(1 - \frac{\omega}{2}\right)} \text{ where } \sigma_s = E_s \epsilon_{cu} \left(\frac{0.8}{\omega} - 1\right), \qquad \text{if } \omega > \omega_{bal}$$

Fatigue check of flexural reinforcement using Markov factor

The fatigue is checked in accordance with SS-EN 1992-1-1:2005, section 6.8.5. To use this method an equivalent damage is needed which is calculated from the moment acting at the foundation using the Markov matrix.

The Markov factor, $\gamma_{\Delta M}$, is a factor to account for the geometry of the foundation and the the tower. Assume that the radius is very big, then the reaction force will move towards the edge of the foundation and thus closer to the the resultant force from the soil. This will decrease the moment in the slab and looking at the formula for the Markov factor it is obvious that it decreases as the radius grows. Thus a small Markov factor renders less moment in the slab.

$$\gamma_{\Delta M} = 0.5 * \frac{\frac{b_{found}}{2} * \frac{2}{3} - 0.9 * r_{tow}}{\frac{b_{found}}{2} * \frac{2}{3}}$$

$$\Delta M = \Delta M_{tower} * \gamma_{\Delta M}$$

$$M_N = -G_{tow}\left(\frac{b_{found}}{8} - \frac{r_{tow} * 2}{2 * \pi}\right)$$

From this a stress can be derived and a required reinforcement area calculated to resist. The capacity is reduced with the two factors $\gamma_{F,fat}$ and $\gamma_{S,fat}$ as follows. Gamma values can be found in SS-EN 1992-1-1:2005.

$$\Delta\sigma_{S,equ}(N^*) \leq \frac{\Delta\sigma_{Rsk}(N^*)}{\gamma_{F,fat}\gamma_{S,fat}}$$

This stress is then used to calculate the required amount of reinforcement:

$$A_{s,fat} = \frac{M}{0.9 d \Delta\sigma_{S,equ}}$$

Which is compared to the previous calculated area needed as flexural reinforcement.

9. Prestressed bolts

In this chapter the stresses in the bolts and the distribution plate are calculated.

Preconditions

A_{bolt} – bolt area

$f_{yk.bolt}$ – bolt proof stress

$f_{tk.bolt}$ – Ultimate tensile strength

n_{bolt} – Number of bolts

$b_{t.flange}$ –width of the distribution plate

The bolts can be post-tensioned to 70 % of the ultimate tensile strength. This gives an indication of what force the bolts should be tensioned with, proposedly to an even number that renders lower stress than the ultimate stress, i.e.

$$f_{t.bolt}$$

An equivalent cross section for the concrete and the bolt is calculated as:

$$EA_{bolt} = E_s n_{bolt} A_{bolt}$$

$$EA_{concrete} = E_{cd}\left(b_{t.flange} + 0.25h\right)\pi 2r_{tow}$$

The bolt and concrete will respectively bear

$$k_{bolt} = \frac{EA_{bolt}}{EA_{bolt} + EA_{concrete}}$$

$$k_{concrete} = \frac{EA_{concrete}}{EA_{bolt} + EA_{concrete}}$$

of the load.

The tensile force from the tower is found from Naviers formula where the gravity contributes negatively and the tilting moment positively.

$$F_{tower} = -\frac{G_{tow}}{A_{cyl}} + \frac{M_{tilt}}{W_{cyl}}$$

The total tensile force is found as

$$F = F_{tower} + \frac{n_{bolt} f_{t.bolt}}{\pi 2r_{tow}}$$

Prestress loss

b_{anchor} - width of anchor plate

The initial compression along the circle of bolts becomes

$$F_{c.initial} = \frac{n_{bolt} f_{t.bolt}}{\pi 2r_{tow}}$$

$\chi = 1.98 * 3^{8*0.7}\left(\frac{500000}{1000}\right)^{0.75*(1-0.7)}$ from Eurocode 2, 3.1.4.

n_{year} – years working life

$$A_c = hb_{found}$$

$u = b_{found}$ – Circumference of the part that is exposed to drying

$$h_0 = \frac{2A_c}{u}$$

$$\beta_{ds} = \frac{365n_{year}}{365n_{year} + 0.04\sqrt{h_0^3}}$$

$$k_h = \begin{matrix} 1\ if\ h_0 \leq 500 \\ 0.7\ otherwise \end{matrix}$$

$RH_{outside}$ –outside relative humidity

RH_0 – initial relative humidity

$a_{ds.1}$ – coefficient dependent on cement class

$a_{cd.2}$ - coefficient dependent on cement class

$$\beta_{RH} = 1.55\left(1 - \left(\frac{RH}{RH_0}\right)^3\right)$$

$$\epsilon_{cd.0} = 0.85\left((220 + 110a_{ds.1})e\text{^}(-a_{cd.2}\frac{f_{cm}}{f_{cm0}}\right)10^{-6}\beta_{RH}$$

The drying shrinkage becomes

$$\epsilon_{cd} = \beta_{ds}k_h\epsilon_{cd.0}$$

The autogenous shrinkage

$$\epsilon_{ca} = 2.5(f_{ck} - 10) * 10^{-6}$$

The bolts are pretensioned after 28 days, then two thirds of the autogenous shrinkage has taken place.

$$\beta_{as} = 1 - e^{-0.2t^{0.5}}$$

An uncertainty factor for the total amount is used and in this case taken as 1.3.

$$\gamma_{uncertainty} = 1.3$$

$$\epsilon_{cs} = \gamma_{uncertainty}\left(\frac{\epsilon_{ca}}{3} + \epsilon_{cd}\right)$$

The creep number is found in figure 3.1 in EC2:

$$\varphi$$

$$\Delta\sigma_s = E_s\epsilon_{cs} + \varphi\frac{E_s}{E_{cd}}\,\sigma_{initial} + 0.8\chi\sigma_s$$

The force after prestress loss is

$$F_{prestres} = (\sigma_s - \Delta\sigma_s)A_{bolt}$$

The force over the bolt ring is then

$$F_{prestress.total} = \frac{n_{bolt}\,F_{prestres}}{\pi 2 r_{tow}}$$

Initial ultimate limit state

Check that a gap does not occur between foundation and tower for frequent loads, thus using $M_{tilt.normal}$.

$$F_{tower.normal} = -\frac{G_{tow}}{A_{cyl}} + \frac{M_{tilt.normal}}{W_{cyl}}$$

If a gap would occur the at the tension side, the concrete compression there will be zero since the bolts are not in contact with the concrete. The force in the bolts will then increase with the factor:

$$\frac{1}{k_{concrete}}$$

So that

$$F_{gap} = \frac{F_{prestress.total}}{k_{concrete}}$$

This force is then compared so that

$$F_{gap} > F_{tower.normal}$$

The fatigue damage is calculated with the fatigue bending moment, $M_{fat.tower}$, as

$$\Delta\sigma_{fat} = \frac{4M_{fat.tower}}{n_{bolt}2r_{tow}}\frac{k_{bolt}}{A_{bolt}}$$

The fatigue strength is calculated in accordance with SS:EN 1992-1-1 2005 using table 6.4N to get the inclinations of the S-N curve. From this table the fatigue strength f_{fat} is taken which renders

$$\Delta\sigma_R = \frac{f_{fat}}{\gamma_s}\left(\frac{N_{cycles}}{N^*}\right)^k$$

N^* - From Eurocode

N_{cycles} – number of cycles

$k = k_1\ or\ k_2,\ depending\ on\ N_{cycles}$, from table 6.4N.

Ultimate limit state before and after prestress loss

The bolted connection is a post-tensioned concrete structure where the prestress force is regarded as an imposed load. The resulting compression reaction is assumed to have elastic (triangular) distribution. The total vertical reaction, i.e. tower plus prestress force, is denoted V and the bending moment, M.

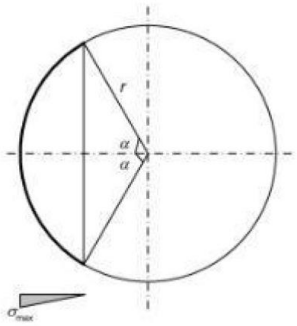

$$\sigma = \sigma_{max}\frac{\cos\varphi - \cos a}{1 - \cos a}$$

The reaction V is

$$V = \int_{-a}^{a} \sigma r d\varphi$$

$$V = \sigma_{max}\frac{r}{1 - \cos a}\int_{-a}^{a} \cos\varphi - \cos a \, d\varphi$$

$$V = \sigma_{max}\frac{r}{1 - \cos a}(2\sin a - 2a\cos a)$$

$$k = \frac{\sigma_{max}}{\sigma_{average}} = \frac{\sigma_{max}}{\frac{V}{2\pi r}} = \pi\frac{1 - \cos a}{\sin a - a\cos a}$$

The bending moment at the centre is

$$M = \int_{-a}^{a} \sigma r d\varphi \cos\varphi \, r$$

$$M = \sigma_{max}\frac{r^2}{1 - \cos a}\int_{-a}^{a} (\cos\varphi - \cos a)\cos\varphi \;\; d\varphi$$

$$M = \sigma_{max}\frac{r^2}{1 - \cos a}(a - \sin a\cos a)$$

The relative eccentricity at the factored extreme bending moment becomes

$$e_r = \frac{e}{r} = \frac{M}{(G_{tow} + n_{bolt} f_{t.bolt}) r_{tow}}$$

Using the previously defined expression for the total vertical force, V and moment, M we can write the relative eccentricity as and find the angle a from,

$$\frac{e}{r} = \frac{M}{Vr} = \frac{1}{2} \frac{a - \sin a \cos a}{\sin a - \mathrm{acos}\, a}$$

And the factor k is solved from

$$k = \frac{\pi(1 - \cos a)}{\sin a - a \cos a}$$

With k the maximum compression reaction under the bolt ring can be calculated as

$$F_{max} = k \frac{G_{tow} + n_{bolt} F_{prestress}}{\pi 2 r_{tow}}$$

The maximum force, F_{max} can then be compared with the previously calculated force due the tower weight and tilting moment. These values should be roughly the same, i.e.

$$F_{max} \approx -\frac{G_{tow}}{A_{cyl}} + \frac{M_{tilt.normal}}{W_{cyl}}$$

The bolts are perfectly elastic up the maximum load during prestressing, however, a set of 0.6 mm has to be compensated. This implies that the maximum force is

$$F_{bolt.max} = f_{t.bolt} + A_{bolt} \frac{0.6mm}{l_{bolt}} E_s$$

Which is compared with

$$F_{gap} = \frac{F_{prestress.total}}{k_{concrete}}$$

The effect of torsional moment and horizontal force

After the tower bottom section is erected, a “pedestal” is cast inside the tower in order to prevent sliding movement of the tower due to horizontal forces. Furthermore, in this way the deformation of the ring beam (bottom flange) will be minimized. The concrete slab is anchored to the foundation by means of hair pins.

$R_H = H$ – Shear force due to horizontal wind load

$R_T = \frac{M}{r_{tow}}$ – Shear force due to torsional moment

$A_{HT} = 0.5\left(2r_{tow} - b_{t.flange}\right)^2$ – Area for shear transfer

$\mu_{HT} = 0.6$ – Untreated surface

$$R_{HT} = \sqrt{R_H^2 + R_T^2}$$

$$\tau = \frac{R_{HT}}{A_{HT}}$$

And the amount of shear reinforcement can be calculated as

$$\rho = \frac{\tau_{HT}}{0.6}\frac{\gamma_s}{f_{yk}}$$

The horizontal force is transferred through the grout into the "pedestal" cast in the tower. The area that transfers the shear force into the center of the tower is defined as

$$A_{grout} = \sqrt{A_{HT}}h_{grout}$$

And the pressure is then

$$q = \frac{H}{A_{grout}}$$

Anchor plate

b_{anchor} – width of plate

$b_{macstag}$ – distance between bolts

f_u – ultimate strength

t_{anchor} – thickness of anchor plate

$d_{bolt.cc}$ – cc-distance between bolts

$d_{bolt.hole}$ – hole diameter

The compression from the anchor bolts

$$R_{anchor} = 1.1\frac{0.95 n_{bolt} f_{tk.bolt} A_{bolt}}{2 r_{tow}\pi}$$

$\sigma_{concrete} = \frac{R_{anchor}}{b_{anchor}}$, to compare with $1.5 f_{cd}$

Moment in the plate is calculated as

$$M_{anchor.hole} = \sigma_{concrete}\frac{\left(b_{anchor} - b_{macstag}\right)^2}{8}$$

Which is compared with the capacity

$$M_R = \frac{0.9 f_u}{1.25}\frac{t_{anchor}^2}{4}\frac{(d_{bolt.cc} - d_{bolt}.hole)^2}{d_{bolt.cc}}$$

When the wind is causing a negative bending moment, i.e. when bottom of the slab is compressed, a favorable triaxle concrete stress develops over the anchor plate in the bottom of the slab. The concrete capacity can then be increased by a factor 1.5. When the wind is acting the other direction, a positive bending moment develops that causes tension in the bottom of the slab. This means that the stress variation in the bolts will be almost zero which implies that also the variation in the concrete will be zero. Recall that the concrete stress is zero if a gap develops on the tension side thus no extra pressure on the bolts. This, in turn, means that it is sufficient to check so that the concrete stress is limited to the basic fatigue strength, f_{fat}.

$f_{fat} = 0.85\frac{f_{ck}}{1.5}\left(1 - \frac{f_{ck}}{250}\right)$, SS-EN 1992-1-1:2005 Eq. 6.61 & 6.57

Which is compared with

$$\sigma_{c.anchor} = \frac{n_{bolt} f_{t.bolt}}{2\pi r_{tow} b_{anchor}}$$

Splitting forces due to prestress

The splitting forces in the concrete is assessed in accordance with EC2 using the previously defined initial force, $F_{c.initial}$.

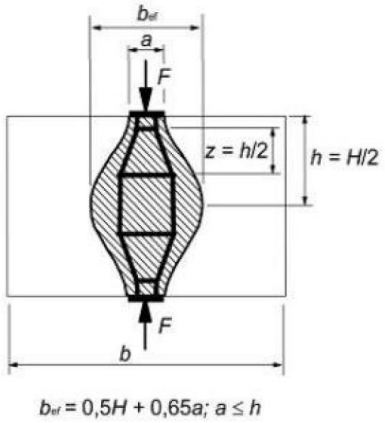

$F_{tie} = 2\frac{1}{4}\left(1 - 0.7\frac{b_{anchor}}{0.5h}\right)F_{c.initial}$, SS-EN 1992-1-1:2005 Eq. 6.59

The total splitting force, H:

$$F_{Hsplit} = F_{tie} 2r_{tow}$$

Splitting reinforcement is added for half the splitting force so that

$$A_T = \frac{F_{Hsplit}}{2f_{yd}}$$

The splitting reinforcement is placed in two layers, one close to the top and close to the bottom.

Distribution ring

$b_{t.flange}$ – ring width

t_{plate} – ring thickness

The compression in the plate due to tower self-weight, tilting moment and prestress force becomes

$$F_{c.plate} = \frac{1.35 m_{bolt} f_{t.bolt}}{\pi 2 r_{tow}} + \left| -\frac{1.35 G_{tow}}{A_{cylinder}} - \frac{M}{W_{cylinder}} \right|$$

$$\sigma_{c.plate} = \frac{F_{c.plate}}{b_{t.flange}}$$

The concrete is triaxially compressed due the bending moment, this implies that the stress should be compared to

$$f_{cd.triax} = 3\, f_{cd}$$

The bending moment in the plate is

$$m_{plate} = F_{c.plate} \frac{b_{t.flange} - b_{tower.flange}}{8}$$

The capacity is

$$m_{R.plate} = \frac{f_y t_{plate}^2}{6}\, 1.75$$

The bending moment at the holes is

$$b_{cantilever} = \frac{b_{t.flange}}{2} - \frac{b_{macstag}}{2}$$

$$m_{holes} = \sigma_{c.plate} \frac{b_{cantilever}^2}{2}$$

$$m_{R.holes} = \frac{0.9 f_u}{1.25} \frac{t_{plate}^2}{4} \frac{d_{bolt.cc} - d_{bolt.hole}}{d_{bolt.cc}}$$

Fatigue

$$\Delta N = \frac{M_{fat.steel}}{W_{cyl}}$$

$$\Delta\sigma = \frac{\Delta N\, b_{cantilever}^2}{2 b_{t.flange}} \frac{6}{t_{plate}^2} \frac{d_{bolt.cc} - d_{bolt.hole}}{d_{bolt.cc}}$$

$$\Delta\sigma_R = \frac{f_{fat}}{\gamma_s} \left(\frac{N_{cycles}}{N^*} \right)^k$$

10. Shear reinforcement

The shear force is concentrated along one quarter of the perimeter of the tower. The control section is at 0.5d outside the outer bolt ring,

$$\upsilon = \frac{V_{max}}{\pi \frac{\left(O_{ring} + 0.5d_{bottom}\right)}{4}}$$

$$\tau = \frac{\upsilon}{d_{bottom}}$$

$$\gamma_c = 1.5$$

$$C_{Rd.c} = \frac{0.18}{\gamma_c}$$

$$f = C_{Rd.c} k (100 \rho_{shear} f_{cd})^{\frac{1}{3}}$$

If shear reinforcement is required:

$$A_{sv} = \frac{V_{max}}{f_{yd}}$$

The shear reinforcement is then placed within circles so that, e.g.,

$$A_1 = \pi(r_2^2 - r_1^2)$$

$$\rho = \frac{4A_{sv}}{2A_1}$$

Anchoring of stirrups

The stirrups are anchored to the top reinforcement and should fulfill the requirements according to case a) in the figure below in accordance with section 8.5, SS-EN 1992-1-1:2005.

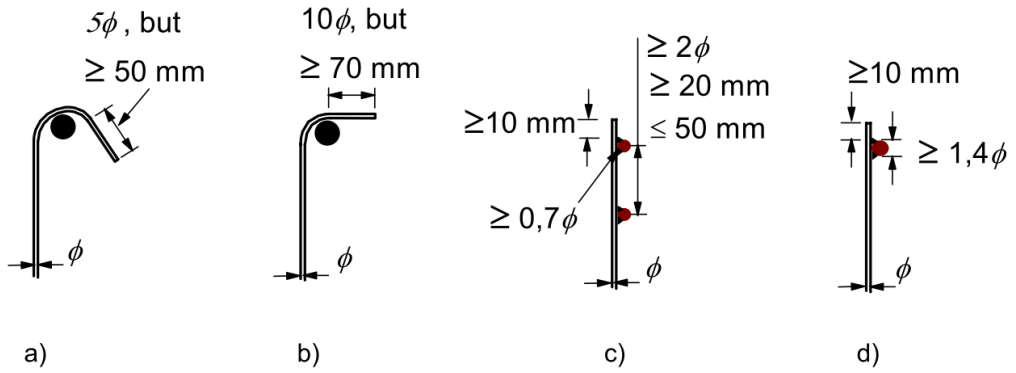

$d_{mandrel}$ – Mandrel diameter

η_1 – section 8.4.2, SS-EN 1992-1-1:2005

η_2 – section 8.4.2, SS-EN 1992-1-1:2005

f_{ctd} – concrete tension strength

$f_{bd} = 2.25\eta_1\eta_2 f_{ctd}$ – eq. 8.2, section 8.4.2, SS-EN 1992-1-1:2005

$l_{b.rqd} = \frac{\Phi}{4}\frac{\sigma_{sd}}{f_{bd}}$ – eq. 8.3, section 8.4.3, SS-EN 1992-1-1:2005

a_1 - a_5 are given in section 8.4.4, SS-EN 1992-1-1:2005

$l_{bd} = a_1 a_2 a_3 a_4 a_5 l_{b.rqd}$ – eq 8.4, section 8.4.4, SS-EN 1992-1-1:2005

Mandrel diameter

The allowed mandrel diameter is checked according to section 8.3, SS-EN 1992-1-1:2005.

$$\phi_{m.min} \geq F_{bt}\frac{\frac{1}{a_b}+\frac{1}{2\phi}}{f_{cd}}$$

Which should fulfill

$$\phi_{mandrel} \geq \phi_{m.min}$$

Extension of stirrups

With the soil reaction at the edge known, the extension length of the stirrup can be calculated using the concrete shear capacity.

f_v – concrete shear capacity

$V_c = f_c d_{bottom}$ – concrete shear capacity per meter

$$x_{extension} = \frac{V_c}{\sigma_{max.soil} - G_{found.backfill}}\frac{b_{found} - 2x_{extension}}{b_{found}}$$

From x and further, closer to the center, the shear reinforcement should be able to carry the force V_c.

Fatigue strength of stirrups

$$I_{found} = \frac{b_{found}^4}{12}$$

$$\Delta\sigma = \frac{M_{fat.tower}}{I_{found}} \frac{b_{found}}{2}$$

The shear force range along one quarter of the tower can be derived as follows. The expression is integrated from 0 to $\frac{b}{2}$ starting from the edge. The expression for the width and soil pressure become

$$b = b_{found} - 2x$$

$$\sigma = \Delta\sigma \frac{\left(\frac{b_{found}}{2} - x\right)}{\frac{b_{found}}{2}}$$

$$\int_0^{\frac{b}{2}} b\sigma \, dx = \frac{2\Delta\sigma}{b_{found}} \int_0^{\frac{b}{2}} \left(\frac{b_{found}}{2} - x\right)\left(b_{found} - 2x\right) dx = \frac{\Delta\sigma b_{found}^2}{6}$$

$$\Delta V = \Delta\sigma b_{found} \, b_{found}$$

The resistance for bent bars should be reduced according to table 6.3N in SS-EN 1992-1-1:2005 so that the capacity becomes

$$f_{fat} = \Delta\sigma_R(0.35 + 0.026 d_{mandrel}/\phi)$$

The force may be reduced if the flexural reinforcement is anchored in several layers.

When the resistance is known the required area can be calculated as:

$V_{fatigue} = \Delta V \frac{f_{yd} 2^{\frac{1}{4}}}{f_{fat}}$ Which is compare to the previously calculated maximum shear force.

Shear inside tower

With elastic stress distribution in the tower the total compression and tension forces from the bending become:

$$V = \frac{M}{\pi r^2} 2r = \frac{2M}{\pi r}$$

Reducing the shear force due to the weight from the tower gives the force that needs to be resisited:

$$V = \frac{2M}{\pi r_{tower}} - 0.5Q$$

The maximum compression capacity in the concrete should, according to Eurocode, fulfill:

$V_{Ed} \leq 0.5 b_w d \nu f_{cd}$ Eq 6.5, SS-EN 1992-1-1:2005

$\nu = 0.6\left[1 - \frac{f_{ck}}{250}\right]$ Eq 6.6, SS-EN 1992-1-1:2005

The anchor bolts will carry some of the shear force. Between the angles β and α the anchor bolts go from 0 % to 100 % active as shear reinforcement and between the angles 45° and β the bolts are 100 % active, recall that in this area the bolts are not effective as moment resistor since that that part is concentrated to one quarter of the circle, i.e. -45° to 45°. The angle α and the factor k is calculate in previous chapters. β is found by seeing the linearly varying pressure and realizing that two equilateral triangles can be formed.

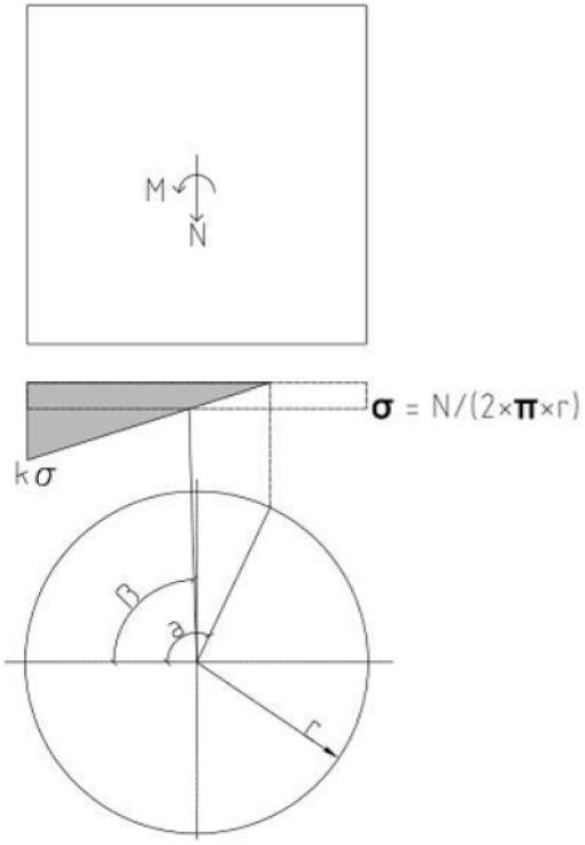

The figure below shows the relation between the triangles which leads to the expression:

$$\frac{1 - \cos\beta}{1 - \cos\alpha} = \frac{k - 1}{k}$$

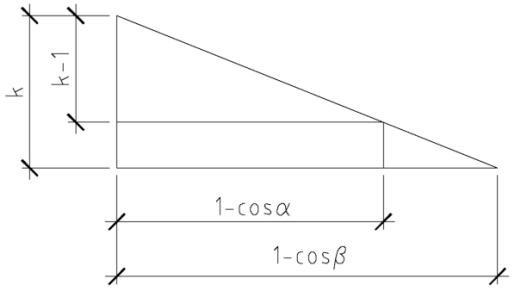

The total capacity of the anchor bolts as shear reinforcement can be calculated using the prestress force after prestress loss as:

$$F = \frac{0.5(\alpha - \beta) + 1.0(\beta - \theta)}{\pi} n_{bolt} F_{prestress}$$

Vertical cracks caused by the global bending moment may reduce the effectiveness of the bolts over the perimeter of the tower. These cracks develop perpendicular to the direction of the moment as indicated in the figure below. The shear force is assumed to be taken by bottle shaped diagonal concrete struts with slope of about 1:2. Because of this, a minimum amount of reinforcement should be provided to assure a ductile behavior after a splitting crack occurring. If the tensile stress across the strut is assumed to have trinaugal variation, the minimum reinforcement ratio for the vertical stirrup becomes:

$$\rho_w = \frac{1}{2} \frac{f_{ctm}}{f_{yk} \sin^2 a}$$

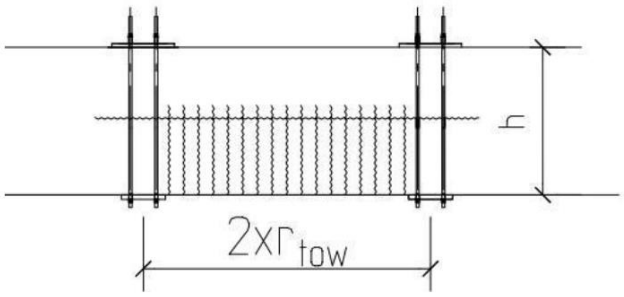

Fatigue

The equivalent bending moment range the slab is calculated from the Markov matrices and thus for the shear force range becomes:

$$V = \frac{2M_{fatigue.tower}}{\pi r_{tower}} - \frac{3}{2}\Delta V$$

Where ΔV is calculated in *Fatigue strength of stirrups*.

Concrete fatigue

The compression strength in the fatigue limit state can be assessed from the Markov matrix. Each load bin is studied in accordance with SS-EN 1992-1-1 and the accumulative damage is calculated as follows.

The basic strength after the first load cycle is given as:

$$f_{fat} = 0.85 f_{cd} \left(1 - \frac{f_{ck}}{250}\right)$$

The fatigue strength σ_{max} at a million cycles varies and is calculated from

$$\sigma_{max} = f_{fat}\left(1 - 0.43\sqrt{1 - R}\right)$$

Where

$$R = \frac{\sigma_{min,i}}{\sigma_{max,i}}$$

$\sigma_{min,i}$ and $\sigma_{max,i}$ are the concrete stresses under the tower distribution ring due to the maximum and minimum bending moments at the studied load cycle plus the stress due to the gravity load reaction and prestressing.

It is assumed that the concrete fatigue strength varies linearly in a log-log diagram from σ_{max} for $N = 10^6$ to f_{fat} for $N = 1$ cycles. Note that this approach is slightly more conservative than the "Bridge formula" in SS-EN 1992-1-1 where the fatigue strength is a curve with convex curvature when represented in a log-log diagram. The difference is small in the range up to a million cycles but above this it is unrealistic.

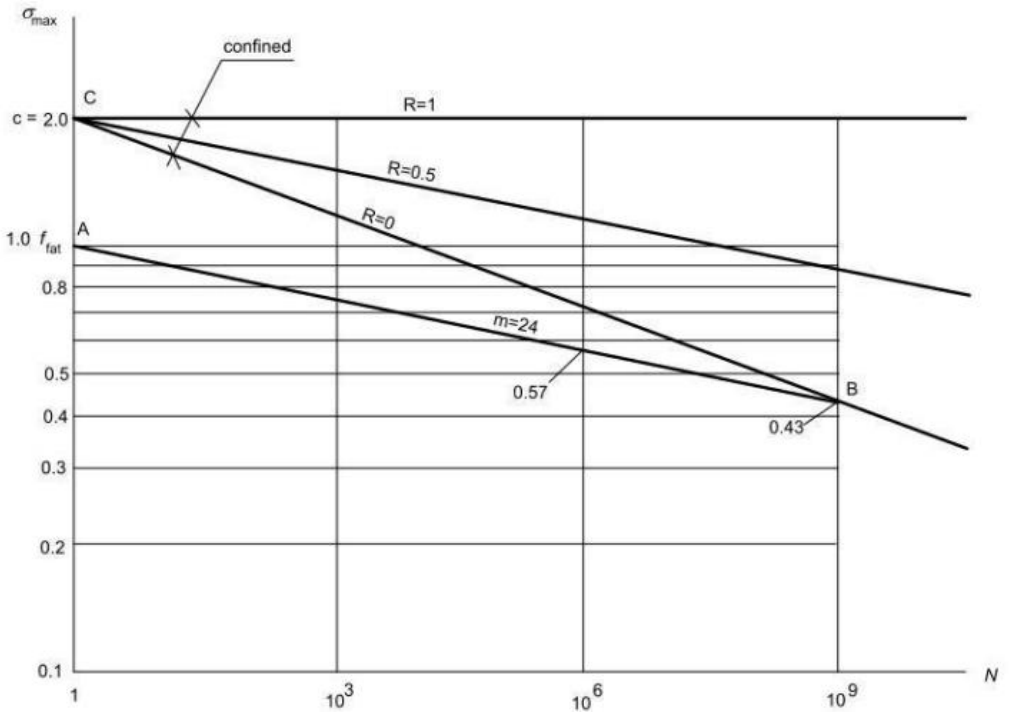

$$m_{AB} = \frac{\log\left(\frac{10^6}{10^0}\right)}{\log\left(\frac{1}{0.57}\right)} = 24.578$$

The stress value for a billion cycles become:

$$\sigma = n_{val} f_{fat}$$

Where

$$n_{val} = 0.57\left(\frac{10^6}{10^9}\right)^{\frac{1}{24}}$$

The wind turbine tower is placed directly on the top surface of the foundation slab. Due to the large bending moment in the tower, the reaction stress is compression and tension respectively on opposite sides of the tower. On the compression side the global bending moment in the foundation gives a horizontal concrete compression stress in all directions under the distribution ring connection. This active confinement together with the passive confinement by the flexural reinforcement due to the poission ratio $\upsilon = 0.20$ gives the confined compression strength.

$$f_{cd.c} = 3f_{cd}$$

On the tension side no active confinement will occur and only the passive confinement by the top reinforcement corresponding to $\upsilon = 0.20$ exists, rearranging gives:

$$1.5f_{cd.c} = 1.125f_{ck} + 2.5 \cdot 0.20f_{cd.c} \Longrightarrow f_{cd.c} = \frac{1.6875f_{ck}}{1.5}$$

The strength increase because the confinement can be expressed by the factor "*c"=3* and *1.7* (Choosing 1.5 respectively in the two described cases above.

Research seem to indicate that the confinement effect for static loading in the ultimate limit state decrease at fatigue loading. The confinement effect is here assumed to vanish at a billion cycles for *R=0*. This is illustrated by the line CB in the figure above.

The compression capacity for a billion cycles becomes:

$$f_{max} = f_{fat}\left(c - (c - 0.43)\sqrt{1 - R}\right)$$

The slope of the studied line is:

$$m_{CB} = \frac{\log(10^9)}{\log\left(\frac{cf_{fat}}{f_{max}}\right)}$$

The partial damage for each row in the matrix becomes:

$$d = \frac{N_i}{10^9}\left(\frac{\sigma_{max,i}}{f_{max}}\right)^m$$

If the total damage $\sum d$ becomes less than 1, the design is OK. The fatigue capacity of the grout below the tower T-flange can be assessed with the confinement factor $c > 1.5$, according to above, because the thin grout layer is confined by the distribution plate.

Foundation stiffness

The concrete slab acts as a beam on elastic layer, see figure below. The fictions length l_0 is an important parameter for the calculation of the behavior of the beam.

$$l_0 = \sqrt[4]{\frac{EI}{bc}}$$

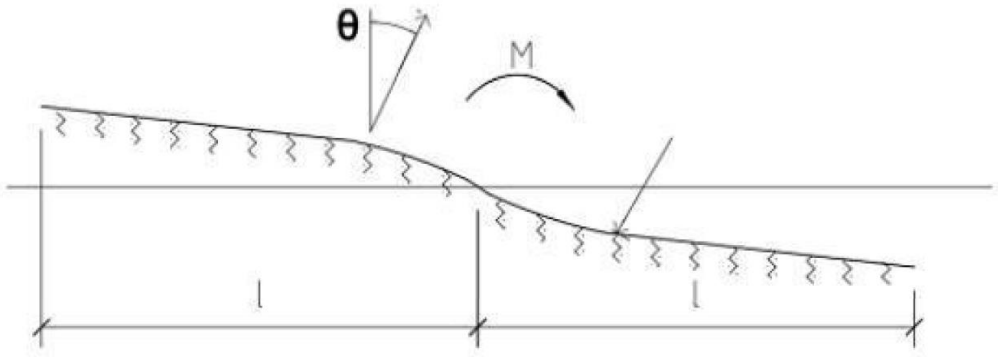

Soil properties

The dynamic compression modulus for the subsoil can several times larger than the static compression modulus, which is evident from the figure below.

$$M_s = \frac{\Delta\sigma}{\Delta\epsilon}$$

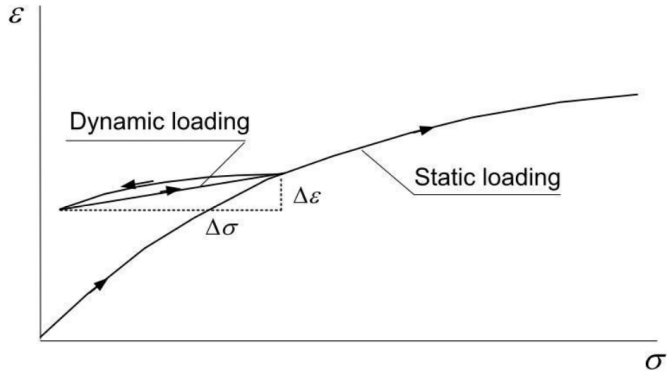

Soft layer

In order to establish a permanently good dynamic behavior of the foundation it is recommended to place a soft layer under the central part of the foundation, see figure below.

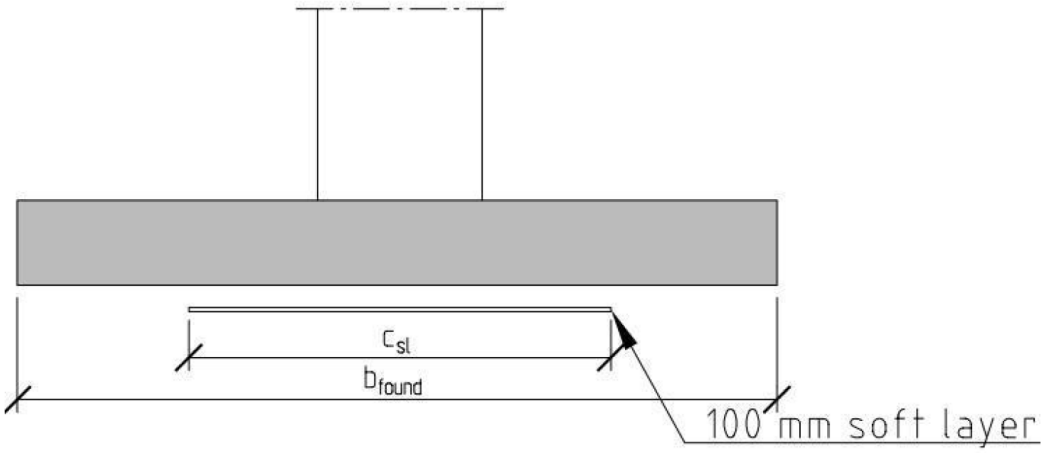

The soft layer should be able to contain the weight from the concrete.

$$q_{d,pressure} = \rho_{concrete} h$$

The strength capacity of the soft layer is:

$\kappa_r = 0.55$ Load type B, depends on load duration

f_k – Strength of the soft layer

$f_d = \frac{\kappa \cdot f_k}{1.3}$ – capacity of the soft layer

Flexural stiffness of the foundation slab

The flexural stiffness EI of the foundation can be assessed as follows. The bending moment in the slab causing slab cracking is assumed to be *1.5* times the average distributed moment over the foundation width.

$$M_{cr} = f_{ctm}\frac{h^2 b_{found}}{6}\frac{1}{1.5}$$

The maximum tower moment is given by the tower supplier and is assessed as:

$$M_{res} = M_{tower.normal} \cdot 0.5\frac{\frac{2}{3}b_{found} - 0.9r_{tow}}{\frac{2}{3}b_{found}}$$

The dynamic stiffness of the foundation of the square foundation is:

$$EI_{\infty} = E_{cd}\frac{b_{found}h^3}{12}$$

The flexural reinforcement for the cracked foundation is calculated as follows. With the average reinforcement of the bottom and top reinforcement, the reinforcement amount is expressed as:

$$A_{s,average} = \frac{A_{s,bottom} + A_{s,top}}{2}$$

$$\rho = \frac{A_{s,average}}{d_{bottom}b_{found}}$$

The relative height of the compression zone becomes:

$$a_e = \frac{E_s}{E_{cd}}$$

$$\xi_1 = a_e\rho\sqrt{1 + \frac{2}{a_e\rho}}$$

The stiffness in the *45°* direction of the square foundation is equal to the stiffness along the main axis. The cracked flexural stiffness in the *45°* direction with orthogonal reinforcement layout is, however, only half the flexural stiffness in the main direction, which is accounted for in the following.

The flexural stiffness of the cracked concrete section is then:

$$EI_{II} = 0.5E_s\rho b_{found}d_{bottom}^3(1 - \xi_1)\left(1 - \frac{\xi_1}{3}\right)$$

An estimate of the resulting stiffness according to EC2, section 7.4.3 gives:

$$\xi_2 = 1 - 0.5\frac{M_{cr}}{M_{res}}$$

The resulting flexural stiffness can be assessed to:

$$EI_{res} = \xi_2 EI_{II} + (1.\xi_2)EI_{\infty}$$

Behavior of foundation slab

Required dynamic:

$$\frac{M}{\theta} = k_{\varphi} \geq 59 \frac{GNm}{rad}$$

The required bed modules becomes:

$$c_{req} = \frac{k_{\varphi}}{\frac{b_{found}^4 - c_{sl}^4}{12}}$$

The fictous length l_0 can then be assessed to:

$$l_0 = \sqrt[4]{\frac{EI_{res}}{b_{found} c_{req}}}$$

$$\frac{\frac{b_{found}}{2}}{l_0\sqrt{2}}$$

From Handbok bygg 1B, it is evident that as long as

$$\frac{l}{l_0\sqrt{2}} \leq 1.6$$

The beam is so stiff that the soil deflection varies linearly, which means that the foundation slab rotates as an almost rigid body during the tower oscillation. The usual assumption, that the foundation stiffness is solely governed by the subsoil is therefore correct in this case – if the tower is attached to the top of the foundation by means of prestressed anchor bolts.

The square foundation is equivalent to a circular foundation with the same rotation stiffness I.

$$\frac{\pi r^4}{12} = \frac{b_{found}^4}{12}$$

For a circular foundation:

$$k_{\varphi} = \frac{4r^3}{3} M_s \frac{1-2v}{1+v} = \frac{4r^3}{3} \frac{E_{soil}}{1-v_s^2}$$

And the dynamic modulus of elasticity

$$E_{soil} = \frac{k_{\varphi} 3(1-v_s^2)}{4r^3}$$

And the required compression modulus of the soil, M_s, becomes:

$$M_s = E_{soil} \frac{1-v_s}{(1+v_s)(1-2v_s)}$$

DNV has a redefined expression to account for a foundation buried in the soil with limited depth to rock.

D - depth from ground level to the faoundation

H – depth from ground level to bedrock

$$k_\varphi = \frac{4r^3}{3}\frac{E}{1-v_s^2}\left(1+\frac{r}{6H}\right)\left(1+\frac{2D}{r}\right)\left(1+\frac{0.7D}{H}\right)$$

Crack widths

The bending moment for permanent loads is calculated as follows:

Axial force from tower gives the bending moment in the foundation

$$m_{found} = G_{tower}\left(\frac{1}{8}-\frac{1}{2\pi}\frac{2r_{tower}}{b_{found}}\right)$$

The maximum average bending moment over the foundation width becomes approximately:

$$m_{average} = 0.5\frac{M_{normal}}{b_{found}}\frac{\frac{b_{found}}{2}\cdot\frac{2}{3}-0.9r_{tow}}{\frac{b_{found}}{2}\cdot\frac{2}{3}}$$

This gives the top and bottom bending moment as:

$$m_{average,top} = m_{average} - m_{found}$$

$$m_{average,bot} = m_{average} + m_{found}$$

The maximum bending moment at the edge of the tower is assumed to be 1.5 times the average moment. The calculations of the crack widths are performed in accordance with SS-EN 1992-1-1:2005.

$$\sigma = \frac{1.5m_{average,top/bottom}}{0.9d_{found}A_s}$$

$\rho_{p,eff} = \frac{A_s}{A_{c,eff}} = \frac{A_s}{2.4(h-d_{found})}$ Eq 7.10, with SS-EN 1992-1-1:2005

$\Delta\epsilon = \epsilon_{sm} - \epsilon_{cm} = \frac{\sigma_s - k_t\frac{f_{ct,eff}}{\rho_{p,eff}}(1+\alpha_e\rho_{p,eff})}{E_s} \geq 0.6\frac{\sigma_s}{E_s}$ Eq 7.9, with SS-EN 1992-1-1:2005

$k_t = 0.4$ – for long term

$k_t = 0.6$ – for short term

The maximum crack spacing is calculated as:

$s_{r,max} = k_3c + k_1k_2k_4\phi/\rho_{p,eff}$ Eq 7.11, with SS-EN 1992-1-1:2005

ϕ – bar diameter

c – concrete cover

k_1 – coefficient for adhesion properties of reinforcement, *0.8* bars with good adhesion and *1.6* for bars with practically smooth surface.

k_2 – factor that accounts for the strain distribution, *0.5* for bending and *1.0* for pure tension.

k_3 – recommended value is *3.4*.

k_4 – recommended value is *0.425*.

The characteristic crack width becomes

$$w_k = s_{r,max}\Delta\epsilon$$

Lap lengths

Worst place to splice the reinforcement is where the moment is maximum.

$f_{bd} = 2.25\eta_1\eta_2 f_{ctd}$ Eq 8.2, with SS-EN 1992-1-1:2005

The average moment is calculated by using the maximum moment, previously calculated, acting in the foundation.

$$m_{splice} = \frac{M_{max}}{b_{found}}$$

$$F_{sd} = \frac{m_{splice}}{d_{found}}$$

$$\sigma_{sd} = \frac{F_{sd}}{A_s} = \frac{F_{sd}}{\pi\frac{\phi^2}{4}\cdot s}$$

$l_{b,rqd} = \frac{\phi}{4}\cdot\frac{\sigma}{f_{bd}}$ Eq 8.3, with SS-EN 1992-1-1:2005

The splice length is given by:

$l_0 = a_1a_2a_3a_4a_5l_{b,drq} \geq l_{0,min}$ Eq 8.4, with SS-EN 1992-1-1:2005

Where a_1, a_2, a_3, a_4, a_5 are given in table 8.2 in SS-EN 1992-1-1:2005 and

$l_{0,min} = \max(0.3a_6l_{b,rqd}; 15\phi; 200mm)$ Eq 8.11, with SS-EN 1992-1-1:2005

Where a_6 is given in table 8.3 in SS-EN 1992-1-1:2005.

Tabell 8.3 – Värden på koefficienten α_6

Area för skarvade stänger i förhållande till total armeringsarea	< 25%	33%	50%	>50%
α_6	1	1,15	1,4	1,5
ANM. Mellanliggande värden får bestämmas med interpolation.				